Gene-Drug Interactions and the Evolution of Antibiotic Resistance

HARVARD UNIVERSITY
Graduate School of Arts and Sciences

DISSERTATION ACCEPTANCE CERTIFICATE

The undersigned, appointed by the

Committee on Higher Degrees in Systems Biology

have examined a dissertation entitled

Gene-drug interactions and the evolution of antibiotic resistance

presented by Adam Christopher Palmer

candidate for the degree of Doctor of Philosophy and hereby certify that it is worthy of acceptance.

Signature: _____

Typed Name: Dr. Timothy Mitchison

Signature: _____

Typed Name: Dr. Michael Springer

Signature: _____

Typed Name: Dr. Jeff Gore

Signature: _____

Typed Name: Dr. Deborah Hung

Date: November 07, 2012

Gene-drug interactions and the evolution of antibiotic resistance

A dissertation presented

by

Adam Christopher Palmer

to

The Committee on Higher Degrees in Systems Biology

in partial fulfillment of the requirements
for the degree of
Doctor of Philosophy
in the subject of

Systems Biology

Harvard University
Cambridge, Massachusetts

October 2012

Gene-drug interactions and the evolution of antibiotic resistance

Abstract

The evolution of antibiotic resistance is shaped by interactions between genes, the chemical environment, and an antibiotic's mechanism of action. This thesis explores these interactions with experiments, theory, and analysis, seeking a mechanistic understanding of how different interactions between genes and drugs can enhance or constrain the evolution of antibiotic resistance.

Chapter 1 investigates the effects of the chemical decay of an antibiotic. Tetracycline resistant and sensitive bacteria were grown competitively in the presence of tetracycline and its decay products. Antibiotic decay did not only remove selection for resistance, but long-lived decay products favored tetracycline sensitivity by inducing costly drug efflux pumps in the resistant strain. Selection against resistance by antibiotic-related compounds may contribute to the coexistence of drug-sensitive and resistant bacteria in nature.

Chapter 2 investigates how genetic interactions can favor particular combinations of resistance-conferring mutations. All possible combinations of a set of trimethoprim resistance-conferring mutations in the drug's target gene were constructed and phenotyped. Incompatibilities between mutations arose in a high-order, not pairwise, manner. One mutation was found to induce this ruggedness and create a multi-peaked adaptive landscape.

Chapters 1 and 2 observed that non-optimal expression of a drug resistance gene or a drug's target could compromise antibiotic resistance. Chapter 3 broadly characterizes non-optimal gene expression under antibiotic treatment, using a functional genetic screen to identify over one hundred pathways to antibiotic resistance through positive and negative changes in gene expression. Genes with the potential to confer antibiotic resistance were found to often go unused during antibiotic stress. The optimization of gene expression for drug-free growth was found to cause non-optimal expression under drug treatment, creating a situation where regulatory mutations can confer resistance by correcting errors in gene expression.

Chapter 4 investigates whether it is beneficial to up-regulate the genes encoding antibiotic targets when they are inhibited. Drug target genes were quantitatively over-expressed, and drug resistance was found to not always increase, but alternatively to remain unchanged or even decrease. These diverse effects were explained by simple models that consider toxicity arising from gene over-expression, and mechanisms of drug action in which drugs induce harmful enzymatic reactions.

Table of contents

A cell can regulate some genes perfectly all of the time, and all genes perfectly some of the time,

but a cell can not regulate all genes perfectly all of the time.

-with apologies to Abraham Lincoln

Chapter 1.

Chemical decay of an antibiotic inverts selection for resistance

Adam C. Palmer[1], Elaine Angelino[1], Roy Kishony[1,2]

[1]Department of Systems Biology, Harvard Medical School, 200 Longwood Ave, Boston, MA 02115.

[2]School of Engineering and Applied Sciences, Harvard University, Cambridge, MA 02138.

Antibiotics are often unstable, decaying into a range of compounds with potential biological activities. We found that as tetracycline degrades, the competitive advantage conferred to bacteria by resistance to it not only diminishes, but reverses to become a prolonged disadvantage due to the activities of more stable degradation products. Tetracycline decay can therefore lead to net selection against resistance, which may help explain the puzzling coexistence of sensitive and resistant strains in natural environments.

More than half of all known antibiotics are secreted by soil bacteria (Kieser et al., 2000),

mediating communication (Fajardo and Martinez, 2008; Linares et al., 2006; Yim et al., 2007),

metabolism (Dantas et al., 2008; Price-Whelan et al., 2006) and warfare (Walsh, 2003). While

resistance to these naturally-occurring antibiotics is prevalent in the soil environment, the

genes conferring resistance do not seem to take over and fixate in these natural populations;

instead resistant and sensitive bacterial strains coexist (D'Costa et al., 2006). It is therefore

likely that while antibiotics select for resistant strains, other natural mechanisms might exist

which select against resistance. Indeed, several natural chemicals are known to specifically

inhibit growth of strains resistant to certain antibiotics (Bochner et al., 1980; Halling-

Sorensen et al., 2002). The ability of any compound to select for or against resistance depends

not only on the selective pressure it exerts, but also on the duration of its activity, determined

by its chemical stability. Many antibiotics are short-lived in the natural environment; they

decay to an assortment of chemical species which may be more stable than the precursor

drug, and may therefore have significant ecological impacts. Thus, competition between

antibiotic resistant and sensitive strains may be influenced both by the short-term effect of an

antibiotic and by the potential long-term effects of its degradation products (Figure 1.1a).

Here we ask how the chemical decay of tetracycline influences selection for resistant strains.

Tetracycline is widely used clinically (Chopra et al., 1992) and agriculturally(Sarmah et al.,

2006), its major degradation pathway is well characterized (Yuen and Sokoloski, 1977), and

its decay products are found in soil, wastewater, and market tetracyclines (Jia et al., 2009;

Sarmah et al., 2006; Walton et al., 1970). One of its decay products, anhydrotetracycline, is

known to preferentially inhibit the growth of bacteria carrying the Tn10 tetracycline

resistance determinant, by binding the *tetR* regulator to induce expression of the costly *tetA* efflux pump (Eckert and Beck, 1989; Lederer et al., 1996; Moyed et al., 1983; Nguyen et al., 1989). We investigated the selective advantage/disadvantage of resistance throughout the degradation process, by directly competing fluorescently labeled tetracycline resistant and sensitive strains of *Escherichia coli*.

Tetracycline (Tet) undergoes reversible epimerization to epitetracycline (ETC) and also irreversible dehydration to anhydrotetracycline (ATC), with both epimerization and dehydration yielding epianhydrotetracycline (EATC) (Yuen and Sokoloski, 1977) (Figure 1.1b). To accelerate the degradation process to convenient timescales we exposed tetracycline to phosphoric acid and high temperatures (Yuen and Sokoloski, 1977); Methods). At different time-points of exposure to these degrading conditions (t_{deg}), samples of the chemical reaction were taken and the reaction was stopped by shifting to neutral pH and freezing. To track the abundance of tetracycline and its degradation products over time, we measured the absorbance spectrum of each sample and compared it to the spectra of the individual compounds (Supplementary Figure 1.1). A previously established kinetic model (Yuen and Sokoloski, 1977), extended to account for the loss of the degradation products at very long timescales, was fully consistent with the spectral data (Figure 1.1c; Methods and Supplementary Figs. 1.2-1.4).

Figure 1.1. Tetracycline degrades into a range of longer lived compounds, with potential ecological impacts on selection for resistance. a, While an antibiotic selects for strains resistant to it, it is not clear what selective pressure is imposed by its soup of degradation products. **b**, Tetracycline degrades into a range of bioactive compounds, which themselves slowly decay further. **c**, Tetracycline decay products have different concentration profiles through time. Degradation is accelerated by pH of 1.5 and temperature of 75°C (Yuen and Sokoloski, 1977). Shaded areas in this stacked plot represent the kinetic model of (Yuen and Sokoloski, 1977) with a correction for long-term decay (Methods). Points are estimated fractions of Tet and its degradation products, obtained by fitting the spectra of pure compounds to a spectrum of the degraded Tet solution at each individual timepoint (Methods). ATC and EATC are not well distinguished spectrally, and so are plotted as their sum. These fitted points confirm the consistency of our samples with the kinetic model of (Yuen and Sokoloski, 1977).
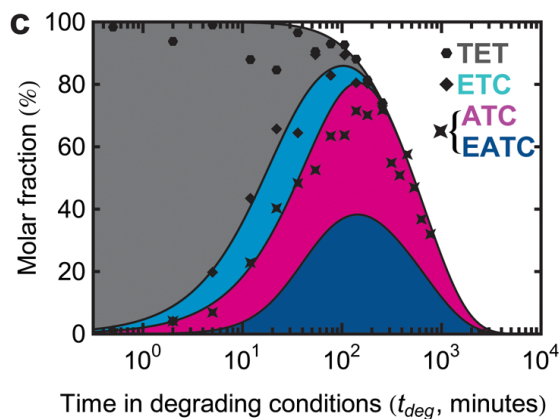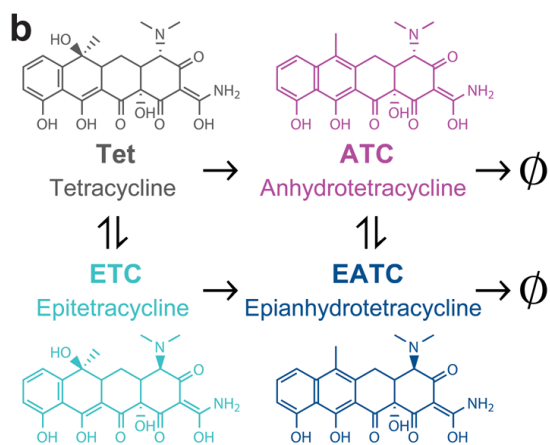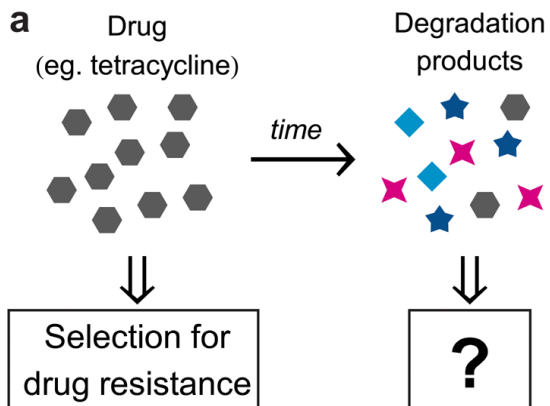
Figure 1.1. Tetracycline degrades into a range of longer lived compounds, with potential ecological impacts on selection for resistance. (Continued)

To measure the selective pressure for tetracycline resistance imposed by samples of Tet that had been exposed to degrading conditions for different times, we used a fluorescence-based competition assay between resistant and sensitive *E. coli* (Chait et al., 2007; Hegreness et al., 2006). Matching Tet resistant (Tet[R]) and sensitive (Tet[S]) strains were generated by supplying MG1655 with a plasmid carrying the *tetR-tetA* genes from the Tn10 transposon, or with the non-resistant parental plasmid, respectively (Lenski et al., 1994). These Tet[S] and Tet[R] strains were differentially labeled with chromosomally encoded cyan and yellow fluorescent proteins; pairs of strains were constructed in both dye permutations. Direct competition between the strains, as well as high-resolution measurements of their individual growth rates (Kishony and Leibler, 2003; Yeh et al., 2006), showed equal fitness of the Tet[S] and Tet[R] strains in the absence of Tet (Supplementary Figure 1.5). To measure selection for or against resistance, Tet[S] and Tet[R] strains were mixed 1:1 in fresh media, a sample of untreated or degraded Tet was added, and the cultures were grown overnight to stationary phase; the final ratio of sensitive cell count ($N_{\text{Tet}}{}^{S}$) to resistant cell count ($N_{\text{Tet}}{}^{R}$) was then measured by flow cytometry (Figure 1.2a).

While Tet strongly selects in favor of resistance, we found that its cocktail of degradation products actually shows selection in favor of sensitivity (Figure 1.2c,d, trajectory 1). Solutions of Tet with little or no exposure to degrading conditions ($t_{deg} <$ ~50 min), applied at high concentrations (1000 ng/mL), strongly favored the growth of resistant bacteria. However, following substantial degradation ($t_{deg} >$ ~50 min), not only did the loss of Tet abolish selection for resistance, but the accumulation of its degradation products caused strong

6

selection against resistance (Figure 1.2c,d, change from red to green along trajectory 1; similar results are seen with chromosomally-integrated tetracycline resistance, in the presence of the naturally occurring compound fusaric acid, Supplementary Figure 1.6). Importantly, while the initial selection in favor of resistance was short lived, the subsequent selection in favor of sensitivity lasted for much longer times, and had not weakened much even at the latest time point of t_{deg}~450 min.

We consider the full ecological impact of an antibiotic as the selective pressure of the antibiotic and its degradation products integrated over time. This integrated selective pressure is represented by the area between the curve of the fold changes in $\log(N_{\text{Tet}}^{S} / N_{\text{Tet}}^{R})$ and the line $\log(N_{\text{Tet}}^{S} / N_{\text{Tet}}^{R}) = 0$ (no selection) (Figure 1.2d). When degradation is the primary means of loss (trajectory 1), the initial selection for resistance by Tet is greatly outweighed by the subsequent longer selection against resistance by more stable degradation products (Figure 1.1c).

In a natural scenario, an initial drug dosage may not only be lost due to degradation, but also due to dilution, or diffusion (Figure 1.2b). To account for dilution in addition to degradation, we applied our Tet^{R}-Tet^{S} competition assay across a 2D gradient created by serial dilution of each of the time samples of the degradation reaction (Figure 1.2c). Dilution of the drug and its degradation products can profoundly affect the overall selection pressure: if Tet loss is dominated by dilution, degradation products do not appear at substantial concentration and so the selective pressure of the initial compound, Tet, is dominant, favoring resistance (Figure

1.2c,d, trajectory 3). In these conditions the net selection is in favor of resistance, demonstrating that dilution can eliminate the ability of degradation products to invert the selective pressure. Tet clearance in the clinical setting and in treatment of farm animals is dominated by dilution rather than degradation (Kelly and Buyske, 1960), consistent with the selective advantage of resistance in these settings (Levy et al., 1976).

More generally, we envision that in the environment a drug may be lost simultaneously by both degradation and dilution. An environment initially containing a fixed dose of Tet will then move through different chemical environments along a linear trajectory across Figure 1.2c, with a slope defined by the ratio between the dilution rate and the degradation rate ($-\lambda_{dil}/\lambda_{deg}$, where λ_{dil}, λ_{deg} are the reciprocals of the drug's half-life due to dilution and degradation, respectively). We find that when both degradation and dilution are active, selective pressure can vary over time in a complex non-monotonic manner. For example, in trajectory 2 (Figure 1.2c,d), the initial selection in favor of resistance is followed by selection against resistance, but then at low concentrations of degradation products weak selection in favor of resistance returns. Since degradation products select in opposing directions depending upon their concentration, net selection depends non-trivially upon both the means of loss and the initial concentration of antibiotic (Supplementary Figure 1.7).

We next asked to what extent these complex trajectories of selective effects, exerted throughout Tet decay, can be rationalized in terms of the individual selective pressures exerted by the drug and each of its degradation products. We measured the effect on the Tet[S]-

Tet[R] competition imposed by Tet, ETC, ATC and EATC as a function of concentration (Supplementary Figure 1.8). We found that each of the degradation products has a different selective impact and that selection against resistance is mediated by ATC. This observation is consistent with the known action of ATC as a strong inducer of the costly tet operon (Eckert and Beck, 1989; Lederer et al., 1996) and adds to the growing evidence of signaling roles for antibiotics (Goh et al., 2002; Linares et al., 2006; Yim et al., 2007). In principle, 'non-additive' interactions may be present in drug combinations, producing effects not explainable by the sum of individual drug effects. We adopt the Bliss definition of additivity, where the effect of drugs in combination is equal to the multiplication of their individual effects (Bliss, 1939). To test for non-additive drug interactions, we measured selective pressures across a 2D gradient of Tet vs. a 1:1 mixture of ATC and EATC, chosen to approximately represent the chemical environments encountered following Tet decay (the epimerization is a relatively fast reaction leading to nearly equal amounts of ATC and EATC at late times, Figure 1.1c). We found that Bliss additivity reproduced all features of the measured 2D gradient, with quantitative deviations only at high drug concentrations, suggesting that interactions amongst Tet and the decay products ATC and EATC are primarily additive (Supplementary Figure 1.9).

An additive model of the selective pressures throughout Tet degradation and dilution was then constructed from the kinetic model of chemical composition (Figure 1.1c, Supplementary Figure 1.3) and the selective effects of each of the individual compounds (Supplementary Figure 1.8). This additive model shows very good qualitative and quantitative agreement with the measured selective pressures along trajectories 1, 2 and 3 (Figure 1.2d,

compare dashed line with filled area). Selection by Tet and its degradation products can therefore be understood as the additive sum of the effects of each of the compounds.

Figure 1.2. Tetracycline degradation inverts the overall selective advantage of resistant strains. a, To measure selection for/against resistance by degraded tetracycline solution, a sample of the degradation reaction is taken at timepoint t_{deg} and is added to a 1:1 mixture of resistant (Tet^R) and sensitive (Tet^S) cells inoculated into fresh media. Fluorescent labels (YFP or CFP) allow changes in the ratio $N_{Tet}{}^S$ / $N_{Tet}{}^R$ to be measured by flow cytometry, after overnight competition. **b**, Loss of the initial drug can occur by either degradation to alternate compounds (across x-axis), or by dilution (down y-axis). **c**, Selective pressure in favor (red) or against (green) resistance as a function of the degradation time t_{deg} and dilution (axes definitions match panel b). Black points mark measurements, between which the color map is interpolated. Numbered black lines are trajectories representing Tet loss by degradation alone (1), dilution alone (3), or a combination of both with respective rates λ_{deg} and λ_{dil} (2). **d**, Selective pressure changes over time as Tet is lost along the three trajectories of panel c. Shaded areas represent the integrated selective pressure in favor (red) or against (green) resistance. The time axis is normalized by net rate of Tet loss (λ_{deg} + λ_{dil}). Dotted black lines are an additive model of selective pressure, constructed by summing the changes in log($N_{Tet}{}^S$ / $N_{Tet}{}^R$) produced by each of the individual compounds (Supplementary Figure 1.8), given their concentrations from the kinetic model of Tet decay (Figure 1.1c).
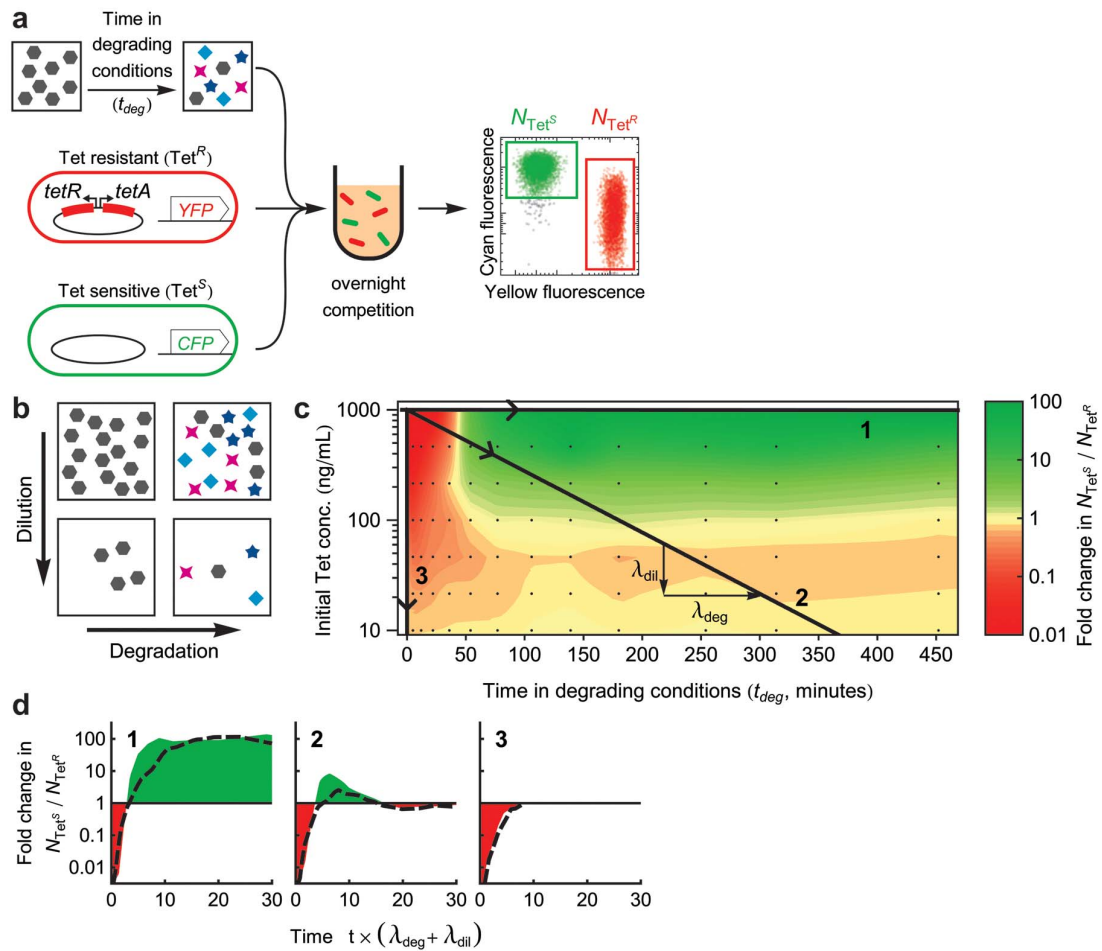
Figure 1.2. Tetracycline degradation inverts the overall selective advantage of resistant strains. (Continued)

In the natural environment, antibiotics are not static - a single drug can decay into a range of compounds, each accumulating and degrading with different kinetics and displaying different selective effects. The simple additive sum of the effects of each of the degradation products can lead to complex, non-monotonic, patterns of selections for and against resistance. Consequently, the net evolutionary impact of a drug depends upon the manner of its eventual loss from the environment. When Tet loss is dominated by degradation, the initial selection for resistance by tetracycline can be substantially outbalanced by the prolonged selection against resistance imposed by its longer lived degradation products. While these results were demonstrated for accelerated degradation of tetracycline, they depend on relative, rather than absolute, stabilities of the drug and its degradation products, and therefore may be of relevance also to the natural environment. Interestingly, ATC is a biosynthetic precursor to Tet in the drug producing microbes (McCormick et al., 1968), and induces Tet efflux pump expression prior to the imminent production of the drug. This provides an evolutionary rationale for non-toxic drug derivatives to be potent inducers of resistant genes. It will be interesting to test the selective effect of decay of other drugs on various resistance mechanisms and via multiple decay pathways; different decay pathways will produce different metabolites, which could be affected by the environment and even by other surrounding microbes (Dantas et al., 2008). Selection against resistance by antibiotic decay may help explain the puzzling coexistence of antibiotic resistant and sensitive microbial strains in the natural soil environment.

Acknowledgements

Author Contributions

A.C.P., E.A. and R.K. designed research; A.C.P. performed research and analyzed data; A.C.P. and R.K. wrote the manuscript.

Methods

Strains and Media

Fluorescently labeled strains MC4100-YFP and MC4100-CFP, described previously(Hegreness et al., 2006), were transformed with plasmid pBT107-6A to create a Tet resistant strain, or with the parent plasmid pACYC177 to create a Tet sensitive strain. pBT107-6A carries the Tn10 tetracycline resistance determinant, with a *tetA* promoter down-mutation which has been demonstrated to provide higher fitness in the presence of 10 μg.mL^{-1} Tet than either stronger or weaker promoters(Daniels and Bertrand, 1985; Lenski et al., 1994).

All fitness measurements were performed in M63 minimal medium (2 g.L^{-1} (NH$_4$)$_2$SO$_4$, 13.6 g.L^{-1} KH$_2$PO$_4$, 0.5 mg.L^{-1} FeSO$_4$•7H$_2$O) supplemented with 0.2% glucose, 0.1% casamino acids, 1mM MgSO$_4$ and 1.5 μM thiamine, and also 100 μg.mL^{-1} ampicillin and 50 μg.mL^{-1} kanamycin for the maintenance of pACYC177 based plasmids. Drug solutions were made from powder stocks (Sigma, Vetranal analytical standard: tetracycline hydrochloride, #3174; epitetracycline hydrochloride, #37918; anhydrotetracycline hydrochloride, #37919; epianhydrotetracycline hydrochloride, #37921) dissolved in ethanol, with drug gradients made by serial dilution in M63 medium.

Tetracycline degradation

Powdered tetracycline was dissolved in 1M phosphoric acid, pH 1.5, at 400µg/mL. Aliquots were incubated at 75°C and transferred to ice at various time points. These frozen samples were diluted 40× into M63 media for fitness assay, or into water for spectroscopy.

Spectroscopy and determination of chemical composition from spectra

All spectra were recorded at 10 µg/mL in aqueous solution, on a Cary 300 spectrophotometer (Varian). The kinetic model of (Yuen and Sokoloski, 1977), modified to include a reaction for the slow further decay of Tet degradation products with rate constant k_{loss}, successfully fitted the time series of spectra (Supplementary Figs. 2, 3) using all other rate constants as previously measured by HPLC (Yuen and Sokoloski, 1977). Allowing all rate constants to be simultaneously fitted to all spectra produces only a 2% reduction in the sum of square errors; the previously measured parameters have values that minimize errors in the spectral alignment, for all parameters for which a well defined minimum exists (Supplementary Figure 1.4, Supplementary Table 1.1). Species concentrations were estimated from spectra at individual timepoints (points in Figure 1.1c) by numerically searching for the local minimum in alignment error over the characteristic wavelength ranges 250-290nm and 325-400nm, starting from the composition predicted by the kinetic model; numerical minimization was performed by the FindMinimum function of *Mathematica 7.0* (Wolfram).

Competitive fitness assay

Selection between resistant and sensitive cells by a particular chemical environment was measured by mixing stationary phase cultures of resistant and sensitive strains at 1:1 ratio, and further diluting 1:100 into fresh media containing the chemical environment of interest. Competitive growth occurred throughout 24 hours of growth with shaking at 30°C in clear, flat bottomed 96-well plates (Corning #3595), sealed with adhesive lids (Perkin Elmer #6005185). Sensitive and resistant cells were differentially labeled with a chromosomally integrated YFP or CFP gene driven by the P_{lac} promoter, which is constitutive in the *lacI* strains used here. To obtain stronger fluorescence signals, the stationary phase cultures obtained after 24 hours of competition were subcultured 1:100 into fresh drug-free media, and grown as before for between 90 and 180 minutes, before the ratio of yellow to cyan fluorescent cells was counted by flow cytometry (Becton Dickinson LSRII; CFP excited at 405nm, emission detected through 505LP and 525/550nm filters; YFP excited at 488nm, emission also detected through 505LP and 525/550nm filters). Plating and colony counting of selected wells confirmed that the final subculturing and brief growth did not alter the ratio $N_{Tet}^{S} / N_{Tet}^{R}$, within the margin of error of counting 200 - 500 colonies per plate. The selective pressures presented in Figure 1.2c and Supplementary Figure 1.8 are the average of two experiments, one where fluorescent labels were swapped between Tet^{S} and Tet^{R} strains. No substantial difference was detected between dye-swaps, indicating that the use of differential dyes does not influence $N_{Tet}^{S} / N_{Tet}^{R}$ ratio (Supplementary Figure 1.10). At least 16 wells per plate were drug-free, for precise measurement of $N_{Tet}^{S} / N_{Tet}^{R}$ ratio in non-selective conditions.

The mean ratio N_{Tet}^S / N_{Tet}^R (mean determined on log scale) in these drug-free wells provided the reference point, determined separately for each plate, for the fold change in N_{Tet}^S / N_{Tet}^R. For Supplementary Figure 1.6, fusaric acid was applied uniformly across the plate, including reference wells, such that any selection (changes in N_{Tet}^S / N_{Tet}^R) due solely to fusaric acid is removed in the normalization to reference wells. Thus, the selective effects seen in Supplementary Figure 1.6 are due to tetracycline and its degradation products, or drug-drug interactions between these compounds and fusaric acid. Sample flow cytometry data from three points in Figure 1.2c are presented in Supplementary Figure 1.11, demonstrating selection for, against, and neutral with respect to resistance.

Growth rate assay

Tet^S and Tet^R strains were transformed with a plasmid-borne, constitutively expressed bacterial bioluminescence operon(Kishony and Leibler, 2003). Photon counting of growing bioluminescent cultures allows precise measurements of cell densities over many orders of magnitudes (e.g. Supplementary Figure 1.5). Cultured were grown in black 96-well plates (Corning #3792) sealed with clear adhesive lids (Perkin Elmer #6005185). Readings were made by a Perkin Elmer TopCount NXT Microplate Scintillation and Luminescence Counter, stored in a 30°C room at 70% humidity, with duplicate 1 second readings per well. Wells contained 100μL of media inoculated with approximately 10 to 100 cells from fresh -80°C frozen cultures. Growth rate is the slope of the logarithm of photon counts per second (c.p.s.), and is taken from the line of best fit spanning the fastest 5 doublings.

References

Bliss, C.I. (1939). The toxicity of poisons applied jointly. Ann Appl Biol *26*, 585-615.

Bochner, B.R., Huang, H.C., Schieven, G.L., and Ames, B.N. (1980). Positive selection for loss of tetracycline resistance. J Bacteriol *143*, 926-933.

Chait, R., Craney, A., and Kishony, R. (2007). Antibiotic interactions that select against resistance. Nature *446*, 668--671.

Chopra, I., Hawkey, P.M., and Hinton, M. (1992). Tetracyclines, molecular and clinical aspects. J Antimicrob Chemother *29*, 245-277.

D'Costa, V.M., McGrann, K.M., Hughes, D.W., and Wright, G.D. (2006). Sampling the antibiotic resistome. Science *311*, 374--377.

Daniels, D.W., and Bertrand, K.P. (1985). Promoter mutations affecting divergent transcription in the Tn10 tetracycline resistance determinant. J Mol Biol *184*, 599--610.

Dantas, G., Sommer, M.O., Oluwasegun, R.D., and Church, G.M. (2008). Bacteria subsisting on antibiotics. Science *320*, 100-103.

Eckert, B., and Beck, C.F. (1989). Overproduction of transposon Tn10-encoded tetracycline resistance protein results in cell death and loss of membrane potential. J Bacteriol *171*, 3557--3559.

Fajardo, A., and Martinez, J.L. (2008). Antibiotics as signals that trigger specific bacterial responses. Curr Opin Microbiol *11*, 161-167.

Goh, E.B., Yim, G., Tsui, W., McClure, J., Surette, M.G., and Davies, J. (2002). Transcriptional modulation of bacterial gene expression by subinhibitory concentrations of antibiotics. Proc Natl Acad Sci U S A *99*, 17025-17030.

Halling-Sorensen, B., Sengelov, G., and Tjornelund, J. (2002). Toxicity of tetracyclines and tetracycline degradation products to environmentally relevant bacteria, including selected tetracycline-resistant bacteria. Arch Environ Contam Toxicol *42*, 263-271.

Hegreness, M., Shoresh, N., Hartl, D., and Kishony, R. (2006). An equivalence principle for the incorporation of favorable mutations in asexual populations. Science *311*, 1615--1617.

Jia, A., Xiao, Y., Hu, J., Asami, M., and Kunikane, S. (2009). Simultaneous determination of tetracyclines and their degradation products in environmental waters by liquid chromatography-electrospray tandem mass spectrometry. J Chromatogr A *1216*, 4655-4662.

Kelly, R.G., and Buyske, D.A. (1960). Metabolism of tetracycline in the rat and the dog. J Pharmacol Exp Ther *130*, 144-149.

Kieser, T., Bibb, M.J., Buttner, M.J., Chater, K.F., and Hopwood, D.A. (2000). Practical Streptomyces Genetics, 1st edn (John Innes Foundation, Norwich, UK).

Kishony, R., and Leibler, S. (2003). Environmental stresses can alleviate the average deleterious effect of mutations. J Biol *2*, 14.

Lederer, T., Kintrup, M., Takahashi, M., Sum, P.E., Ellestad, G.A., and Hillen, W. (1996). Tetracycline analogs affecting binding to Tn10-Encoded Tet repressor trigger the same mechanism of induction. Biochemistry *35*, 7439--7446.

Lenski, R.E., Souza, V., Duong, L.P., Phan, Q.G., Nguyen, T.N., and Bertrand, K.P. (1994). Epistatic effects of promoter and repressor functions of the Tn10 tetracycline-resistance operon of the fitness of Escherichia coli. Mol Ecol *3*, 127--135.

Levy, S.B., FitzGerald, G.B., and Macone, A.B. (1976). Changes in intestinal flora of farm personnel after introduction of a tetracycline-supplemented feed on a farm. N Engl J Med *295*, 583--588.

Linares, J.F., Gustafsson, I., Baquero, F., and Martinez, J.L. (2006). Antibiotics as intermicrobial signaling agents instead of weapons. Proc Natl Acad Sci U S A *103*, 19484-19489.

McCormick, J.R., Jensen, E.R., Johnson, S., and Sjolander, N.O. (1968). Biosynthesis of the tetracyclines. IX. 4-Aminodedimethylaminoanhydrodemethylchlortetracycline from a mutant of Streptomyces aureofaciens. J Am Chem Soc *90*, 2201-2202.

Moyed, H.S., Nguyen, T.T., and Bertrand, K.P. (1983). Multicopy Tn10 tet plasmids confer sensitivity to induction of tet gene expression. J Bacteriol *155*, 549--556.

Nguyen, T.N., Phan, Q.G., Duong, L.P., Bertrand, K.P., and Lenski, R.E. (1989). Effects of carriage and expression of the Tn10 tetracycline-resistance operon on the fitness of Escherichia coli K12. Mol Biol Evol *6*, 213--225.

Price-Whelan, A., Dietrich, L.E., and Newman, D.K. (2006). Rethinking 'secondary' metabolism: physiological roles for phenazine antibiotics. Nat Chem Biol *2*, 71-78.

Sarmah, A.K., Meyer, M.T., and Boxall, A.B. (2006). A global perspective on the use, sales, exposure pathways, occurrence, fate and effects of veterinary antibiotics (VAs) in the environment. Chemosphere *65*, 725-759.

Walsh, C. (2003). Antibiotics : actions, origins, resistance (Washington, D.C.: ASM Press).

Walton, V.C., Howlett, M.R., and Selzer, G.B. (1970). Anhydrotetracycline and 4-epianhydrotetracycline in market tetracyclines and aged tetracycline products. J Pharm Sci *59*, 1160-1164.

Yeh, P., Tschumi, A.I., and Kishony, R. (2006). Functional classification of drugs by properties of their pairwise interactions. Nat Genet *38*, 489--494.

Yim, G., Wang, H.H., and Davies, J. (2007). Antibiotics as signalling molecules. Philos Trans R Soc Lond B Biol Sci *362*, 1195-1200.

Yuen, P.H., and Sokoloski, T.D. (1977). Kinetics of concomitant degradation of tetracycline to epitetracycline, anhydrotetracycline, and epianhydrotetracycline in acid phosphate solution. J Pharm Sci *66*, 1648--1650.

Chapter 2.

A multi-peaked adaptive landscape arising from high-order genetic interactions

Adam C. Palmer[1,¶], Erdal Toprak[1, 2, ¶], Seungsoo Kim[3], Adrian Veres[3], Shimon Bershtein[4],

Roy Kishony[1,5]

[1]Department of Systems Biology, Harvard Medical School, 200 Longwood Ave, Boston, MA 02115.

[2]Faculty of Engineering and Natural Sciences, Sabanci University, Istanbul, Turkey

[3]Faculty of Arts and Sciences, Harvard University, Cambridge, MA 02138.

[4]Department of Chemistry and Chemical Biology, Harvard University, Cambridge, MA 02138.

[5]School of Engineering and Applied Sciences, Harvard University, Cambridge, MA 02138.

[¶]These authors contributed equally to this work.

Multiple sets of mutations can arise under antibiotic selection, all producing strongly drug-resistant genotypes. We investigated the genetic interactions that separate adaptive peaks, by constructing and characterizing all combinatorial sets of trimethoprim resistance-conferring mutations in the *DHFR* gene, drawn from the results of parallel evolution experiments. The resulting adaptive landscape is almost maximally rugged, with direct and indirect evolutionary trajectories leading to multiple distinct peaks. Pairwise interactions could not explain the existence of multiple peaks, but rather, high-order genetic interactions were

responsible for a rugged and multi-peaked adaptive landscape. One mutation could profoundly influence the course of evolution: its presence or absence strongly altered the ruggedness or smoothness of the adaptive landscape. High-order genetic interactions constrain but do not confound the evolution of antibiotic resistance: evolution can always find a way to a highly drug-resistant genotype.

Antibiotic resistance can evolve through the sequential accumulation of multiple resistance-conferring mutations in a single gene (Lozovsky et al., 2009; Toprak et al., 2012; Weinreich et al., 2006). These evolutionary pathways have been studied by examining the feasibility of all possible genotypic transitions leading from the ancestor to the evolved drug resistant genotype. Across different experimental systems, these studies have observed that only a limited number of pathways lead to a single adaptive genotype (Lozovsky et al., 2009; Weinreich et al., 2006). However, since these studies examined sets of mutations drawn from a single adaptive genotype, it is known *a priori* that it is ultimately beneficial to acquire all mutations, even though the sequence of acquisition may be constrained. However, in a recent laboratory evolution experiment where five isogenic, drug-sensitive *Escherichia coli* populations were evolved in parallel under dynamically sustained trimethoprim selection, multiple distinct genotypes that shared similar drug resistant phenotypes were observed (Toprak et al., 2012). Across all replicate experiments a total of six types of mutations were observed in the dihydrofolate reductase (*DHFR*) gene (five amino acids were mutated and the *DHFR* promoter was mutated), but each evolving population accumulated a total of four of these mutations. Furthermore, the evolutionary trajectories had significant similarities: of five drug-adapted cultures, there were two pairs of genotypes that contained the same set of mutated residues. This observation suggests that some combinations of mutations were superior to others, and yet the different final adaptive genotypes reached remarkably similar levels of trimethoprim resistance. We sought to understand the nature of the genotypic landscape that produces multiple adaptive genotypes sharing a common drug-resistant phenotype.

To map genotype to phenotype, we constructed and characterized all combinatorial sets of the six types of trimethoprim resistance-conferring mutations previously observed in *DHFR* (Toprak et al., 2012). We studied the effects of one promoter mutation (-35C>T, position indicated relative to the transcription start site) and five mutated amino acids; one site had been observed to have two different amino acid changes in different adaptive genotypes, making for six mutations in total: P21L, A26T, L28R, W30G, W30R, and I94L (Figure 2.1a). All combinations amounted to 96 possible variants of *DHFR* ($2^5 \times 3^1$), which were synthesized and recombined into the *E.coli* chomosome in place of the wildtype *DHFR* gene (Methods) (Bershtein et al., 2012; Datsenko and Wanner, 2000). We were unable to generate 6 mutant strains out of 96 despite repeated attempts; we hypothesize that these particular combinations of mutations in an essential gene may be unviable (Supplementary Figure 2.1). The trimethoprim resistance of the mutant strains was quantified by measuring all strains' growth rates across a gradient of trimethoprim concentrations (Figure 2.1b and Supplementary Figure 2.1). Each mutant strain was characterized by two parameters derived from these measurements: r_0 is the growth rate in the absence of drug, and IC50 is the trimethoprim concentration that inhibits growth to 50% of the uninhibited wildtype growth rate ($r_0^{WT}/2$) (Figure 2.1c). From this network of genotypes and their associated growth rates in trimethoprim we assembled the adaptive landscape of trimethoprim resistance (Figure 2.1d). Amongst each set of genotypes with the same overall number of mutations, a wide distribution in trimethoprim resistance was observed. Although each mutation conferred significantly increased trimethoprim resistance when acquired on a wildtype background, many combinations of two to five mutations generated approximately wildtype susceptibility

to trimethoprim. This indicates the presence of strong genetic interactions, in particular 'sign epistasis', where a mutation that is beneficial when it arises on one genetic background is deleterious when acquired on a different genetic background.

Figure 2.1. Synthetic construction and phenotyping of all combinations of seven trimethoprim resistance mutations. a, Trimethoprim resistance can be conferred by any of seven different mutations in the target of trimethoprim, *DHFR*. Each combination of these mutations was synthesized and recombined into the *E.coli DHFR* gene. **b**, The growth rate of each mutant strain was measured in liquid cultures spanning a range of trimethoprim (TMP) concentrations. Growth rate is the slope of a linear fit to $\log(OD_{600})$ over time (gray lines). **c**, Fitness costs of mutations are measured by the growth rate in the absence of trimethoprim (r_0). The trimethoprim concentration that inhibits growth to 50% of the wildtype growth rate (IC50) is the intersection of the inhibition curve with the horizontal line where growth rate = $r_0^{WT} / 2$. The growth rates marked by squares (no drug) and triangles (11 µg/mL TMP) are derived from the growing cultures shown in Figure 2.1b. **d**, Mutant strains are distributed in rows sorted by number of mutations. Each mutant's genotype is represented by colored circles atop a column (see colors in Figure 2.1a) whose height is proportional to the trimethoprim resistance (IC50) of that genotype. Each gain of mutation throughout the network of genotypes is shown as a line colored by the mutation gained; the series of thick lines starting at wildtype are adaptive trajectories observed in a long-term evolution experiment (Toprak et al., 2012). The trimethoprim resistance of the wildtype strain and each single mutant is shown in a vertically enlarged box for contrast.
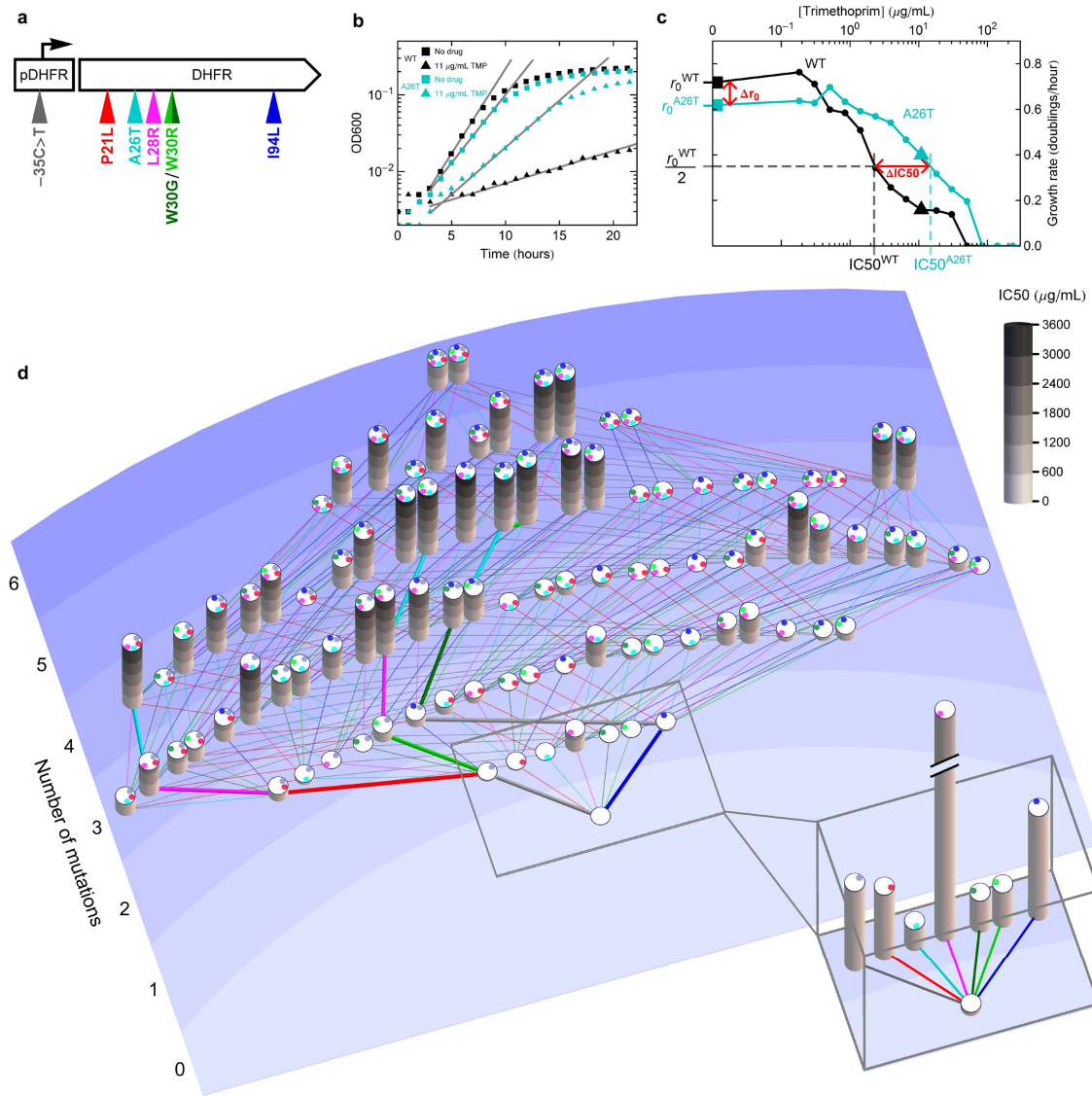
Figure 2.1. Synthetic construction and phenotyping of all combinations of seven trimethoprim resistance mutations. (Continued)

We investigated the prevalence of fitness costs in the evolution of trimethoprim resistance by determining the correlation between growth rates in the absence of drug (r_0) and either the number of mutations, or the level of trimethoprim resistance (IC50) (Figure 2.2). While the fitness r_0 declined with an increasing number of mutations ($r = -0.41$, $P<10^{-4}$), there was no correlation between fitness and IC50 ($r = -0.02$ against $\log$(IC50), $P = 0.8$). Indeed, many combinations of mutations produced high trimethoprim resistance with no significant fitness cost, and some other combinations of mutations were not particularly resistant but did incur large costs to fitness. Thus, while drug resistance mutations may compromise native protein function and incur fitness costs, such fitness costs are not an inevitable consequence of drug resistance, because selected combinations of mutations can ameliorate one another's deleterious effects and compensate for fitness costs. These observations in *E.coli* are consistent with a previous study of the evolution of pyrimethamine resistance through multiple mutations in the dihydrofolate reductase gene of *Plasmodium falciparum* (Brown et al., 2010).

Figure 2.2. Though the accumulation of resistance mutations on average incurs fitness costs, genotypes exist with high resistance and no cost. **a**, Fitness costs of mutations are assessed by the growth rate in the absence of trimethoprim, and are seen to gradually accrue with increasing numbers of mutations. Each point is a genotype positioned by its number of mutations and drug-free growth rate; points are color coded green to blue by the number of mutations, and a small horizontal scatter is added to improve the visibility of overlapping data. **b**, Each point is a genotype positioned by its trimethoprim resistance (IC50) and drug-free growth rate (no added scatter), color coded by the same scheme as Figure 2.2a. Because of the existence of highly resistant genotypes with no fitness cost, and also weakly resistant genotypes with significant fitness costs, IC50 does not correlate negatively or positively with growth rate in the absence of trimethoprim.
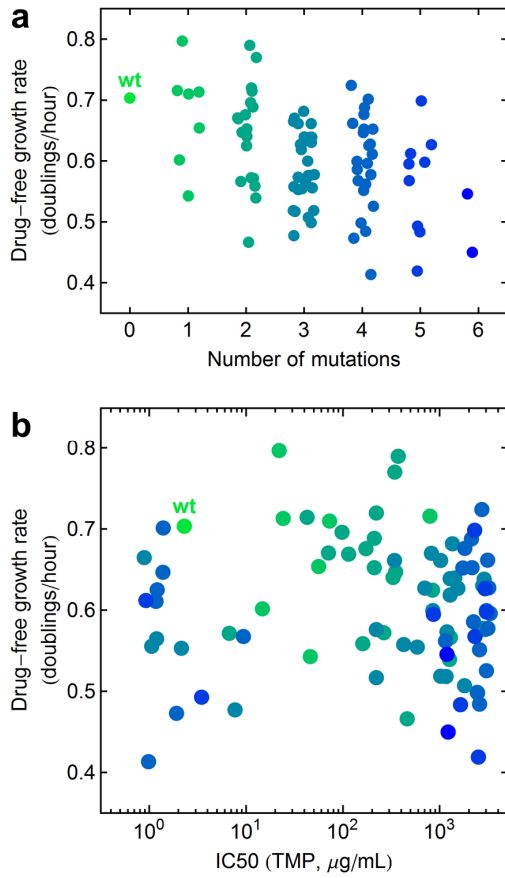
Figure 2.2. Though the accumulation of resistance mutations on average incurs fitness costs, genotypes exist with high resistance and no cost. (Continued)

We examined how evolving populations might move through this landscape by evaluating all possible adaptive trajectories. We find 423 possible trajectories along which new mutations may be gained, previously acquired mutations may be lost, or an existing mutation can convert to a different (non-ancestral) mutation at the same locus; this latter option is possible at W30 where two different drug resistance alleles were observed in evolutionary experiments (Toprak et al., 2012). Every step in these 423 trajectories continuously improves IC50; neither drift nor transient decreases in resistance are permitted, and so they terminate at locally adaptive peaks. Examining the mutations that are acquired, and possibly lost, along these trajectories, we find that only the promoter mutation (−35C>T) is always acquired, and all but one of the amino acid changing mutations has some probability of being acquired and subsequently lost or converted in the process of adaption to trimethoprim (Figure 2.3a). These instances of mutational reversions must arise from sign epistasis, and demonstrate that strong negative genetic interactions produce a landscape on which both direct and indirect paths can be taken to adaptive peaks. These observations are supported by the observation of indirect adaptive trajectories in the experimental evolution studies that identified this set of mutations (Toprak et al., 2012), and are consistent with the fitness landscape of the TEM-1 β-lactamase which also produces indirect adaptive trajectories (DePristo et al., 2007).

It is unclear whether evolutionary trajectories in a rugged, multi-peaked adaptive landscape are guaranteed to find a path to a highly adaptive peak, or whether evolution might be trapped at local optima (Poelwijk et al., 2007). The rugged and multi-peaked landscape of trimethoprim resistance through mutations in *DHFR* allows us to address this question. For

each genotype we asked what is the most advantageous step (best change in IC50) accessible from that genotype? Genotypes have neighbours that are accessible by gaining, losing, or converting a mutation; for example, a genotype with four mutations (Figure 2.3b, pillar at center) can make seven possible genetic changes, including two gains of mutation, four losses of mutation, and possibly a conversion of a mutation. In the example in Figure 2.3b, only two changes can improve trimethoprim resistance: either loss of P21L or conversion of W30G to W30R, with the latter being the most advantageous step. The best possible improvement in IC50 from each genotype is plotted as a function of that genotype's initial IC50 (Figure 2.3c, black points), and when the best step is not to gain a mutation, we also show what the best step would be if only the gain of mutations was permitted (Figure 2.3c, orange points show best possible gain when this is an inferior option to a loss or conversion). We found that the best possible steps starting from low resistance were very large, and with increasing levels of initial resistance, the best possible steps became smaller in proportion to the reduced difference between the initial IC50 and the largest observed IC50. Any genotype where the best possible step is negative is a local optima within this set of mutations, since no further change in genotype can improve resistance - it is these points that may reveal the existence of 'evolutionary dead-ends'. This landscape contained seven adaptive peaks, all carrying 4 mutations, where no further gain, loss or conversion of mutations could improve resistance (Figure 2.3c, blue points). These genotypes can be thought of as three truly distinct peaks: two genotypes that are not neighbours of any other peaks (Figure 2.3d, two genotypes to far right), and a set of five genotypes that are connected by almost neutral drift through two other genotypes that carry 5 mutations (Figure 2.3d, connected set of genotypes). At many

genotypes the best possible *gain* of a new mutation confers less improvement in resistance than is possible by loss or conversion of a previously held mutation. In particular, many of these genotypes would be a local optimum if there were not advantageous steps out of these states through the loss or conversion of mutations. Thus, this adaptive landscape would be difficult to navigate by only gaining mutations: evolutionary trajectories could be trapped by many local optima, but these evolutionary 'dead-ends' are escaped by beneficial losses or conversions of mutations. Strong genetic interactions are thus the antidote to their own poison: sign epistasis can give rise to genotypes where the further gain of usually beneficial mutations is instead deleterious, but sign epistasis also acts upon previously acquired and previously beneficial mutations to make their loss or conversion a beneficial step facilitating continued adaptation.

Figure 2.3. Conversion and reversions bypass evolutionary dead ends, guaranteeing a path to reach one of several highly adaptive peaks. a, Simulated evolutionary trajectories over the adaptive landscape of *DHFR* (Figure 2.1d) show that when evolving trimethoprim resistance, it can be advantageous to lose a previously acquired 'resistance' mutation. **b**, Genotypes can change by the gain, loss, or conversion of mutations. Starting from the genotype encircled in black, the best possible improvement in IC50 is shown as a black arrow. Alternatively, one can evaluate the accessibility of the landscape if only the gain of new mutations is permitted; the best gain of mutation is shown as an orange arrow, which in this example lowers resistance. **c**, Determining the best possible improvement in IC50 shows that significant steps towards the maximum trimethoprim resistance are possible from all genotypes, provided that gain, loss, or conversion of mutations are permitted (black points). For genotypes where the best step is a loss or conversion of a mutation, the inferior option presented by only gaining new mutations is shown in orange. Orange points within the gray zone (below '×1' change in IC50) would be local optima, where an evolving population could be trapped at intermediate trimethoprim resistance, if it were not for escape by the loss or conversion of mutations. True peaks (blue points) are genotypes where no further gain, loss, or conversion of mutations can improve IC50. **d**, Seven genotypes each with 4 mutations are adaptive peaks. Five of these can be conceived of as a single 'adaptive plateau' (genotypes on left side) since they are connected through almost neutral transitions to two genotypes with 5 mutations (colored lines indicate the mutations gained or lost in these transitions). No pair of mutated sites is intrinsically incompatible - every possible pair co-exists in an adaptive peak.
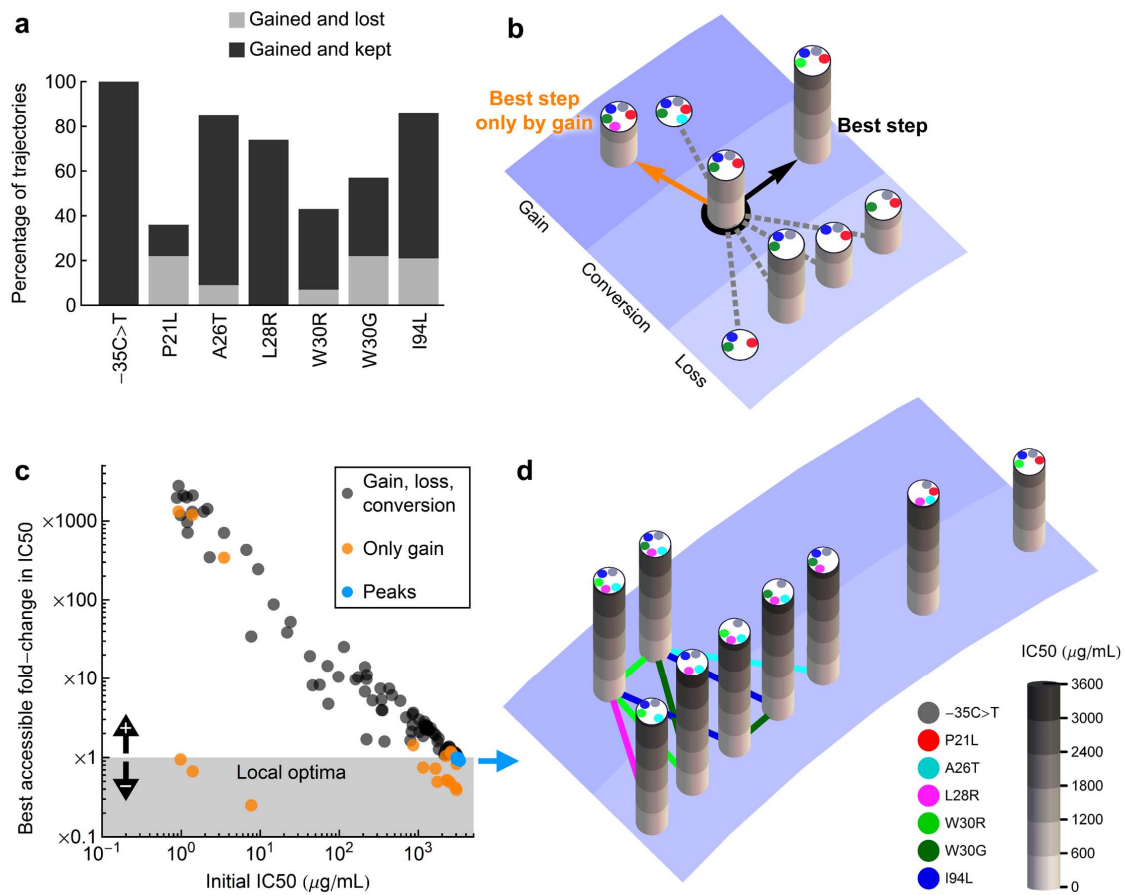
Figure 2.3. Conversion and reversions bypass evolutionary dead ends, guaranteeing a path to reach one of several highly adaptive peaks. (Continued)

We next investigated the genetic interactions that produce distinct adaptive peaks. It can be proven mathematically that an adaptive landscape can only contain multiple peaks in the presence of peak-separating 'reciprocal sign epistasis', where two mutations (e.g. $A \to a$ and $B \to b$) each change the sign of their effect when applied together; i.e. the transition $AB \to aB$ has an opposite effect to $Ab \to ab$, and $AB \to Ab$ also has an opposite effect to $aB \to ab$. This scenario is necessary to create losses of fitness along all genetic paths between two adaptive peaks, without which there would only be a single adaptive peak (Poelwijk et al., 2011). The separation of adaptive peaks by reciprocal sign epistasis has been previous observed as arising from pairwise incompatibility between two mutations; i.e. mutations a and b are individually beneficial, but deleterious when applied in combination. This interaction creates two separate evolutionary lineages, one with a and one with b, leading to separate adaptive peaks (Kvitek and Sherlock, 2011; Salverda et al., 2011). However, simple pairwise incompatibility cannot explain the multiple adaptive peaks observed in this landscape, because each possible pair of mutations is found to co-occur in an adaptive peak (Figure 2.3c). Since there are no intrinsically incompatible pairs of mutations, the genetic interactions that separate adaptive peaks must be more complex in nature.

Inspecting the genetic interactions between pairs of mutations revealed high-order genetic interactions where a given pair of mutations could display a variety of qualitatively different interactions with each other, depending upon the presence of yet other mutations (Figure 2.4a). 'Ruggedness' is the propensity for genetic interactions to change the sign of a mutation's

37

phenotypic effect (from advantageous to deleterious or vice versa); to understand the ruggedness of this adaptive landscape we investigated higher-order interactions by quantifying how each mutation affects the interactions amongst all other mutations. We defined a metric for ruggedness where each mutation i is assigned an information entropy H_i, calculated from the probability that acquiring the mutation has a beneficial (p^+) or deleterious (p^-) effect, over all possible genotypes on which it could be acquired: $H_i = -p^+.\ln(p^+) -p^-.\ln(p^-)$. The overall ruggedness is the sum of each mutation's information entropy ($\Sigma_i H_i$). When the IC50s of two neighboring genotypes are within experimental error (Methods), we regard this as a neutral transition that does not contribute to the calculation of ruggedness. This definition permits that even if some mutations are beneficial and some are deleterious, the ruggedness is 0 provided each mutation is *always* beneficial or neutral, or *always* deleterious or neutral. Ruggedness is maximized when every mutation has equal chance of being beneficial or deleterious. Strikingly, by this metric the adaptive landscape as a whole (Figure 2.1d) is 83% as rugged as the theoretical maximum. For each mutation, ruggedness was calculated for the subset of the adaptive landscape lacking that mutation, and over the subset of the landscape always possessing that mutation (Figure 2.4b). For four mutations (−35C>T, A26T, W30R, I94L) their presence or absence had no effect on ruggedness, two mutations (L28R, W30G) modestly increased ruggedness when present, and one mutation, P21L, was the largest contributor: its presence nearly doubled ruggedness (49% vs. 90% of the theoretical maximum). Importantly, P21L is not simply incompatible with other mutations; P21L exists together with every other type of mutation in adaptive peaks, whose resistance would (by definition) decrease if P21L reverted to wildtype (Figure 2.3d). Rather, the presence

of P21L dramatically increases the likelihood that acquiring other commonly beneficial mutations will instead be deleterious (Figure 2.4b). We viewed the relation between IC50 and number of mutations, with or without P21L, to investigate how this ruggedness-inducing mutation affects the evolutionary process. Without P21L the maximum possible resistance increases rapidly at first before reaching a peak at certain combinations of 4 mutations, and including all 5 mutations besides P21L is approximately equal in resistance to the peak (Figure 2.4c, Figure 2.3d). This 'diminishing returns' epistasis is consistent with other studies of interactions between advantageous mutations, and may be a general property of adaptive evolution (Chou et al., 2011; Khan et al., 2011). However, in the presence of P21L the continued accrual of 'trimethoprim-resistance' mutations generates *worse* than diminishing returns: after resistance reaches a maximum at a combination of 4 mutations, the resistance of any set of 5 or 6 mutations is lower (Figure 2.4c). Similarly, many combinations of 3 to 5 mutations that include P21L produce lower trimethoprim resistance than is found with any single mutation.

Figure 2.4. Ruggedness is the result of high-order genetic interactions, which are strongly induced by one mutation. a, P21L (red) and W30R (green) possess widely varying genetic interactions with one another when acquired on different genetic backgrounds. Mutations are indicated by colored dots and column height represents trimethoprim resistance (IC50). Red and green arrows point in the favorable direction for gaining or losing the P21L or W30R mutations, respectively. **b**, Ruggedness is calculated from the information entropy of mutations' effects: zero when each mutation's effect has a consistent sign, and maximised when each mutation has equal chance of being beneficial or deleterious. Calculating ruggedness from subsets of the adaptive landscape that excluding or including each mutation reveals that P21L is most responsible for ruggedness; when absent, other mutations are rarely deleterious, but when present, beneficial or deleterious effects are equally probable (pie charts over P21L). In contrast the presence or absence of I94L, for example, does not substantially alter the probability that other mutations are beneficial or deleterious (pie charts over I94L). **c**, Without P21L, trimethoprim resistance evolves with diminishing returns: fold-increases in IC50 become progressively smaller, until the addition of further 'resistance' mutations makes no significant change to resistance. Adaptation in the presence of P21L is much more rugged: acquiring fifth or sixth 'resistance' mutations lowers resistance from the peak, and many genotypes of 3 to 5 mutations are almost equally or even more susceptible to trimethoprim than wildtype. Solid red and black lines show the maximum level of trimethoprim resistance obtained with a given number of mutations (with or without P21L respectively). Points are shown with a small horizontal scatter to improve the visibility of overlapping data.
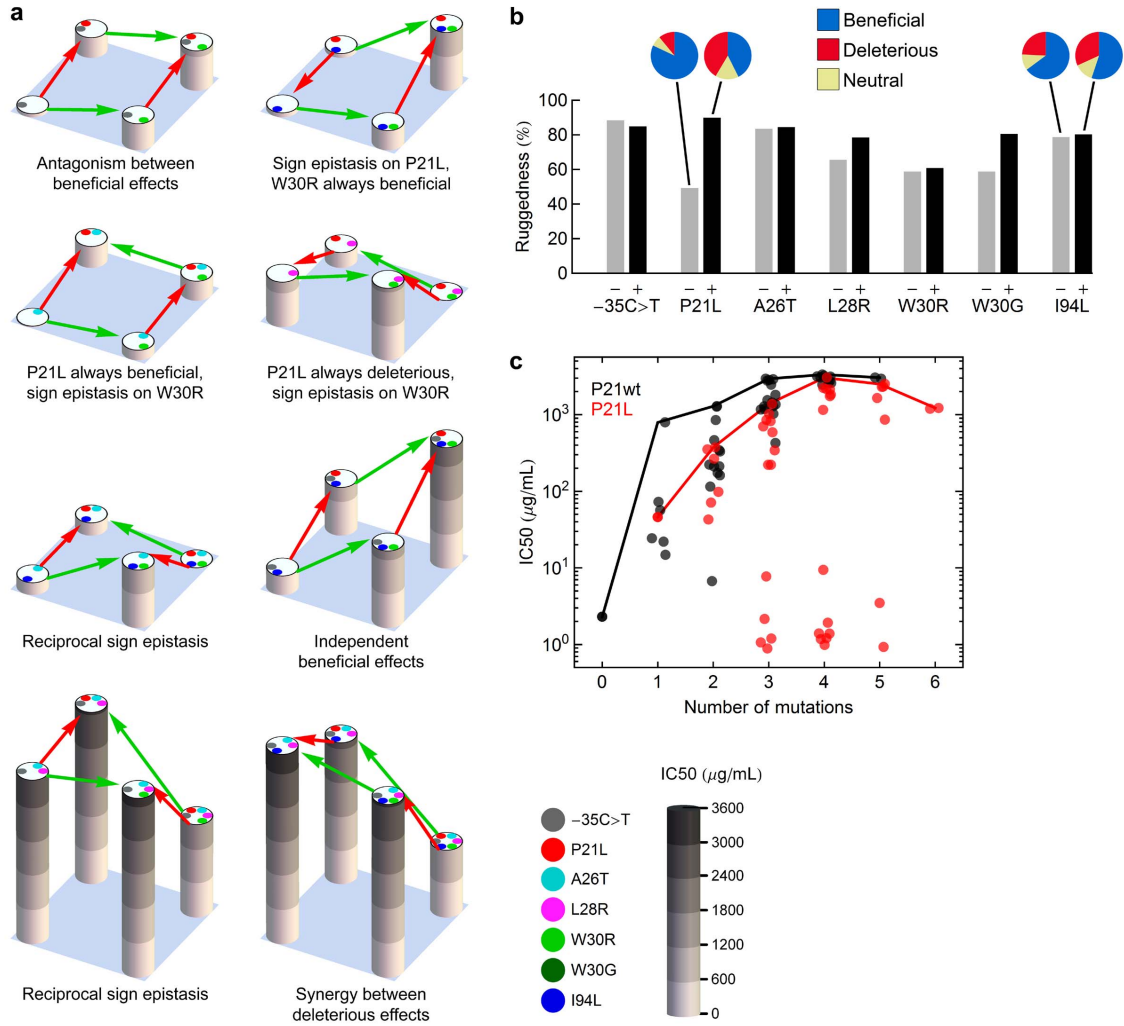
Figure 2.4. Ruggedness is the result of high-order genetic interactions, which are strongly induced by one mutation. (Continued)

The evolution of trimethoprim resistance through mutations in the drug's target *DHFR* is characterized by erratic genetic interactions. Adaptive pathways can take indirect paths, gaining, losing, or converting mutations along the way to any of several adaptive peaks. These multiple adaptive peaks are separated not by consistent pairwise incompatibilities between mutations, but by high-order genetic interactions where the genetic interaction between a pair of mutations widely varies depending on other mutations in the background genotype. One mutation has the ability to induce a level of ruggedness that is close to the theoretical maximum, giving rise to 'worse than diminishing' returns that prevent the continued gain of otherwise advantageous mutations. Despite these effects, indirect mutational paths can circumvent dips in fitness and thereby guarantee evolving populations a path to a highly drug-resistant genotype.

Acknowledgements

Author Contributions

E.T., S.K., A.V. and S.B. performed experiments; A.C.P., E.T. and R.K. analyzed data and wrote the manuscript.

Methods

Strains and media

All *DHFR* mutant strains were constructed in MG1655 attTn7::pRNA1-tdCherry (gift from N.D. Lord). Growth rate measurements were performed in M9 minimal medium (6 g.L^{-1} Na$_2$HPO$_4$, 3 g.L^{-1} KH$_2$PO$_4$, 1 g.L^{-1} NH$_4$Cl, 0.5 g.L^{-1} NaCl, 3 mg.L^{-1} CaCl$_2$) supplemented with 0.4% glucose, 0.2% casamino acids, and 1mM MgSO$_4$. Drug solutions were made from powder stock (Sigma Aldrich: chloramphenicol, C0378; kanamycin, K1876; trimethoprim, T7883).

Chromosomal Integration

Mutant *DHFR* strains were constructed by replacing the endogenous (coding and noncoding regions) of the *DHFR* gene with chemically synthesized mutant *DHFR* sequences, following the method of (Datsenko and Wanner, 2000) specifically adapted for *DHFR* (Bershtein et al., 2012). Briefly, mutant *DHFR* genes, including the native *DHFR* promoter, were synthesized and cloned into a plasmid with flanking kanamycin and chloramphenicol resistance genes. The integration cassette was PCR-amplified with primers possessing 60 nucleotide homology to the genes immediately upstream (*kefC*) and downstream (*apaH*) of *DHFR* in the *E.coli* chromosome. PCR products were DpnI digested (New England Biolabs, R0176) and

electroporated into strains carrying the lambda Red recombinase expression plasmid pKD46 (Datsenko and Wanner, 2000). Integrants were selected on Lysogeny Broth (LB) agar with 30 mg.L^{-1} kanamycin and 25 mg.L^{-1} chloramphenicol. Colony purification at 42°C removed the pKD46 plasmid, which was confirmed by a failure to grow on LB agar with 100 mg.L^{-1} ampicillin. Single colonies were Sanger sequenced to verify the sequence of the mutated *DHFR* locus. Mutated *DHFR* genes were transduced by phage P1 into naive MG1655 attTn7::pRNA1-tdCherry, transductants were selected on LB agar with kanamycin and chlorampenicol, and single transductant colonies were sequenced to again confirm the mutated *DHFR* sequence. Gene synthesis services were provided by GenScript, and DNA sequencing services were provided by GENEWIZ.

Phenotyping assay

Frozen stocks of all mutant strains were prepared in one master 96-well plate (LB with 15% glycerol). Approximately 0.3µL of each frozen stock was transferred by a pin replicator (V&P Scientific, VP408) to the corresponding wells of a range of 96-well plates, with 150µL of M9 minimal media per well. Each of these plates possessed one trimethoprim concentration out of a 23-point range from 0.2 to 3000 µg.mL^{-1}, plus duplicate cultures with no trimethoprim. Plates were incubated with shaking at 30°C and 70% humidity in an environmental room, and each well's optical density at 600nm (OD600) was measured every 60 minutes. To more precisely measure growth rate in the absence of drug, the assay was repeated with fewer plates (duplicate cultures with no trimethoprim) and more frequent measurements (every 15

minutes); additionally growth was measured at 3600 µg.mL^{-1} trimethoprim to verify that this concentration inhibited the growth of all mutant strains.

Growth rate and IC50 determination

A background optical density of 0.03 units was subtracted from each OD600 measurement, based upon the optical density of a control empty well present in all assays. Along the experimentally measured functions of log(OD600) over time, linear fits were made to each series of four data points (four hours of growth). A time series of growth rates was constructed from the slopes of these linear fits, which was then smoothed by a median filter (median of 3 consecutive growth rates). The most rapid growth rate of this median-smoothed series was taken as the growth rate of that culture at that trimethoprim concentration. For the more frequently measured cultures with no trimethoprim, the same protocol was applied except that linear fits were made to every 7 consecutive log(OD600) measurements, and the median filter was taken over 5 consecutive growth rates.

The trimethoprim resistance of each strain was quantified by the IC50, as calculated from the function of growth rate versis trimethoprim concentrations. Specifically, linear interpolations of growth vs log([trimethoprim]) were constructed, and IC50 was calculated as the largest trimethoprim concentration at which this linear interpolation of growth rate was equal to half of the uninhibited wildtype growth rate (half of 0.7 doublings/hour = 0.35 doublings/hour).

To quantify the experimental error in IC50 measurements, a distribution of IC50 estimates was acquired by performing the above protocol on an ensemble of 1000 functions of growth rate versus trimethoprim, where for every member of the ensemble each growth rate measurement is multiplied by a number drawn from a normal distribution with a mean of 1 and a standard deviation of 0.07; chosen such that the artificially 'noisy' data set has a Z-score that is twice the Z-score of the duplicate experimental measurements with no trimethoprim. From this ensemble, a standard deviation was calculated for each genotype's IC50; this standard deviation was small when growth is inhibited over a narrow range of trimethoprim concentrations, and large when growth gradually declines over a wide range of trimethoprim concentrations. When simulating evolutionary trajectories (Figure 2.3a) and calculating landscape ruggedness (Figure 2.4b), we required 99% confidence that the IC50 values of neighboring genotypes were not equal, or else they were considered to be connected by neutral drift. Drift transitions between genotypes were not permitted in simulated evolutionary trajectories, and drift transitions did not contribute to the calculation of ruggedness, where information entropy was calculated only from confidently beneficial or confidently deleterious transitions.

References

Bershtein, S., Mu, W., and Shakhnovich, E.I. (2012). Soluble oligomerization provides a beneficial fitness effect on destabilizing mutations. Proceedings of the National Academy of Sciences of the United States of America *109*, 4857-4862.

Brown, K.M., Costanzo, M.S., Xu, W., Roy, S., Lozovsky, E.R., and Hartl, D.L. (2010). Compensatory mutations restore fitness during the evolution of dihydrofolate reductase. Mol Biol Evol *27*, 2682-2690.

Chou, H.H., Chiu, H.C., Delaney, N.F., Segre, D., and Marx, C.J. (2011). Diminishing returns epistasis among beneficial mutations decelerates adaptation. Science *332*, 1190-1192.

Datsenko, K.A., and Wanner, B.L. (2000). One-step inactivation of chromosomal genes in Escherichia coli K-12 using PCR products. Proceedings of the National Academy of Sciences of the United States of America *97*, 6640-6645.

DePristo, M.A., Hartl, D.L., and Weinreich, D.M. (2007). Mutational reversions during adaptive protein evolution. Molecular biology and evolution *24*, 1608-1610.

Khan, A.I., Dinh, D.M., Schneider, D., Lenski, R.E., and Cooper, T.F. (2011). Negative epistasis between beneficial mutations in an evolving bacterial population. Science *332*, 1193-1196.

Kvitek, D.J., and Sherlock, G. (2011). Reciprocal sign epistasis between frequently experimentally evolved adaptive mutations causes a rugged fitness landscape. PLoS genetics *7*, e1002056.

Lozovsky, E.R., Chookajorn, T., Brown, K.M., Imwong, M., Shaw, P.J., Kamchonwongpaisan, S., Neafsey, D.E., Weinreich, D.M., and Hartl, D.L. (2009). Stepwise acquisition of pyrimethamine resistance in the malaria parasite. Proc Natl Acad Sci U S A *106*, 12025-12030.

Poelwijk, F.J., Kiviet, D.J., Weinreich, D.M., and Tans, S.J. (2007). Empirical fitness landscapes reveal accessible evolutionary paths. Nature *445*, 383-386.

Poelwijk, F.J., Tanase-Nicola, S., Kiviet, D.J., and Tans, S.J. (2011). Reciprocal sign epistasis is a necessary condition for multi-peaked fitness landscapes. Journal of theoretical biology *272*, 141-144.

Salverda, M.L., Dellus, E., Gorter, F.A., Debets, A.J., van der Oost, J., Hoekstra, R.F., Tawfik, D.S., and de Visser, J.A. (2011). Initial mutations direct alternative pathways of protein evolution. PLoS Genet *7*, e1001321.

Toprak, E., Veres, A., Michel, J.B., Chait, R., Hartl, D.L., and Kishony, R. (2012). Evolutionary paths to antibiotic resistance under dynamically sustained drug selection. Nat Genet *44*, 101-105.

Weinreich, D.M., Delaney, N.F., Depristo, M.A., and Hartl, D.L. (2006). Darwinian evolution can follow only very few mutational paths to fitter proteins. Science *312*, 111-114.

Chapter 3.

Diverse pathways to drug resistance by changes in gene expression

Adam C. Palmer[1], Remy Chait[1,2], Roy Kishony[1,3]

[1]Department of Systems Biology, Harvard Medical School, 200 Longwood Ave, Boston, MA 02115.

[2]Institute of Science and Technology - Austria, Am Campus 1, A-3400, Klosterneuburg, Austria.

[3]School of Engineering and Applied Sciences, Harvard University, Cambridge, MA 02138.

The effects of antibiotics are mediated by their direct or indirect interactions with individual proteins in the cell, as well as by the abundance of those proteins. Hence, antibiotic resistance can evolve not only by mutations that change the amino acid sequences of proteins, but also by mutations that change the expression level of proteins. To explore the potential of changes in gene expression to confer antibiotic resistance, we implemented a pooled diffusion-based assay to screen all viable gene over-expression and gene deletion mutants of *Escherichia coli* against a broadly representative panel of 31 antibiotics. We found 136 positive or negative changes in gene expression that confer drug-specific or multi-drug resistance. These genes span a diverse range of functions and most were not previously associated with antibiotic resistance; only 4 are drug targets. By quantitatively adjusting gene expression and measuring resistance, we find that intrinsic antibiotic defense systems, and also 'protoresistance' genes that hold enormous potential for resistance, are often regulated so as to actually confer little resistance to the wildtype strain. We rationalize the abundance and diversity of hits by

viewing gene-regulation as an optimization problem: because antibiotic treatment results in the non-optimal expression of some genes, there exist many possibilities for the evolution of drug resistance through regulatory mutations that deploy latent defense capabilities or correct other errors in gene expression.

Mutations can confer antibiotic resistance by changing the amino acid sequence of a protein (coding mutations) or by altering the expression level of proteins in a cell (non-coding, regulatory mutations). Resistance mutations have been identified in regulatory sequences in antibiotic resistant isolates from the clinic and from laboratory evolution experiments. These mutations have been found to confer antibiotic resistance by mechanisms such as over-expression of a drug's target, over-expression of drug defense systems, and the down-regulation or deletion of genes required for drug entry or enzymatic activation of a pro-drug. Examples include: trimethoprim resistance acquired by over-expression of its target enzyme dihydrofolate reductase (Flensburg and Skold, 1987); penicillin resistance acquired by the over-expression of drug degrading beta-lactamases (Bergstrom and Normark, 1979); and cephalosporin resistance acquired by loss of porins through which the drug enters the cell (Curtis et al., 1985). However, these and other examples have generally been identified individually, and because regulatory mutations can act in trans it remains challenging to systematically identify regulatory pathways to drug resistance by genotypic approaches (Courvalin, 2005). This limitation can be overcome through the use of genome-wide libraries of strains where each has a defined change in gene expression, e.g. deletion or over-expression. Genome-wide screens with such libraries have identified gene deletions which confer antibiotic hypersensitivity (Girgis et al., 2009; Tamae et al., 2008), and gene duplications which confer stress resistance; although the latter study utilized a competitive growth method that only identified 1 to 3 genes per stress (Soo et al., 2011). The most comprehensive such studies screened all viable homozygous and heterozygous gene deletions in diploid *S. cerevisiae* or all viable gene deletions in *E. coli* against hundreds of chemical

stresses (Hillenmeyer et al., 2008; Nichols et al., 2011). However, as both of these studies aimed to measure phenotypic signatures for each gene, stresses were applied only at sub-inhibitory levels, and so gene deletions that confer survival at normally lethal stress levels were not identified. Thus, a systematic and sensitive screen for positive and negative changes in gene expression that confer antibiotic resistance is absent.

In this study, we perform functional genetic screens in *E. coli* for drug-specific and multi-drug resistance conferred by increasing or decreasing gene expression levels, using a panel of antibiotics representing most classes effective against gram-negative bacteria. To accomplish this, we developed a robust genome-wide screen to identify gene expression changes conferring drug resistance. We employ two *E.coli* strain libraries: the 'KEIO' collection of strains containing each viable gene deletion (Baba et al., 2006), and the 'ASKA' collection wherein each gene is individually expressed from an IPTG-inducible promoter on a plasmid (Kitagawa et al., 2005). The ASKA collection of plasmids was transformed from its host cloning strain to the 'wildtype' MG1655 *ΔlacIZYA* for healthy growth; additionally the *lacIZYA* deletion allows IPTG to exclusively induce plasmid-based expression without fitness effects from induction of the *lac* operon. Screening large strain collections for drug-resistant mutants typically requires exploring a range of discrete, finely-tuned drug concentrations using high-throughput laboratory automation. We have addressed these challenges with a simple two-step pooled diffusion-based screen on agar (Figure 3.1a): (1) a strain library (deletion or over-expression) is pooled and seeded as a lawn on agar. An aliquot of concentrated drug solution is spotted in the center of the plate, as in a classical disc-diffusion

assay, and diffuses through the media to form a continuous spatial gradient of drug concentrations. Typically, following incubation, the wild type strain will grow into a dense lawn across the plate, except in a zone of clearing surrounding the drug source, where drug concentrations are high enough to preclude growth. Strains with enhanced resistance to the drug can grow in the higher drug concentrations closer to the center, and are thus visible as individual colonies inside the zone of inhibition; (2) Drug resistant colonies are picked and identified by Sanger sequencing of the expression plasmid or of the chromosome adjacent to the site of a gene deletion (Supplementary Methods). Because the diffusion gradient samples a continuum of drug concentration space, this rapid and inexpensive assay is robust with respect to drug concentrations and sensitively detects improvements in drug resistance.

We employed our assay on 31 antibiotics, representing all major classes of antibiotics effective against gram-negative bacteria (Table 3.1). The gene deletion collection represents the extreme case of down-regulation, and utilizing the IPTG-inducible promoter driving the gene over-expression collection, we screened against both weak and strong up-regulation (using 15μM and 150μM IPTG, respectively). 48 colonies were picked and sequenced for each of three expression conditions per drug (deletion, weak over-expression, strong over-expression). Inspection of the assay plates reveals discrete colonies within the high drug concentration zones of clearing, showing that both gene deletion and gene over-expression can confer drug resistance. The presence and abundance of drug-resistant gene expression mutants is highly variable across drugs, with very strongly resistant mutants appearing on some drugs (e.g. penicillin G, trimethoprim) while some drugs permitted no resistant

mutants (e.g. colistin) (Figure 3.1b). In contrast, the 'wildtype' reference plates rarely show colonies in the zone of inhibition, representing infrequent spontaneous drug resistance mutations. To avoid false identifications from the occurrence of spontaneous resistance mutations, we required two or more observations of each specific gene-drug interaction (false discovery rate ≤ 1%). We also noted a few interactions where a change in gene expression that had been repeatedly observed to resist one drug (satisfying the previous criteria) was also observed once with a second drug of the same mode of action (false discovery rate ≤ 5%).

Table 3.1. List of antibiotics used in this study, mechanism of action, and abbreviation.

Mechanism of action	Drug class	Drug name	Abbr.
Cell Wall Synthesis	Cephalosporin	Cephalexin	CLX
		Cefoxitin	FOX
		Cefsulodin	CFS
	Glycopeptide	Vancomycin	VAN
	Penicillin	Ampicillin	AMP
		Carbenicillin	CRB
		Mecillinam	MEC
		Penicillin G	PEN
Cell Membrane	Polypeptide	Colistin	COL
		Polymyxin B	PMB
	Fatty acid synthesis inhibitor	Triclosan	TCL
Transcription	Rifamycin	Rifamycin SV	RIF
Translation	Aminoglycoside	Amikacin	AMK
		Streptomycin	STR
		Tobramycin	TOB
	Macrolide	Azithromycin	AZI
		Erythromycin	ERY
		Spectinomycin	SPX
		Spiramycin	SPR
	Lincosamide	Clindamycin	CLI
	Tetracycline	Doxycycline	DOX
		Tetracycline	TET
DNA Synthesis	Quinolone	Ciprofloxacin	CPR
		Lomefloxacin	LOM
		Nalidixic acid	NAL
	Folate synthesis inhibitor	Trimethoprim	TMP
		Sulfacetamide	SCM
		Sulfamethoxazole	SMX
Free radical production	Glycopeptide	Bleomycin	BLM
		Phleomycin	PHM
	Nitrofuran	Nitrofurantoin	NIT

Figure 3.1. A genome-wide screen identifies changes in gene expression that confer antibiotic resistance. a, A library of *E.coli* strains with genes deleted or overexpressed is pooled and plated as a lawn on agar. A drug spot is applied which creates a zone of growth inhibition. Members of the strain library with increased drug resistance grow inside the zone of inhibition (yellow colonies), and are picked and identified by DNA sequencing. **b**, Photographs of assay plates for five example drugs (out of 31 drugs in total) illustrate that both gene deletion and over-expression can confer drug resistance, and the possible levels of resistance range from none at all (e.g. colistin), to modest (e.g. clindamycin, vancomycin), to very strong (e.g. penicillin, trimethoprim). Plate images of all drugs are shown in Supplementary Figure 3.1.
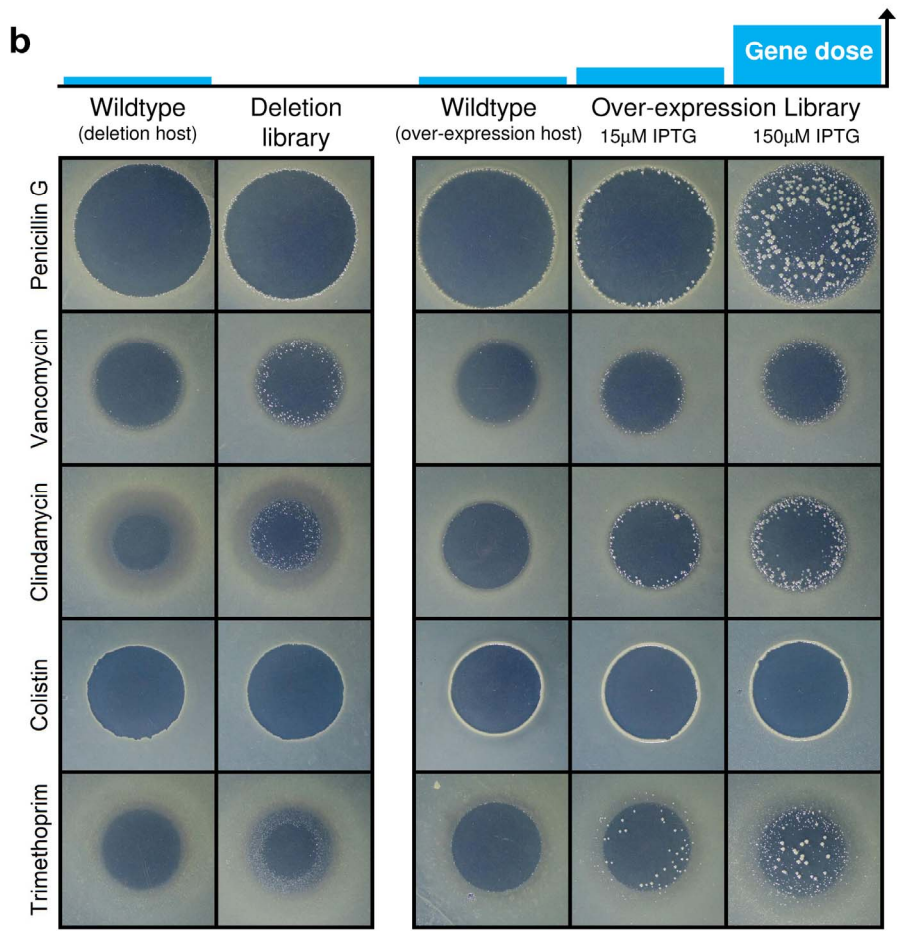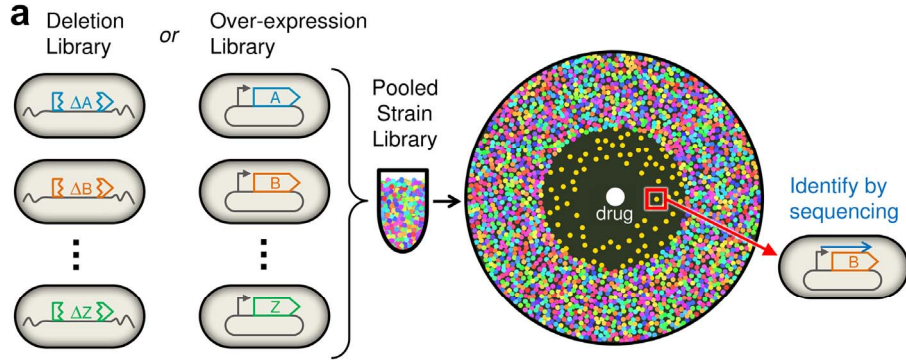
Figure 3.1. A genome-wide screen identifies changes in gene expression that confer antibiotic resistance. (Continued)

We sequenced over 2400 drug resistant colonies and identified over 200 gene-drug interactions where a change in gene expression was repeatedly observed to increase resistance to an antibiotic. These changes in gene expression consisted of a mixture of over-expression and deletion (59% and 41% of genes, respectively) (Figure 3.2). For only 4 of 31 drugs did we not identify any changes in individual gene expression that confer resistance, and 2 of these were the membrane-disrupting drugs colistin and polymyxin B where it is unclear how an internal change in gene expression might improve resistance. The majority of expression changes were observed to increase resistance to drugs only within a single mechanistic class (93% of genes), and have not been previously associated with drug resistance (83% of genes). Amongst those genes known to be associated with antibiotic resistance, we have reproduced several drug-specific and multi-drug resistant regulatory mutations previously identified in clinical isolates or experiments (Supplementary Table 3.1). These results demonstrate that for most antibiotics there are many regulatory mutations with the potential to increase resistance.

Figure 3.2. Many positive and negative changes in gene expression can confer drug resistance. Drugs (black hexagons) are grouped by mechanism of action (see Table 3.1 for abbreviations). *E. coli* genes are marked by red circles when deletion confers drug resistance and blue circles when over-expression confers drug resistance; known drug targets whose over-expression confers resistance are outlined in dark blue. Changes in gene expression that resist only one mechanism of drug action are grouped around the drugs of that mechanism, while those that resist multiple classes of drug are shown in the center. Pale colored links denote changes in gene expression that were identified only once as resisting a particular drug, that are included because they were repeatedly observed to resist another drug of the same mechanism of action. Supplementary Table 3.1 lists all gene-drug interactions
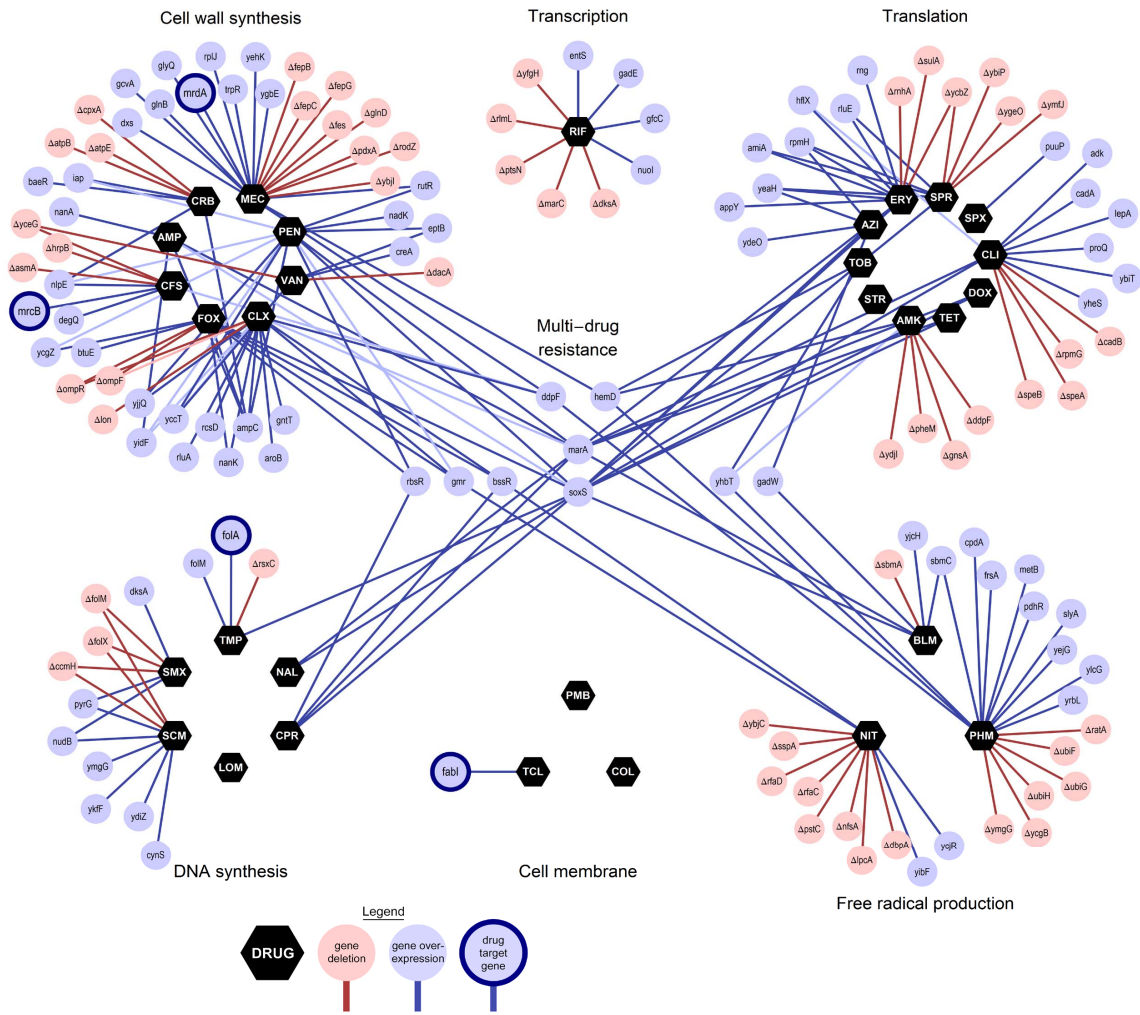
Figure 3.2. Many positive and negative changes in gene expression can confer drug resistance. (Continued)

A multitude of drug-specific pathways to resistance were observed. Amongst those genes with annotated functions, a diverse range of possible resistance mechanisms are demonstrated or suggested. Resistance mechanisms suggested by functional annotations include modification of the cellular process affected by a drug, increased flux through a drug-inhibited pathway, modification of cell permeability, chemical modification of a drug, and the activation of drug efflux and acid resistance systems (Table 3.2). Additionally, resistance to various antibiotics resulted from changes in the expression levels of numerous genes involved in the metabolism or transport of lipopolysaccharide, enterobactin, polyamines, and ubiquinone. These cases where a resistance mechanism can be inferred, or at least a particular metabolic process is implicated, represent only one third of the changes in gene expression that increase antibiotic resistance, while the remaining two thirds act by yet unclear mechanisms.

Table 3.2. Mechanisms of drug resistance mediated by changes in gene expression.

See Supplementary Table 3.1 for all gene-drug interactions and functional annotations.

Genetic change	Putative resistance mechanism
Modification of a cellular process affected by drug	
sbmC	Inhibits DNA Gyrase and confers resistance to DNA damage by phleomycin
ΔdacA	Alters the peptidoglycan moiety bound by vancomycin
ΔrodZ	Loss of a binding partner of the target of mecillinam confers mecillinam resistance
ΔdksA	Loss of an RNA Polymerase binding protein increases resistance to the RNA Polymerase inhibitor rifamycin SV
hflX	Over-expression of ribosome component increases resistance to the translation inhibitors clindamycin and erythromycin
ΔrpmG	Loss of ribosome component increases clindamycin resistance
Alteration of cell permeability	
ΔompF, ΔompR, ΔasmA	Loss of the porins through which cephalosporins enter the cell
ΔsbmA	Loss of a transporter through which antimicrobial peptides enter the cell
amiA	Increased expression of a peptidoglycan amidase
bssR	Increased expression of a biofilm regulator
Increased flux through drug-inhibited pathway	
nudB	Increased rate of first reaction in folic acid synthesis pathway
ΔfolM, ΔfolX	Increased flux through folic acid synthesis pathway by preventing substrate use for tetrahydromonapterin synthesis
folM	Drug-insensitive replacement for a drug-inhibited enzyme
folA, mrcB, mrdA, fabI	Increased expression of a drug-inhibited enzyme
Drug modification	
ΔnfsA	Loss of enzyme that catalyzes pro-drug activation
ampC	Expression of enzyme that inactivates drug
Drug resistance / drug efflux systems	
marA, soxS	Transcriptional activation of multidrug resistance systems
Δlon, ΔrsxC	Loss of enzyme required for inactivation of *mar* or *sox* systems, respectively
ycjR	Component of SdsRQP efflux pump
baeR	Increased transcription of MdtABC efflux pump
Acid resistance systems	
cadA, cadB	Activation of Lysine-dependent acid resistance system
gadE, gadW, ydeO	Activation of Glutamic acid decarboxylase acid resistance system
Lipopolysaccharide metabolism	
ΔlpcA, ΔrfaC, ΔrfaD	Defects in lipopolysaccharide synthesis and modification
eptB	Increased phosphoethanolamine modification of lipopolysaccharide
Enterobactin transport and modification	
ΔfepB, ΔfepC, ΔfepG	Loss of ferric enterobactin ABC transporter
Δfes	Loss of ferric enterobactin hydrolysis
entS	Increased expression of enterobactin transporter
Polyamine metabolism and transport	
puuP	Increased expression of putrescine transporter
rpmH	Decreased polyamine synthesis, but increased intracellular polyamines
ΔspeA, ΔspeB	Loss of putrescine biosynthesis
Ubiquinone metabolism	
ΔubiF, ΔubiG, ΔubiH	Loss of ubiquinone biosynthesis
nuoI	Increased expression of NADH:ubiquinone oxidoreductase

We also identified 9 genes whose over-expression increases resistance against multiple mechanisms of drug action (e.g. both cell wall synthesis drugs and DNA synthesis drugs), including the known multi-drug resistance genes marA and soxS, and 7 novel multi-drug resistance genes of varied functions. gadW is a transcriptional regulator of acid resistance; bssR regulates biofilm formation and may confer multidrug resistance through altered permeability; and ddpF is a putative component of an ABC transporter. The functional annotations of the remaining 4 multi-drug resistance genes (hemD, yhbT, gmr, and rbsR; see Supplementary Table 3.1) do not suggest potential mechanisms of resistance.

Regulatory mutations in the specific targets of drugs are of particular interest. While many antibiotics are not inhibitors of a single protein (instead inhibiting a large complex, a family of related enzymes, or damaging a non-protein target such as the cell membrane), 10 of the 31 antibiotics in our screen specifically bind to one or two enzymes. If an antibiotic acts by disrupting the activity of its target, a higher concentration of the target might be able to restore its activity. Strikingly, only 4 of these 10 antibiotics were resisted by over-expression of their target gene, and 2 of these only when over-expressed weakly, not strongly (Figure 3.2, Table 3.3). Thus, a drug's direct target can be absent from the set of regulatory mutations that confer drug resistance.

Table 3.3. Many specific inhibitors are not resisted by over-expression of their target.

Only 4 antibiotics were resisted by over-expression of their specific target gene(s), and for 2 of these resistance was only conferred by weak, but not strong, target over-expression (genes with *). Conversely, antibiotic resistance can often be increased by the over-expression of certain non-target genes.

Antibiotic	Target over-expression confers resistance?		Non-target genes that confer resistance when over-expressed (#)
	Yes	No	
Cephalexin		ftsI	12
Cefsulodin	mrcB*	mrcA	3
Mecillinam	mrdA*		11
Trimethoprim	folA		2
Sulfamethoxazole		folP	3
Sulfacetamide		folP	6
Ciprofloxacin		gyrA, parC	4
Lomefloxacin		gyrA, parC	0
Nalidixic acid		gyrA, parC	2
Triclosan	fabI		0

These gene-drug interactions identify genes for which a change in expression improves survival, and therefore are not optimally regulated under antibiotic stress in the wildtype cell. For these genes the response of a wildtype cell to antibiotic treatment produces less than, or perhaps even none, of its maximal potential for antibiotic resistance that could be achieved with an optimal regulatory response. We investigated what fraction of the maximum potential resistance is realized by *E. coli* for the 2 most broadly protective multi-drug resistance genes, *marA* and *soxS*, and for 2 strong drug-specific resistance genes, *ampC* and *sbmC*. To answer this question it is necessary to remove the native transcriptional regulation mechanisms and obtain full experimental control over these genes' expression. We achieve this by constructing hybrid 'gene deletion - gene expression' strains in which a plasmid bearing IPTG-regulated gene expression is transformed into a strain where the matching gene is deleted from the chromosome (Figure 3.3a). Two-dimensional gradients of drug dose and IPTG-controlled gene dose were constructed across microtiter plates and bacterial growth rates were measured using a bioluminescence assay with sensitivity far exceeding optical density techniques (Kishony and Leibler, 2003). These experiments assessed how drug resistance depends on gene expression and how the maximal possible drug resistance compares to the resistance of the wildtype strain and a strain lacking the gene.

MarA and SoxS are global regulatory transcription factors with partially overlapping sets of target genes whose activation confers resistance to multiple antibiotics, organic solvents, and oxidative stresses through mechanisms such as upregulation of efflux pumps and downregulation of porins (Alekshun and Levy, 1999; Martin and Rosner, 2002). The growth

of strains with regulated expression of either *marA* or *soxS* were examined in concentration gradients of 9 antibiotics representing the 4 modes of action that were observed to interact with *marA* and *soxS*. We find that *marA* and *soxS* have the potential to boost resistance to ampicillin, mecillinam, clindamycin, doxycycline, ciprofloxacin and trimethoprim (Figure 3.3b). However, this potential for resistance is only well used by the wildtype strain in the case of clindamycin (*marA* and *soxS*) and trimethoprim (*soxS* only), and then only under strong growth inhibition, and not at moderate growth inhibition. (Figure 3.3c, Supplementary Figure 3.3a). Thus, many antibiotics could potentially be resisted by intrinsic stress response systems, but remain effective because of a regulatory failure to fully utilize those defenses. This phenomenon underlies the clinical observation of mutations that activate the *mar* or *sox* operons in multi-drug resistant *E. coli* isolates (Koutsolioutsou et al., 2005; Maneewannakul and Levy, 1996).

Figure 3.3. Multi-drug resistance systems are often poorly utilized. a, The optimality of a gene's response to antibiotic treatment was investigated by comparing the drug susceptibility of three *E. coli* strains: one lacking the gene (black), one with wildtype gene regulation (green), and one where susceptibility can be measured over a range of experimentally controlled gene expression levels (red). **b**, The optimality of the responses of the multi-drug resistance factors *marA* and *soxS* were studied in 9 antibiotics. Drug concentrations are normalized by the IC50 (concentration for 50% inhibition) of the strain lacking the gene of interest. For regulated gene over-expression, the growth rate shown is the highest over all expression levels. For those drugs where gene expression (red) increased resistance relative to gene deletion (black), the wildtype strain (green) frequently used only a fraction of the potential for drug resistance. **c**, On an empirical fitness landscape (growth rate vs drug dose and gene expression) the gene expression response that maximizes growth at each drug dose (red line) can be compared with the wildtype response (green), which is inferred by matching the wildtype growth rate to the level of controlled gene expression producing the same growth rate. In ampicillin and ciprofloxacin, a sub-optimal use of *marA* is observed. In clindamycin the wildtype cell does not use *marA* for drug resistance until growth inhibition is greater than 50%, after which *marA* use becomes optimal.
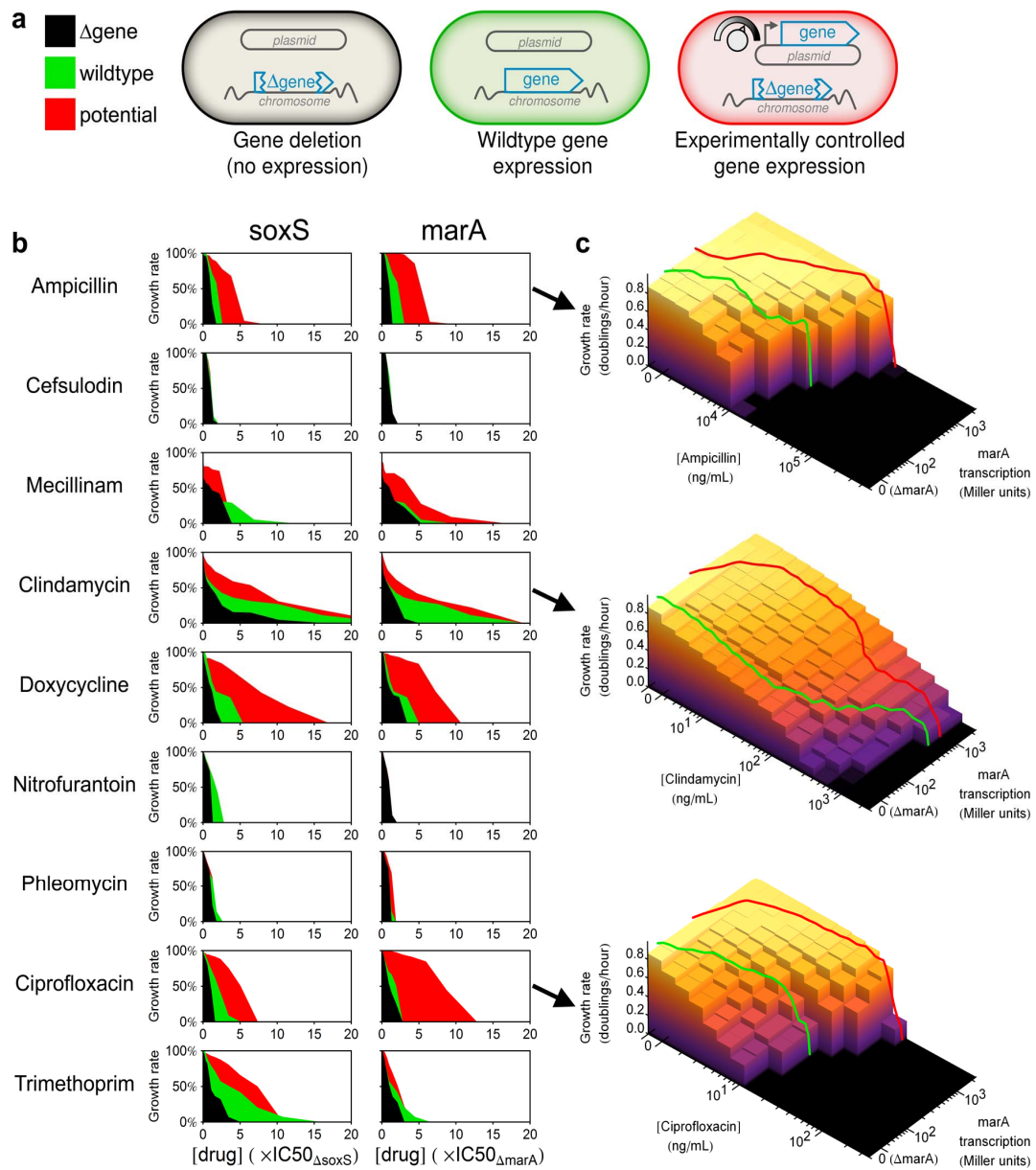
Figure 3.3. Multi-drug resistance systems are often poorly utilized. (Continued)

AmpC is both a beta-lactamase and a peptidoglycan hydrolase required for normal cell morphology (Bishop and Weiner, 1993; Henderson et al., 1997). Regulatory mutations that increase *ampC* expression have been observed in clinical and experimental isolates and confer strong penicillin and cephalosporin resistance (Bergstrom and Normark, 1979). Under treatment by either a penicillin or a cephalosporin, we observe that wildtype *ampC* expression levels provide negligible resistance relative to a Δ*ampC* strain, despite the potential to confer 100-fold resistance when over-expressed (Figure 3.4a, Supplementary Figure 3.3b). The lack of *ampC*-mediated resistance in wildtype *E. coli* suggests that rather than being a drug resistance gene, *ampC* is a 'protoresistance' gene (Morar and Wright, 2010); the primary role of *ampC* is in cell morphology, but it has the capacity to evolve into a beta-lactam resistance gene through mutations that increase its expression level.

SbmC is a DNA gyrase inhibitory protein that acts as an antitoxin to DNA gyrase-specific protein toxins such as microcin B17, and is induced by the SOS response to DNA damage (Baquero et al., 1995; Chatterji and Nagaraja, 2002; Nakanishi et al., 1998; Oh et al., 2001). Here we observed that sbmC over-expression confers resistance to phleomycin, a glycopeptide that generates free radicals leading to DNA cleavage. Comparing the phleomycin susceptibility of Δ*sbmC*, wildtype, and *sbmC* over-expressing strains we found that, despite the SOS-inducibility of *sbmC*, only a small fraction of the potential *sbmC*-mediated phleomycin resistance was used by a wildtype strain (Figure 3.4b, Supplementary

Figure 3.3b). Thus even a specific stress-inducible toxin resistance gene can be inadequately

utilized against toxins that it can resist.

Figure 3.4. Proto-resistance genes hold unrealized potential for strong drug resistance.
The use of *ampC* and *sbmC* under antibiotic treatment was examined by comparing the drug resistance of *E. coli* strains lacking the gene of interest (black), wildtype strains (green), and strains with experimentally controlled gene expression that demonstrate the potential for drug resistance (red) (see Figure 3.3a). **a**, *ampC* encodes a potent beta-lactamase: over-expression can confer 100-fold resistance to penicillins or cephalosporins. However, with wildtype expression regulation of *ampC* (green) almost none of this potential resistance (red) is used. **b**, *sbmC* encodes a DNA gyrase inhibitor whose over-expression confers resistance to the DNA-damaging drug phleomycin. However, a wildtype strain (green) treated with phleomycin uses very little of the potential resistance offered by *sbmC* (red).
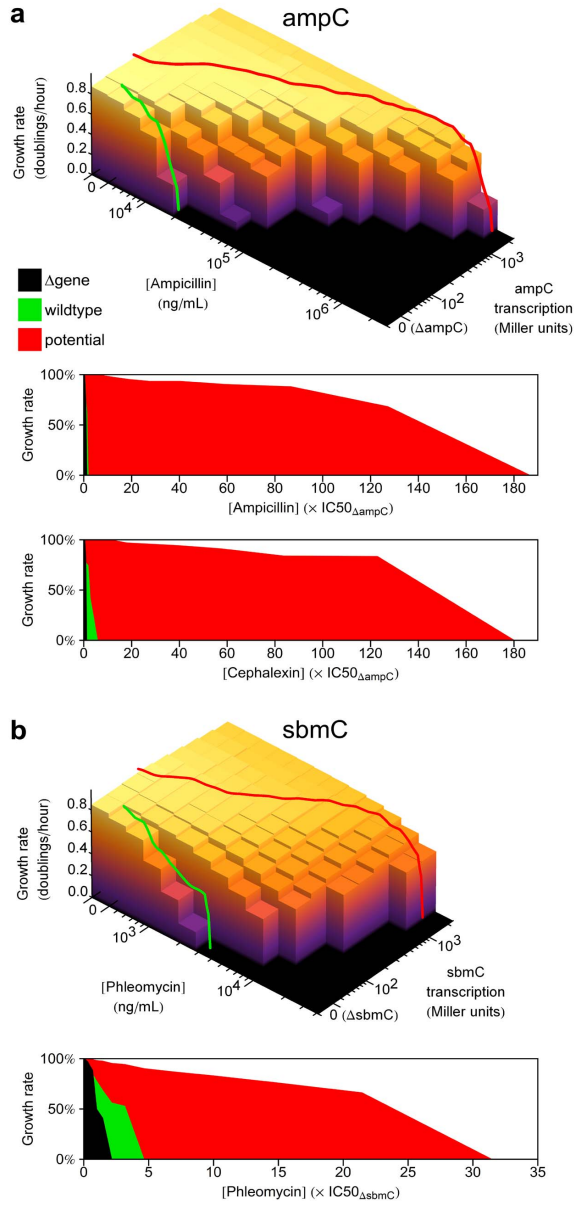
Figure 3.4. Proto-resistance genes hold unrealized potential for strong drug resistance.

(Continued)

In principle, a mutation can only produce a beneficial effect by changing a gene's expression level if that gene's expression was initially sub-optimal, i.e. fitness would be larger at either higher or lower expression. Therefore, all non-coding mutations that are beneficial only under antibiotic treatment are made possible by a non-optimality in gene expression in the presence of the drug. To illustrate this phenomenon, we measured growth rate as a function of gene expression for *nfsA* under nitrofurantoin treatment, and *ampC* under ampicillin treatment. As expected from the previous theoretical arguments, the optimum *nfsA* expression level is lowered by increasing doses of nitrofurantoin, until the expression level that is optimal for growth without the drug is lethally sub-optimal in its presence (Figure 3.5). In scenarios such as this, mutations that lower or abolish gene expression will confer drug resistance. Conversely, the optimum *ampC* expression level increases with increasing doses of ampicillin (Figure 3.5). If actual *ampC* expression is maintained at the level that optimizes growth without drug, the strain will die at drug doses that could have been resisted with greater *ampC* expression; in this type of scenario, gene over-expression will confer drug resistance. These two examples illustrate a universal phenomenon: non-optimal gene expression is the pre-condition for a change in gene expression to be beneficial. The simplest situation that may give rise to non-optimal gene expression under antibiotic treatment is if a gene's expression is optimized for growth in the absence of drug and is not differentially regulated in response to drug treatment. There are also examples of more elaborate reasons for sub-optimal gene expression: a drug or drug mixture may induce serious physiological imbalances between cellular components, outside the usual range of their global regulation

(Bollenbach et al., 2009) or may even induce a harmful regulatory response in drug resistance
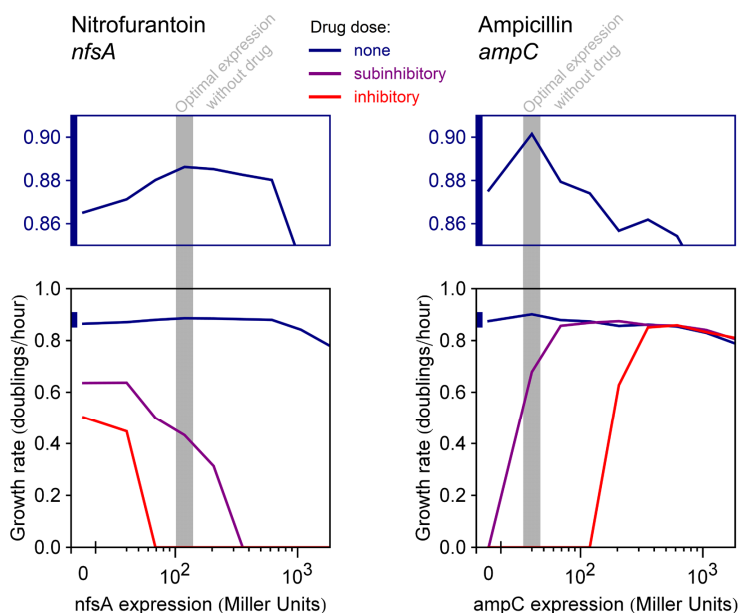
systems (Palmer et al., 2010).

Figure 3.5. **Antibiotic treatments can change optimal gene expression levels.** The growth rate of *E. coli* was measured as a function of *nfsA* or *ampC* expression levels when grown in variable doses of nitrofurantoin or ampicillin, respectively; using strains for experimentally controlled gene expression as per Figure 3.3a. Nitrofurantoin concentrations were $3\mu g.mL^{-1}$ (subinhibitory to the wildtype strain) and $4.4\mu g.mL^{-1}$ (inhibitory to the wildtype strain); and ampicillin concentrations were $16\mu g.mL^{-1}$ (subinhibitory) and $100\mu g.mL^{-1}$ (inhibitory). Plots at top zoom in on growth rates in the absence of drug; gray lines highlight the gene expression level that optimizes growth without drug. Nitrofurantoin treatment lowers the optimal *nfsA* expression level, thus selecting for mutations that lower *nfsA* expression. Ampcillin treatment raises the optimal *ampC* expression level, thus selecting for mutations that elevate *ampC* expression.

Antibiotics inhibit or damage essential processes at micromolar to nanomolar concentrations and come in diverse structural forms; the task of detecting and responding to these compounds must be a challenge, at which drug-sensitive bacteria succeed partially at best. Fitness is an environment-dependent function of gene expression (Dekel and Alon, 2005), and antibiotic treatment changes the optimal expression level of many genes that can influence drug susceptibility. For each and every such gene, if there is a failure to appropriately respond to drug treatment, then regulatory mutations can exist that change gene expression, correct this non-optimality, and thereby improve drug resistance. We have identified an abundance of functionally diverse pathways to antibiotic resistance by such changes in gene expression. While many of these changes have modest drug-specific effects, even potent drug resistance genes and multi-drug resistance systems are subject to mutations that change gene expression, due to their inadequate or complete lack of usage against many antibiotics. Thus, while bacteria can achieve antibiotic resistance by acquiring functional mutations and specific resistance mechanisms, we find that they can also draw on an unappreciatedly vast pool of mutations that correct gene-regulatory failures and activate latent defense mechanisms.

Acknowledgements

Author Contributions

A.C.P., R.C. and R.K. designed research; A.C.P. performed research and analyzed data; A.C.P., R.C. and R.K. wrote the manuscript.

Methods

Strains and Media

All selection experiments and growth rate assays were performed in M63 minimal medium (2g.L^{-1} (NH$_4$)$_2$SO$_4$, 13.6g.L^{-1} KH$_2$PO$_4$, 0.5mg.L^{-1} FeSO$_4$•7H2O, adjusted to pH 7.0 with KOH) supplemented with 0.2% glucose, 0.1% casamino acids, 1mM MgSO$_4$ and 0.5mg.L^{-1} thiamine.

Escherichia coli strain BW25113 is the host for the KEIO gene deletion library (Baba et al., 2006; Datsenko and Wanner, 2000). The strains of the KEIO gene deletion library (Baba et al., 2006) were grown individually in 384-well plates with 80μL of Lysogeny Broth (LB) per well, with incubation at 37°C and shaking at 900rpm for 24 hours. All cultures were then collected in a single beaker and mixed, passed through 5 micron cellulose acetate filters to disrupt cell clumps, and frozen in aliquots at −80°C in 10% glycerol. As the ASKA Open Reading Frame (ORF) library of plasmids was supplied in the AG1 cloning strain (Kitagawa et al., 2005), the plasmids were purified and transformed in pools into the 'wildtype' strain MG1655 *rph+* Δ*lacIZYA* (gift from K.E. Shearwin; constructed from BW30270 (CGSC7925) by precise deletion of *lacIZYA* (EcoCyc MG1655: 360527-366797) by recombineering) to minimize artifacts arising from the poor health of the cloning strain; additionally the *lacIZYA* deletion allows the use of IPTG to exclusively induce plasmid-based expression without additional fitness effects due to induction of the *lac* operon. No such alterations were required for the deletion library as BW25113 has only minor perturbations relative to wildtype MG1655, and IPTG was not required to induce a change in gene expression. The AG1 strains of the ASKA

library were grown by the same protocol as described for the KEIO library, and the chloramphenicol resistance and ORF-encoding pCA24N plasmids were isolated as a pooled mixture from each 384-well plate by a QIAGEN Spin Miniprep kit. Plasmid pools were transformed into MG1655 rph^+ $\Delta lacIZYA$ by the one-step protocol of (Chung et al., 1989). To enrich for plasmid transformed cells, liquid cultures of transformed *E. coli* (~10^9 c.f.u) were inoculated into 10mL of M63 minimal medium with 30μg.mL^{-1} chloramphenicol and were incubated overnight at 37°C with shaking at 300rpm. All transformant pools were added to a single flask, mixed, and frozen in aliquots at −80°C in 10% glycerol. A wildtype reference for the ASKA library was constructed by transforming MG1655 rph^+ $\Delta lacIZYA$ with a pCA24N plasmid encoding yellow fluorescent protein (*yfp*), but with the promoter deleted (pCA24N-ΔpT5lac-*yfp*).

In growth rate assays (Figures 3.3 and 3.4), 'wildtype' refers to BW25113, 'gene deletion' refers to the member of the KEIO deletion library lacking the gene of interest (BW25113 - *gene*::Kan^R), where the Kanamycin resistance cassette was been excised by FLP recombinase from a temperature-sensitive helper plasmid, yielding a strain BW25113 *gene*::FRT (Datsenko and Wanner, 2000). Excision of kanamycin resistance and loss of the helper plasmid, by colony purification at 43°C, was verified by testing for loss of antibiotic resistances. Controlled gene expression was produced by complementing a gene deletion strain with a pCA24N plasmid with isopropyl β-D-1-thiogalactopyranoside (IPTG)-inducible expression of the deleted gene; these plasmids were obtained from the ASKA library and the Open

Reading Frames were sequenced to confirm gene identity (Kitagawa et al., 2005). As *lacIZYA* is deleted in BW25113, IPTG does not incur fitness costs for *lac* operon production (Stoebel et al., 2008), and graded induction is possible without the LacY permease, that would otherwise cause all-or-none induction of LacI-regulated promoters (Choi et al., 2008; Novick and Weiner, 1957). For consistency both 'wildtype' and 'gene deletion' strains were transformed with pCA24N-ΔpT5lac-*yfp*. All strains were then transformed with plasmid pCSλ which encodes a constitutively expressed bacterial bioluminescence operon (Kishony and Leibler, 2003).

Drug solutions were made from powder stocks (from Sigma Aldrich unless specified otherwise: amikacin, A1774; ampicillin, A9518; azithromycin, Tocris 3771; bleomycin, Selleck S1214; carbenicillin, C1613; cephalexin, C4895; cefoxitin, C4786; cefsulodin, C8145; ciprofloxacin, 17850; chloramphenicol, C0378; clindamycin, Indofine C0117; colistin, C4461; doxycycline, D9891; erythromycin, Fluka 45673; isopropyl β-D-1-thiogalactopyranoside, Omega Bio-Tek AC121; kanamycin, K1876; lomefloxacin, L2906; mecillinam, 33447; nalidixic acid,N3143; nitrofurantoin, N7878; ortho-nitrophenyl-β-galactoside, N1127; penicillin G, Fluka 13750; phleomycin, P9564; polymyxin-B, P0972; rifamycin SV, Biochemika 83909; spectinomycin, S9007; spiramycin, S9132; streptomycin, S6501; sulfacetamide, S8627; sulfamethoxazole, S7507; tetracycline, 87128; tobramycin,T4014; triclosan, TCI America T1872; trimethoprim, T7883; vancomycin,V8138). Drug and IPTG gradients were made by serial dilution in M63 medium.

Pooled-library drug diffusion assay

Frozen aliquots of BW25113 (deletion library host), pooled deletion library, MG1655 *rph*⁺ Δ*lacIZYA* pCA24N-ΔpT5lac-*yfp* (over-expression library host), or pooled over-expression library were thawed, and 10^7 cells were spread by glass beads on wet 10cm petri dishes containing 25mL of 1.5% agar M63 minimal media; with 15μM or 150μM IPTG only when plating the pooled over-expression library. Plates were briefly dried in a biosafety cabinet before an aliquot of antibiotic was pipetted in the center of the plate. Plates were incubated at 37°C for 48 hours before being photographed by a custom plate imager (Chait et al., 2010). Plates treated with sulfacetamide and sulfamethoxazole were instead incubated for 1 week due to the slow growth of drug resistant colonies; in all other drugs, resistant colonies either appeared within 48 hours or were not apparent even after 1 week. Up to 48 drug resistant colonies per plate (not including wildtype reference plates) were viewed in a Nikon SMZ-745T stereomicroscope, picked by a flame-sterilized 0.25mm nichrome wire, and struck on selective agar: 50 μg.mL⁻¹ kanamycin for the gene deletion library and 30 μg.mL⁻¹ chloramphenicol for the gene over-expression library. Streak plates were incubated at room temperature for several days, a single colony from each plate was inoculated into a liquid culture of selective LB in a 96-well microtiter plate. Microtiter plates were incubated overnight at 37°C with shaking at 900 rpm, and glycerol was added to each well to a final concentration of 15%. Microtiter plates were stored frozen at -80°C. The genes that confer drug resistance to selected members of the gene over-expression library were identified by sending bacterial cultures to GENEWIZ to Sanger sequencing the Open Reading Frame (ORF) of the pCA24N plasmid using the primer ASKAseqLF (CACCATCACCATCACCAT

ACG). The gene deletions that confer drug resistance to selected members of the KEIO library were identified by Sanger sequencing the products of a 2-step hemi-nested PCR reaction that amplified a portion of chromosome adjacent to the Kanamycin resistance cassette that replaces each deleted gene. Both PCR steps used 20μL reactions with 2 units of OneTaq DNA Polymerase (New England Biolabs M0480), 200nM of each primer (Integrated DNA Technologies), and 200μM of each dNTP (New England Biolabs N0447). The first PCR reaction was inoculated with 1μL of liquid bacterial culture, and used the three primers KEIOseq1 (TGAAGTTCCTATTCCGAAGTTCCTATTCTC), CEKG2C (GGCCACGCGTC GACTAGTACNNNNNNNNNNNGATAT), and CEKG2D (GGCCACGCGTCGACTAGTAC NNNNNNNNNNACGC) in the following reaction cycle: first 5' at 95°C; 6 cycles of 30" at 95°C, 30" at 42°C (lowering by 1°C per cycle), 3' at 68°C; then 24 cycles of 30" at 95°C, 30" at 45°C, 3' at 68°C; and finally 5' at 68°C. The second PCR reaction was inoculated with 0.5μL per well of the completed first PCR reaction, and used the primers KEIOseq3 (TCGAAGCAG CTCCAGCCTAC) and CEKG4 (GGCCACGCGTCGACTAGTAC) in the following reaction cycle: 30 cycles of 30" at 95°C, 30" at 56°C, 3' at 68°C; and finally 5' at 68°C. Products of this final PCR reaction were sent to GENEWIZ for sequencing by the KEIOseq3 primer. Sequences were aligned with blastn to the *E. coli* MG1655 genome (NC_000913.2) to determine gene identity (Altschul et al., 1990; Blattner et al., 1997). Alignments that started more than 100 nucleotides from the expected start of alignment were discarded: gene over-expression sequences should align shortly after the start codon of an ORF; gene deletion sequences should align shortly after the stop codon of an ORF.

Growth rate assay

pCSλ confers constitutive bioluminescence that enables cell densities in growing cultures to be precisely measured over many orders of magnitude by photon counting (Kishony and Leibler, 2003). Cultures were grown in black 96-well plates with white wells (Perkin Elmer 6005039) sealed with clear adhesive lids (Perkin Elmer 6005185). Wells contained 200μL of media inoculated with approximately 100 to 300 cells from freshly thawed -80°C frozen cultures. Plates were incubated in a 30°C room at 70% humidity, and growth was assayed by a Perkin Elmer TopCount NXT Microplate Scintillation and Luminescence Counter that measured each well for 1 second. Experiments of 10 to 20 plates allowed each plate to be measured every 30 to 60 minutes. Plate stacks were ventilated by fans to eliminate spatial temperature gradients and ensure uniform growth conditions across each plate. In each experiment, distributed throughout the plate stack were 3 control plates of uniform media conditions to verify the absence of growth rate gradients within plates or across the plate stack. Growth rate is the slope of the logarithm of photon counts per second (c.p.s.), and is taken from the fastest growing line of best fit observed in any 6 hour timespan; this time corresponds to 5 doublings of a healthy culture. The slope of the logarithm of c.p.s. is unaffected by changes in luminescence per cell, such as might result from antibiotic treatments or changes in gene expression (Kishony and Leibler, 2003).

Beta-galactosidase assay

The transcription rates of genes encoded in the pCA24N plasmid at different IPTG concentrations were measured by kinetic beta-galactosidase (LacZ) assays of pCA24N-*lacZ*, using a method adapted from (Dodd et al., 2001). Liquid cultures of BW25113 pCA24N-*lacZ* were prepared in a 96-well plate in the same manner as for growth rate assays. The plate was incubated at 30°C with shaking until the plate average OD_{600} equalled 0.1 (mid log phase), as measured by a Perkin Elmer Victor plate reader. 20μL of each well was promptly transferred to the corresponding well of a microtiter plate pre-warmed to 30°C, in which each well contained 30μL of sterile media and 190μL of lysis / assay buffer, consisting of 100mM Tris-HCl pH 8.0, 1mM $MgSO_4$, 10mM KCl, 10g.L^{-1} β-mercaptoethanol, 100mg.L^{-1} polymyxin B, and 850mg.L^{-1} ortho-nitrophenyl-β-galactoside. The lysis / assay plate was transferred to a Tecan Sunrise plate reader in a 30°C room at 70% humidity, and OD_{410} was measured every minute for 2 hours, with 20 seconds of shaking between each reading. For each well, promoter activity in Miller Units was calculated from the slope of OD_{410} versus time, multiplied by 200,000, divided by the OD_{600} of the culture that was transferred to that well, and divided by the volume (in μL) of the culture assayed (here 20μL) (Supplementary Figure 3.2).

References

Alekshun, M.N., and Levy, S.B. (1999). The mar regulon: multiple resistance to antibiotics and other toxic chemicals. Trends Microbiol *7*, 410-413.

Altschul, S.F., Gish, W., Miller, W., Myers, E.W., and Lipman, D.J. (1990). Basic local alignment search tool. J Mol Biol *215*, 403-410.

Baba, T., Ara, T., Hasegawa, M., Takai, Y., Okumura, Y., Baba, M., Datsenko, K.A., Tomita, M., Wanner, B.L., and Mori, H. (2006). Construction of Escherichia coli K-12 in-frame, single-gene knockout mutants: the Keio collection. Mol Syst Biol *2*, 2006 0008.

Baquero, M.R., Bouzon, M., Varea, J., and Moreno, F. (1995). sbmC, a stationary-phase induced SOS Escherichia coli gene, whose product protects cells from the DNA replication inhibitor microcin B17. Mol Microbiol *18*, 301-311.

Bergstrom, S., and Normark, S. (1979). Beta-lactam resistance in clinical isolates of Escherichia coli caused by elevated production of the ampC-mediated chromosomal beta-lactamase. Antimicrob Agents Chemother *16*, 427-433.

Bishop, R.E., and Weiner, J.H. (1993). Complementation of growth defect in an ampC deletion mutant of Escherichia coli. FEMS Microbiol Lett *114*, 349-354.

Blattner, F.R., Plunkett, G., 3rd, Bloch, C.A., Perna, N.T., Burland, V., Riley, M., Collado-Vides, J., Glasner, J.D., Rode, C.K., Mayhew, G.F.*, et al.* (1997). The complete genome sequence of Escherichia coli K-12. Science *277*, 1453-1462.

Bollenbach, T., Quan, S., Chait, R., and Kishony, R. (2009). Nonoptimal microbial response to antibiotics underlies suppressive drug interactions. Cell *139*, 707-718.

Chait, R., Shrestha, S., Shah, A.K., Michel, J.B., and Kishony, R. (2010). A differential drug screen for compounds that select against antibiotic resistance. PLoS One *5*, e15179.

Chatterji, M., and Nagaraja, V. (2002). GyrI: a counter-defensive strategy against proteinaceous inhibitors of DNA gyrase. EMBO reports *3*, 261-267.

Choi, P.J., Cai, L., Frieda, K., and Xie, X.S. (2008). A stochastic single-molecule event triggers phenotype switching of a bacterial cell. Science *322*, 442-446.

Chung, C.T., Niemela, S.L., and Miller, R.H. (1989). One-step preparation of competent Escherichia coli: transformation and storage of bacterial cells in the same solution. Proc Natl Acad Sci U S A *86*, 2172-2175.

Courvalin, P. (2005). Antimicrobial Drug Resistance: "Prediction Is Very Difficult, Especially about the Future". Emerg Infect Dis *11*, 1503-1506.

Curtis, N.A., Eisenstadt, R.L., Turner, K.A., and White, A.J. (1985). Porin-mediated cephalosporin resistance in Escherichia coli K-12. J Antimicrob Chemother *15*, 642-644.

Datsenko, K.A., and Wanner, B.L. (2000). One-step inactivation of chromosomal genes in Escherichia coli K-12 using PCR products. Proc Natl Acad Sci U S A *97*, 6640-6645.

Dekel, E., and Alon, U. (2005). Optimality and evolutionary tuning of the expression level of a protein. Nature *436*, 588-592.

Dodd, I.B., Perkins, A.J., Tsemitsidis, D., and Egan, J.B. (2001). Octamerization of lambda CI repressor is needed for effective repression of P(RM) and efficient switching from lysogeny. Genes & development *15*, 3013-3022.

Flensburg, J., and Skold, O. (1987). Massive overproduction of dihydrofolate reductase in bacteria as a response to the use of trimethoprim. European journal of biochemistry / FEBS *162*, 473-476.

Girgis, H.S., Hottes, A.K., and Tavazoie, S. (2009). Genetic architecture of intrinsic antibiotic susceptibility. PLoS One *4*, e5629.

Henderson, T.A., Young, K.D., Denome, S.A., and Elf, P.K. (1997). AmpC and AmpH, proteins related to the class C beta-lactamases, bind penicillin and contribute to the normal morphology of Escherichia coli. J Bacteriol *179*, 6112-6121.

Hillenmeyer, M.E., Fung, E., Wildenhain, J., Pierce, S.E., Hoon, S., Lee, W., Proctor, M., St Onge, R.P., Tyers, M., Koller, D.*, et al.* (2008). The chemical genomic portrait of yeast: uncovering a phenotype for all genes. Science *320*, 362-365.

Kishony, R., and Leibler, S. (2003). Environmental stresses can alleviate the average deleterious effect of mutations. J Biol *2*, 14.

Kitagawa, M., Ara, T., Arifuzzaman, M., Ioka-Nakamichi, T., Inamoto, E., Toyonaga, H., and Mori, H. (2005). Complete set of ORF clones of Escherichia coli ASKA library (a complete set of E. coli K-12 ORF archive): unique resources for biological research. DNA Res *12*, 291-299.

Koutsolioutsou, A., Pena-Llopis, S., and Demple, B. (2005). Constitutive soxR mutations contribute to multiple-antibiotic resistance in clinical Escherichia coli isolates. Antimicrob Agents Chemother *49*, 2746-2752.

Maneewannakul, K., and Levy, S.B. (1996). Identification for mar mutants among quinolone-resistant clinical isolates of Escherichia coli. Antimicrob Agents Chemother *40*, 1695-1698.

Martin, R.G., and Rosner, J.L. (2002). Genomics of the marA/soxS/rob regulon of Escherichia coli: identification of directly activated promoters by application of molecular genetics and informatics to microarray data. Mol Microbiol *44*, 1611-1624.

Morar, M., and Wright, G.D. (2010). The genomic enzymology of antibiotic resistance. Annual review of genetics *44*, 25-51.

Nakanishi, A., Oshida, T., Matsushita, T., Imajoh-Ohmi, S., and Ohnuki, T. (1998). Identification of DNA gyrase inhibitor (GyrI) in Escherichia coli. The Journal of biological chemistry *273*, 1933-1938.

Nichols, R.J., Sen, S., Choo, Y.J., Beltrao, P., Zietek, M., Chaba, R., Lee, S., Kazmierczak, K.M., Lee, K.J., Wong, A., *et al.* (2011). Phenotypic landscape of a bacterial cell. Cell *144*, 143-156.

Novick, A., and Weiner, M. (1957). Enzyme Induction as an All-or-None Phenomenon. Proc Natl Acad Sci U S A *43*, 553-566.

Oh, T.J., Jung, I.L., and Kim, I.G. (2001). The Escherichia coli SOS gene sbmC is regulated by H-NS and RpoS during the SOS induction and stationary growth phase. Biochemical and biophysical research communications *288*, 1052-1058.

Palmer, A.C., Angelino, E., and Kishony, R. (2010). Chemical decay of an antibiotic inverts selection for resistance. Nat Chem Biol *6*, 105-107.

Soo, V.W., Hanson-Manful, P., and Patrick, W.M. (2011). Artificial gene amplification reveals an abundance of promiscuous resistance determinants in Escherichia coli. Proc Natl Acad Sci U S A *108*, 1484-1489.

Stoebel, D.M., Dean, A.M., and Dykhuizen, D.E. (2008). The cost of expression of Escherichia coli lac operon proteins is in the process, not in the products. Genetics *178*, 1653-1660.

Tamae, C., Liu, A., Kim, K., Sitz, D., Hong, J., Becket, E., Bui, A., Solaimani, P., Tran, K.P., Yang, H., *et al.* (2008). Determination of antibiotic hypersensitivity among 4,000 single-gene-knockout mutants of Escherichia coli. J Bacteriol *190*, 5981-5988.

Chapter 4.

The dependence of antibiotic resistance on target expression

Adam C. Palmer[1] & Roy Kishony[1,2]

[1]Department of Systems Biology, Harvard Medical School, 200 Longwood Ave, Boston, MA 02115.

[2]School of Engineering and Applied Sciences, Harvard University, Cambridge, MA 02138.

Increased expression of a drug's target gene sometimes confers drug resistance; this can facilitate the evolution of drug resistance in bacteria, protozoa, and cancer, and can be used to identify drugs' molecular targets. However, it is unclear why this phenomena occurs with some drugs but not others. Here we quantitatively over-expressed *Escherichia coli* genes encoding antibiotic targets and observed that drug resistance does not only increase: it can remain unchanged, decrease, or first increase and then decrease. We explain these effects with simple models of drug action that consider toxicity from gene over-expression, and drugs that do not inhibit an enzyme but instead induce harmful enzyme-catalyzed reactions. The relation between drug resistance and target expression may reveal unexpectedly complex mechanisms of drug action.

Many drugs that inhibit an enzyme's function can be resisted by over-expression of the gene encoding their target protein. For drugs where this is true, this principle has two important effects. Firstly, disease-causing organisms from bacteria to tumor cells can evolve strong drug resistance by gene amplification or over-expression of the drug's target (Chen et al., 2009; Coderre et al., 1983; Flensburg and Skold, 1987; Schimke et al., 1978; Then, 1982). Secondly, the molecular target of the drug can be identified by a genetic screen for over-expression mutants that are drug resistant (Banerjee et al., 1994; Belanger et al., 1996; Luesch et al., 2005; Payne et al., 2004; Rine et al., 1983; Tokunaga et al., 1983). Resistance by target over-expression is common but not universal, and despite its importance in the evolution of drug resistance and as a tool in drug discovery, it remains unclear why this property applies to some drugs but not others. Here we use antibiotics of known mechanisms in *Escherichia coli* as a case study to understand the general factors that enable or prevent the acquisition of drug resistance by target over-expression.

The principle of resistance through target over-expression is most relevant for drugs with a single protein target. There are three broad mechanisms of action in which a drug does *not* act on a single protein target: (1) drugs may target multi-protein complexes (e.g. ribosome, RNA polymerase, or proteasome inhibitors), (2) a drug's efficacy may rely upon polypharmacology (e.g. many beta-lactams and kinase inhibitors), and (3) drugs may act primarily upon non-protein targets (e.g. polymyxins, nitrofurans, vancomycin, DNA intercalators, artemisinin). It is easy to understand that for these mechanisms, resistance cannot result from over-expression of 'the target gene' for the simple reason that no such gene

can be defined. We therefore focused on drugs that primarily target a single protein and investigated how drug resistance changes when the target gene is over-expressed.

We selected six antibiotics that primarily target a single protein, spanning a variety of essential targets (Table 1; for two drugs we investigated both the primary and a secondary target). For each drug we constructed a strain expressing the target gene from an IPTG-inducible promoter (Figure 4.1a) (Kitagawa et al., 2005). This target over-expression strain was grown in liquid cultures spanning two dimensional gradients of drug-dose and IPTG-induced gene expression; the latter was quantified by beta-galactosidase assays of a strain expressing *lacZ* in place of a drug target (Supplementary Figure 4.1). A sensitive bioluminescence-based assay was used to measure bacterial growth rates and thereby to determine how drug susceptibility is altered as a function of target gene expression.

Table 1. List of drugs and drug targets utilized in this study. * indicates primary target when there is a secondary target of lower affinity or lesser importance to growth (Drlica and Zhao, 1997; Kong et al., 2010).

Drug name	Target	Target function	Target process	Gene
Trimethoprim	DHFR	Dihydrofolate reductase	Folate synthesis	*folA*
Sulfamethoxazole	DHPS	Dihydropteroate synthase	Folate synthesis	*folP*
Triclosan	ENR	Enoyl acyl carrier protein reductase	Fatty acid synthesis	*fabI*
Ciprofloxacin	Gyrase * Topo IV	DNA gyrase Topoisomerase IV	DNA replication	*gyrA* *parC*
Cefsulodin	PBP1A PBP1B *	Murein polymerase Murein polymerase	Cell wall synthesis	*mrcA* *mrcB*
Mecillinam	PBP2	Peptidoglycan transpeptidase	Cell wall synthesis	*mrdA*

Over-expression of a drug's target gene had qualitatively different effects on drug resistance for different drugs (Figure 4.1b). The drug concentration that inhibits growth by 50% (IC50) was increased by expressing the targets of trimethoprim (DHFR) and triclosan (ENR), and decreased when expressing the targets of cefsulodin (PBP1A, PBP1B) and ciprofloxacin (Gyrase, Topo IV). Resistance to sulfamethoxazole, a sulfonamide-class antibiotic, was independent of its target (DHPS) expression level, and most curiously, the IC50 of mecillinam increased with mild over-expression of its target (PBP2) but decreased with stronger over-expression.
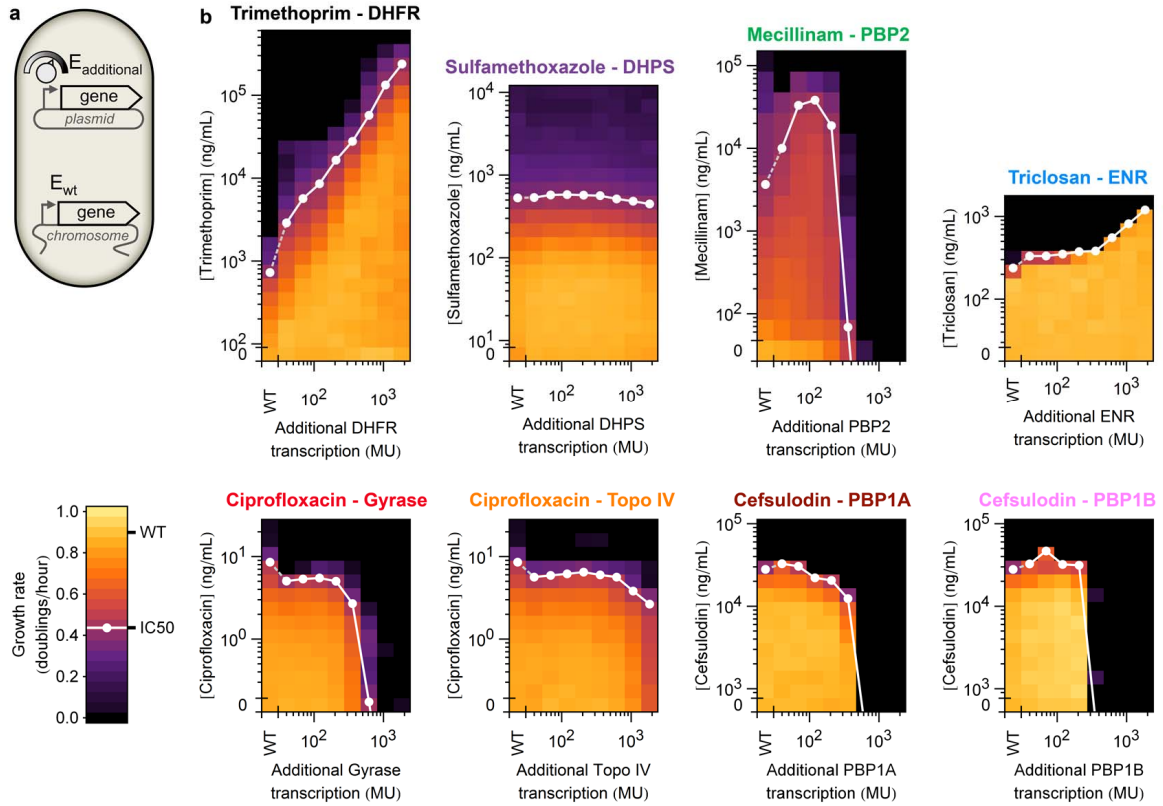
Figure 4.1. Over-expression of a drug's target gene can increase, decrease, or have no effect on drug resistance. (**a**) *E. coli* strains were constructed with IPTG adjustable over-expression of drug target genes. (**b**) For each drug-gene pair, bacterial growth rates were measured over gradients of drug dose (vertical axis) and IPTG-induced gene dose (horizontal axis). Additional target expression is quantified in Miller Units (MU) from kinetic beta-galactosidase assays of a matching plasmid encoding *lacZ* (Supplementary Figure 4.1). Heatmap color indicates growth rate, from uninhibited growth (yellow) to no growth (black). WT denotes a strain without any additional drug target expression, since its plasmid contains neither a promoter nor a drug target gene. At each level of gene expression, the drug concentration that inhibits growth to 50% of the uninhibited wildtype growth (IC50) is overlaid in white.

Figure 4.1. Over-expression of a drug's target gene can increase, decrease, or have no effect on drug resistance. (Continued)

There was no trend within target pathways as to which target genes conferred drug resistance upon over-expression; for example both DHPS and DHFR are enzymes in the folate biosynthesis pathway, but only DHFR confers resistance to its inhibitor when over-expressed. These observations are consistent with clinical isolates of drug resistant bacteria: trimethoprim resistant mutants have been reported with promoter mutations and elevated DHFR expression (Flensburg and Skold, 1987; Then, 1982), but DHPS regulatory mutations have not been reported in sulfonamide resistant mutants, despite characterization of many resistant mutants (Skold, 2000). Similar supportive results have also been observed for triclosan where resistant mutants have been found with elevated ENR expression (Chen et al., 2009), and for ciprofloxacin where, while amino acid changes in Gyrase and Topoisomerase IV are associated with resistance, no regulatory mutations have been reported (Ruiz, 2003).

We sought to understand the relation between drug resistance and drug target expression levels using simple mathematical models of the fitness costs of gene expression and enzyme inhibition. We define the target enzyme concentration as the sum of a wildtype level of enzyme (E_{wt}) and an additional amount ($E_{additional}$). We built mass action models of competitive and non-competitive inhibition and calculated drug susceptibility under the simplifying assumption that 50% growth inhibition (IC50) occurs when the net flux through an essential enzyme is 50% inhibited. Both the competitive and non-competitive inhibition models yield a linear dependence of IC50 on the fold over-production of the enzyme: $IC50/IC50_{wt} = 2 \times (E_{wt}+E_{additional}) / E_{wt} - 1$ (Figure 4.2a, h^-; Supplementary Figure 4.2a,b). For example, if the enzyme is over-expressed 100-fold then 99.5% of the enzyme will have to be

inhibited in order to have half of the flux of the wild-type, which will require 200 times more drug. We observed that many drug targets incurred small to lethal fitness costs when over-expressed, even in the absence of drug (Figure 4.1b). When the models include the fitness cost of over-expression as an independent mechanism of toxicity (treated as a second drug that is 'Bliss additive' with the actual drug(Bliss, 1939)), we find that $IC50/IC50_{wt} = 2 \times (E_{wt} + E_{additional}) / E_{wt} \times (1 - \text{cost}(E_{additional}) - 1$ (Figure 4.2a, $h^- c^+$; Supplementary Figure 4.2a,b). This simple model quantitatively explains the increase in resistance from over-expressing the targets of both trimethoprim (DHFR) and triclosan (ENR) (Figure 4.2b, $h^- c^-$), as well as the increase and subsequent decrease in IC50 resulting from over-expression of mecillinam's target (PBP2) (Figure 4.2b, $h^- c^+$). Thus, drug target over-expression can confer resistance by compensating for inhibited target genes, but the potential for resistance may be limited if target gene over-expression is costly. Additionally, the level of resistance depends on the magnitude of E_{wt}, which can explain the differences between trimethoprim and triclosan (Supplementary Figure 4.3).

If drug target over-expression induces large fitness costs before there is a significant fold-increase in expression, then there might be no expression level that increases drug resistance. This alone might explain the lack of resistance from over-expressing the targets of ciprofloxacin and cefsulodin, but it cannot explain the absence of sulfamethoxazole resistance, whose target DHPS incurs no significant fitness cost upon over-expression. Sulfonamide antibiotics inhibit the synthesis of dihydropteroate from pteridine diphosphate

and para-aminobenzoic acid (PABA) by competing with PABA for binding to the enzyme DHPS(Brown, 1962). Interestingly, sulfonamides do not simply inhibit DHPS, but are covalently attached to pteridine diphosphate in place of PABA, yielding a dihydropterin-sulfonamide product (Bock et al., 1974; Roland et al., 1979) (Supplementary Figure 4.4). While dihydropterin-sulfonamide is not toxic to *E. coli* (Roland et al., 1979), this reaction is harmful to growth by depleting the essential metabolite pteridine diphosphate. We modeled this system treating pteridine diphosphate as being synthesized at a constant rate by the upstream folate synthesis enzymes, and consumed by DHPS-catalyzed condensation to dihydropteroate or dihydropterin-sulfonamide. Strikingly, this model shows that when a drug induces a harmful enzyme-catalyzed reaction with a rate-limiting substrate, pathway inhibition is independent of the enzyme concentration (Figure 4.2a, h^+; Supplementary Figure 4.2c). Taking sulfonamides as an example, the fraction of pteridine diphosphate that is converted to the correct product dihydropteroate is defined not by the abundance of uninhibited enzyme, but only by the ratio of sulfonamide to PABA. This result is consistent with the observation that increased PABA synthesis confers sulfonamide resistance (Landy et al., 1943) and explains why, in contrast, increased expression of DHPS confers no protection against a sulfonamide (Figure 4.2b, h^+c^-). Sulfonamides may thus be more accurately described as poisons that deplete pteridine diphosphate, rather than inhibitors of DHPS. While this modeling framework is not appropriate to describe the DNA damage that results from the binding of ciprofloxacin to Gyrase or Topo IV near the DNA replication fork, it nonetheless illustrates a principle that applies to ciprofloxacin and other drugs: drugs that

only inhibit an enzyme's catalytic activity may be resisted by additional enzyme production, while drugs that induce an enzyme to catalyze harmful reactions will not be resisted by an excess of that enzyme; to this category belongs antibiotics such as aminoglycosides (Davis, 1987), fluoroquinolones (Pan et al., 2001), and sulfonamides. Indeed, the over-expression of a drug target that does not confer resistance but does incur fitness costs will only decrease drug resistance (Figure 4.2b, h^+c^+).

Figure 4.2. Over-expression of drug target genes can confer both resistance and fitness costs, resulting in diverse changes in drug resistance. a, Mass-action models of enzyme inhibition quantified the relation between drug concentration, growth inhibition, and enzyme expression (wildtype enzyme abundance = E_{wt}, additional enzyme = $E_{additional}$). Drug-induced growth inhibition and fitness costs due to gene over-expression are treated as independent mechanisms of toxicity. Changes in the drug concentration that inhibits growth by 50% (IC50) are found to depend upon two factors: whether drug binding only inhibits the enzyme (h^-) or also induces harmful reactions when bound (h^+), and the degree of fitness costs from additional drug target expression; for example lethal, partial, or no fitness costs (c^+ *lethal* / c^+*partial* / c^-). Mechanistic models demonstrate that drug target over-expression protects against enzyme inhibitors (h^-), but not against drugs that damage an enzyme's substrate (h^+) (Supplementary Figure 4.2). **b**, The theory presented in (**a**) results in diverse changes in drug resistance as drug targets are over-expressed. Possible changes in drug resistance upon drug target over-expression include an increase, decrease, first increase then decrease, or no change; differences in E_{wt} influence the level of resistance that may be achieved. This theory rationalizes the diverse experimentally observed behaviors (IC50 lines from Figure 4.1b).
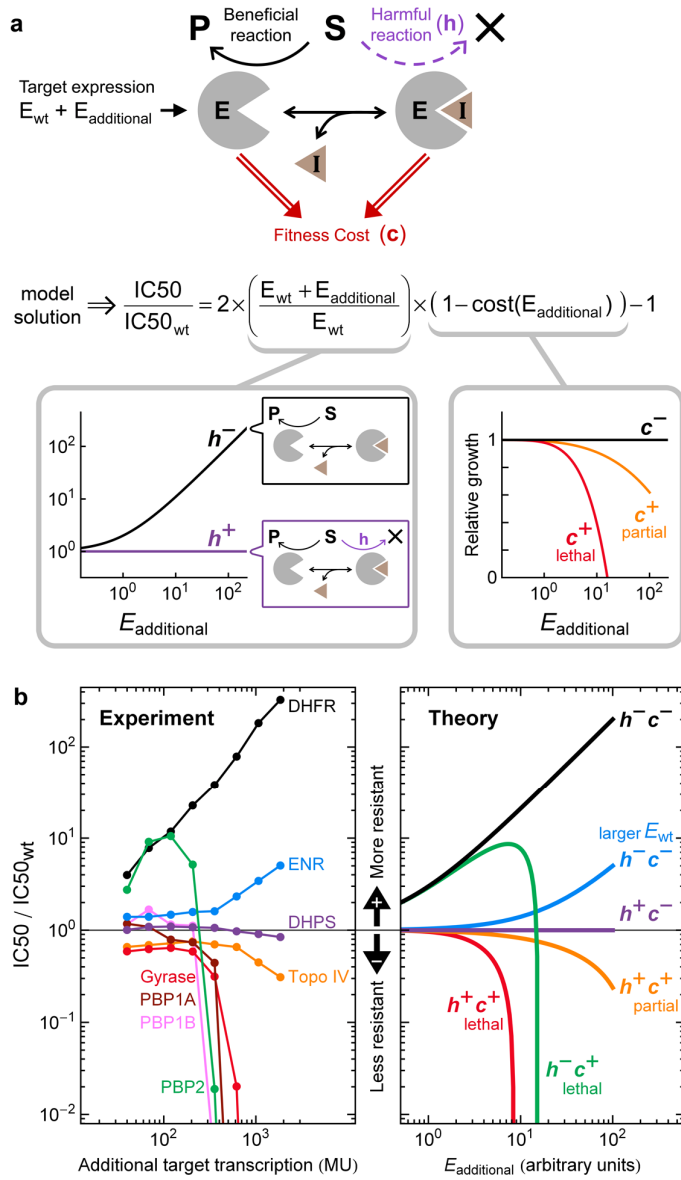
Figure 4.2. Over-expression of drug target genes can confer both resistance and fitness costs, resulting in diverse changes in drug resistance. (Continued)

This study shows that increasing the expression of drug's target gene can have a wide range of effects on resistance to that drug; the simple expectation that resistance will monotonically increase is one of several possibilities. These diverse effects can be understood as the result of two factors: firstly whether a drug solely inhibits a beneficial reaction or induces a harmful reaction; and secondly whether drug target over-expression incurs fitness costs. These results suggest that efforts to identify the molecular targets of compounds by searching for drug resistance via target over-expression will, for better or worse, yield predictably biased results. This approach will succeed in identifying the targets of compounds that are strictly an inhibitor of a single non-costly gene, but may fail for compounds that inhibit costly genes, that act upon multiple targets, or that induce harmful reactions such as damaging a substrate. However, unexpectedly complex mechanisms of drug action can be revealed if the over-expression of a known drug target fails to confer resistance. Finally, these results suggest that the development of compounds that inhibit costly genes, or that inhibit a pathway by damaging pathway-essential metabolites, will produce drugs less prone to the evolution of resistance through target over-expression.

Acknowledgements

Author Contributions

A.C.P and R.K. designed research; A.C.P. performed research, analyzed data, and built mathematical models; A.C.P. and R.K. wrote the manuscript.

Methods

Strains and Media

E. coli strain BW25113 was the host for all studies(Datsenko and Wanner, 2000). As *lacZYA* is deleted in BW25113, IPTG does not incur fitness costs for *lacZYA* production(Stoebel et al., 2008), and graded induction is possible without the LacY permease, that would otherwise cause all-or-none induction of LacI-regulated promoters(Choi et al., 2008; Novick and Weiner, 1957). BW25113 was transformed with plasmid pCSλ, encoding a constitutively expressed bacterial bioluminescence operon(Kishony and Leibler, 2003). Plasmids encoding each target gene (in a pCA24N backbone) were obtained from the ASKA *E. coli* Open Reading Frame collection(Kitagawa et al., 2005), sequenced to confirm gene identity, and were transformed into BW25113 pCSλ. The cefsulodin target gene PBP1B (*mrcB*) was not found at the expected position in the ASKA collection, and was instead isolated by plating a pooled mixture of the entire ASKA collection on 1.5% agar plates of Luria Bertani broth with a range of isopropyl β-D-1-thiogalactopyranoside (IPTG) concentrations, and screening for colonies resistant to a 100µg point source of cefsulodin. At 15µM IPTG, many mildly resistant colonies were isolated that carried pCA24N plasmids encoding PBP1B, according to sequencing. This IPTG concentration corresponds to the point in Figure 4.1B where PBP1B over-expression confers modest cefsulodin resistance. Wildtype drug susceptibilities were determined using a matching strain with no additional drug target gene expression; BW25113 pCSλ pCA24N-Δpromoter-*yfp*; where the IPTG-inducible promoter in pCA24N had been deleted, and yellow fluorescent protein was encoded in place of a drug target gene. All

experiments were performed in M63 minimal medium (2g.L^{-1} (NH$_4$)$_2$SO$_4$, 13.6g.L^{-1} KH$_2$PO$_4$, 0.5mg.L^{-1} FeSO$_4$•7H2O, adjusted to pH 7.0 with KOH) supplemented with 0.2% glucose, 0.01% casamino acids, 1mM MgSO$_4$ and 0.5mg.L^{-1} thiamine, and also 10mg.L^{-1} chlorampenicol and 25mg.L^{-1} kanamycin for the maintenance of the pCA24N and pCSλ plasmids, respectively. Drug solutions were made from powder stocks (from Sigma Aldrich unless otherwise specified: cefsulodin, C8145; chloramphenicol, C0378; ciprofloxacin, 17850; isopropyl β-D-1-thiogalactopyranoside (IPTG), Omega Bio-Tek AC121; kanamycin, K1876; mecillinam, 33447; ortho-nitrophenyl-β-galactoside, N1127; polymyxin-B, P0972; sulfamethoxazole, S7507; triclosan, TCI America T1872; trimethoprim, T7883). Drug and IPTG gradients were made by serial dilution in M63 medium.

Growth rate assay

The constitutive bioluminescence that results from pCSλ enables cell densities in growing cultures to be precisely measured over many orders of magnitude by photon counting(Kishony and Leibler, 2003). Cultures were grown in black 96-well plates with white wells (Perkin Elmer 6005039) sealed with clear adhesive lids (Perkin Elmer 6005185). Wells contained 200μL of media inoculated with approximately 100 to 300 cells from freshly thawed -80°C frozen cultures. Plates were grown in a 30°C room at 70% humidity, and growth was assayed by a Perkin Elmer TopCount NXT Microplate Scintillation and Luminescence Counter that measured each well for 1 second. Experiments of 10 to 16 plates allowed each plate to be measured every 30 to 50 minutes. Plate stacks were ventilated by fans to eliminate spatial temperature gradients and ensure uniform growth conditions across each plate. In

each experiment, distributed throughout the plate stack were 3 control plates of uniform media conditions to verify the absence of growth rate gradients within plates or across the plate stack. Growth rate is the slope of the logarithm of photon counts per second (c.p.s.), and is taken from the fastest growing line of best fit observed in any 6 hour timespan; this time corresponds to 5 doublings of a healthy culture. The slope of the logarithm of c.p.s. is unaffected by changes in luminescence per cell, such as might result from antibiotic treatments or changes in gene expression(Kishony and Leibler, 2003).

Beta-galactosidase assay

The transcription rates of genes encoded in the pCA24N plasmid at different IPTG concentrations were measured by kinetic beta-galactosidase (LacZ) assays of pCA24N-*lacZ*, using a method adapted from (Dodd et al., 2001). Liquid cultures of BW25113 pCA24N-*lacZ* were prepared in a 96-well plate in the same manner as for growth rate assays. The plate was incubated at 30°C with shaking until the plate average OD_{600} equalled 0.1 (mid log phase), as measured by a Perkin Elmer Victor plate reader. 20μL of each well was promptly transferred to the corresponding well of a microtiter plate pre-warmed to 30°C, in which each well contained 30μL of sterile media and 190μL of lysis / assay buffer, consisting of 100mM Tris-HCl pH 8.0, 1mM $MgSO_4$, 10mM KCl, 10g.L^{-1} β-mercaptoethanol, 100mg.L^{-1} polymyxin B, and 850mg.L^{-1} ortho-nitrophenyl-β-galactoside. The lysis / assay plate was transferred to a Tecan Sunrise plate reader in a 30°C room at 70% humidity, and OD_{410} was measured every minute for 2 hours, with 20 seconds of shaking between each reading. For each well,

promoter activity in Miller Units was calculated from the slope of OD_{410} versus time, multiplied by 200,000, divided by the OD_{600} of the culture that was transferred to that well, and divided by the volume (in μL) of the culture assayed (here 20μL) (Supplementary Figure 4.1).

References

Banerjee, A., Dubnau, E., Quemard, A., Balasubramanian, V., Um, K.S., Wilson, T., Collins, D., de Lisle, G., and Jacobs, W.R., Jr. (1994). inhA, a gene encoding a target for isoniazid and ethionamide in Mycobacterium tuberculosis. Science *263*, 227-230.

Belanger, A.E., Besra, G.S., Ford, M.E., Mikusova, K., Belisle, J.T., Brennan, P.J., and Inamine, J.M. (1996). The embAB genes of Mycobacterium avium encode an arabinosyl transferase involved in cell wall arabinan biosynthesis that is the target for the antimycobacterial drug ethambutol. Proceedings of the National Academy of Sciences of the United States of America *93*, 11919-11924.

Bliss, C.I. (1939). The toxicity of poisons applied jointly. Ann Appl Biol *26*, 585-615.

Bock, L., Miller, G.H., Schaper, K.J., and Seydel, J.K. (1974). Sulfonamide structure-activity relationships in a cell-free system. 2. Proof for the formation of a sulfonamide-containing folate analog. Journal of medicinal chemistry *17*, 23-28.

Brown, G.M. (1962). The biosynthesis of folic acid. II. Inhibition by sulfonamides. The Journal of biological chemistry *237*, 536-540.

Chen, Y., Pi, B., Zhou, H., Yu, Y., and Li, L. (2009). Triclosan resistance in clinical isolates of Acinetobacter baumannii. Journal of medical microbiology *58*, 1086-1091.

Choi, P.J., Cai, L., Frieda, K., and Xie, X.S. (2008). A stochastic single-molecule event triggers phenotype switching of a bacterial cell. Science *322*, 442-446.

Coderre, J.A., Beverley, S.M., Schimke, R.T., and Santi, D.V. (1983). Overproduction of a bifunctional thymidylate synthetase-dihydrofolate reductase and DNA amplification in methotrexate-resistant Leishmania tropica. Proceedings of the National Academy of Sciences of the United States of America *80*, 2132-2136.

Datsenko, K.A., and Wanner, B.L. (2000). One-step inactivation of chromosomal genes in Escherichia coli K-12 using PCR products. Proceedings of the National Academy of Sciences of the United States of America *97*, 6640-6645.

Davis, B.D. (1987). Mechanism of bactericidal action of aminoglycosides. Microbiological reviews *51*, 341-350.

Dodd, I.B., Perkins, A.J., Tsemitsidis, D., and Egan, J.B. (2001). Octamerization of lambda CI repressor is needed for effective repression of P(RM) and efficient switching from lysogeny. Genes & development *15*, 3013-3022.

Drlica, K., and Zhao, X. (1997). DNA gyrase, topoisomerase IV, and the 4-quinolones. Microbiology and molecular biology reviews : MMBR *61*, 377-392.

Flensburg, J., and Skold, O. (1987). Massive overproduction of dihydrofolate reductase in bacteria as a response to the use of trimethoprim. European journal of biochemistry / FEBS *162*, 473-476.

Kishony, R., and Leibler, S. (2003). Environmental stresses can alleviate the average deleterious effect of mutations. Journal of biology *2*, 14.

Kitagawa, M., Ara, T., Arifuzzaman, M., Ioka-Nakamichi, T., Inamoto, E., Toyonaga, H., and Mori, H. (2005). Complete set of ORF clones of Escherichia coli ASKA library (a complete set of E. coli K-12 ORF archive): unique resources for biological research. DNA research : an international journal for rapid publication of reports on genes and genomes *12*, 291-299.

Kong, K.F., Schneper, L., and Mathee, K. (2010). Beta-lactam antibiotics: from antibiosis to resistance and bacteriology. APMIS : acta pathologica, microbiologica, et immunologica Scandinavica *118*, 1-36.

Landy, M., Larkum, N.W., Oswald, E.J., and Streightoff, F. (1943). Increased synthesis of p-aminobenzoic acid associated with the development of sulfonamide resistance in staphylococcus aureus. Science *97*, 265-267.

Luesch, H., Wu, T.Y., Ren, P., Gray, N.S., Schultz, P.G., and Supek, F. (2005). A genome-wide overexpression screen in yeast for small-molecule target identification. Chemistry & biology *12*, 55-63.

Novick, A., and Weiner, M. (1957). Enzyme Induction as an All-or-None Phenomenon. Proceedings of the National Academy of Sciences of the United States of America *43*, 553-566.

Pan, X.S., Yague, G., and Fisher, L.M. (2001). Quinolone resistance mutations in Streptococcus pneumoniae GyrA and ParC proteins: mechanistic insights into quinolone action from enzymatic analysis, intracellular levels, and phenotypes of wild-type and mutant proteins. Antimicrobial agents and chemotherapy *45*, 3140-3147.

Payne, D.J., Gwynn, M.N., Holmes, D.J., and Rosenberg, M. (2004). Genomic approaches to antibacterial discovery. Methods Mol Biol *266*, 231-259.

Rine, J., Hansen, W., Hardeman, E., and Davis, R.W. (1983). Targeted selection of recombinant clones through gene dosage effects. Proceedings of the National Academy of Sciences of the United States of America *80*, 6750-6754.

Roland, S., Ferone, R., Harvey, R.J., Styles, V.L., and Morrison, R.W. (1979). The characteristics and significance of sulfonamides as substrates for Escherichia coli dihydropteroate synthase. The Journal of biological chemistry *254*, 10337-10345.

Ruiz, J. (2003). Mechanisms of resistance to quinolones: target alterations, decreased accumulation and DNA gyrase protection. The Journal of antimicrobial chemotherapy *51*, 1109-1117.

Schimke, R.T., Kaufman, R.J., Alt, F.W., and Kellems, R.F. (1978). Gene amplification and drug resistance in cultured murine cells. Science *202*, 1051-1055.

Skold, O. (2000). Sulfonamide resistance: mechanisms and trends. Drug resistance updates : reviews and commentaries in antimicrobial and anticancer chemotherapy *3*, 155-160.

Stoebel, D.M., Dean, A.M., and Dykhuizen, D.E. (2008). The cost of expression of Escherichia coli lac operon proteins is in the process, not in the products. Genetics *178*, 1653-1660.

Then, R.L. (1982). Mechanisms of resistance to trimethoprim, the sulfonamides, and trimethoprim-sulfamethoxazole. Reviews of infectious diseases *4*, 261-269.

Tokunaga, M., Loranger, J.M., and Wu, H.C. (1983). Isolation and characterization of an Escherichia coli clone overproducing prolipoprotein signal peptidase. The Journal of biological chemistry *258*, 12102-12105.

Supplementary Material for Chapter 1.

Chemical decay of an antibiotic inverts selection for resistance
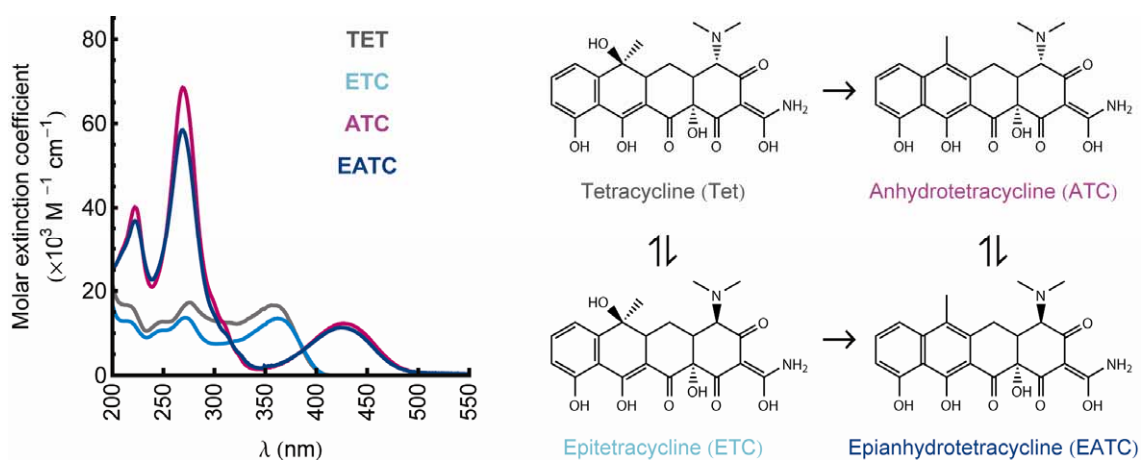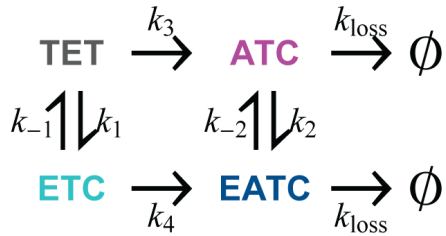

Supplementary Figure 1.1. Absorbance spectra and structures of tetracycline and its degradation products. Absorbance spectra measured in aqueous solution, at 10µg/mL, of tetracycline (Tet; gray), epitetracycline (ETC; cyan), anhydrotetracycline (ATC; magenta) and epianhydrotetracycline (EATC; dark blue).

Supplementary Figure 1.2. Measured and modeled spectra of degraded tetracycline solutions. Measured spectra of tetracycline solutions exposed to degrading conditions for different lengths of time (black), aligned with modeled spectra (gray). Modeled spectra are calculated as a linear combination of the spectra of individual compounds (Supplementary Figure 1.1), with coefficients given by the kinetic model of tetracycline decay (Supplementary Figure 1.3), which describes the proportion of each compound as a function of time in degrading conditions (see Figure 1.1c). After very prolonged degradation (t_{deg} = 2500 min) the spectrum is flat but non-zero, and so the linear combination of spectra also contains a term for the t_{deg} =2500 min spectrum, with coefficient given by the proportion of further degradation products, i.e. following further decay of ATC and EATC (denoted "∅" in the kinetic model; Supplementary Figure 1.3). The parameter k_{loss} is fitted to minimize the sum of square errors between these measured and modeled spectra. To maximize distinction between the similar spectra of epimers, errors were only summed over the most characteristic absorption peaks, located at the wavelength ranges 250-290nm and 325-400nm.
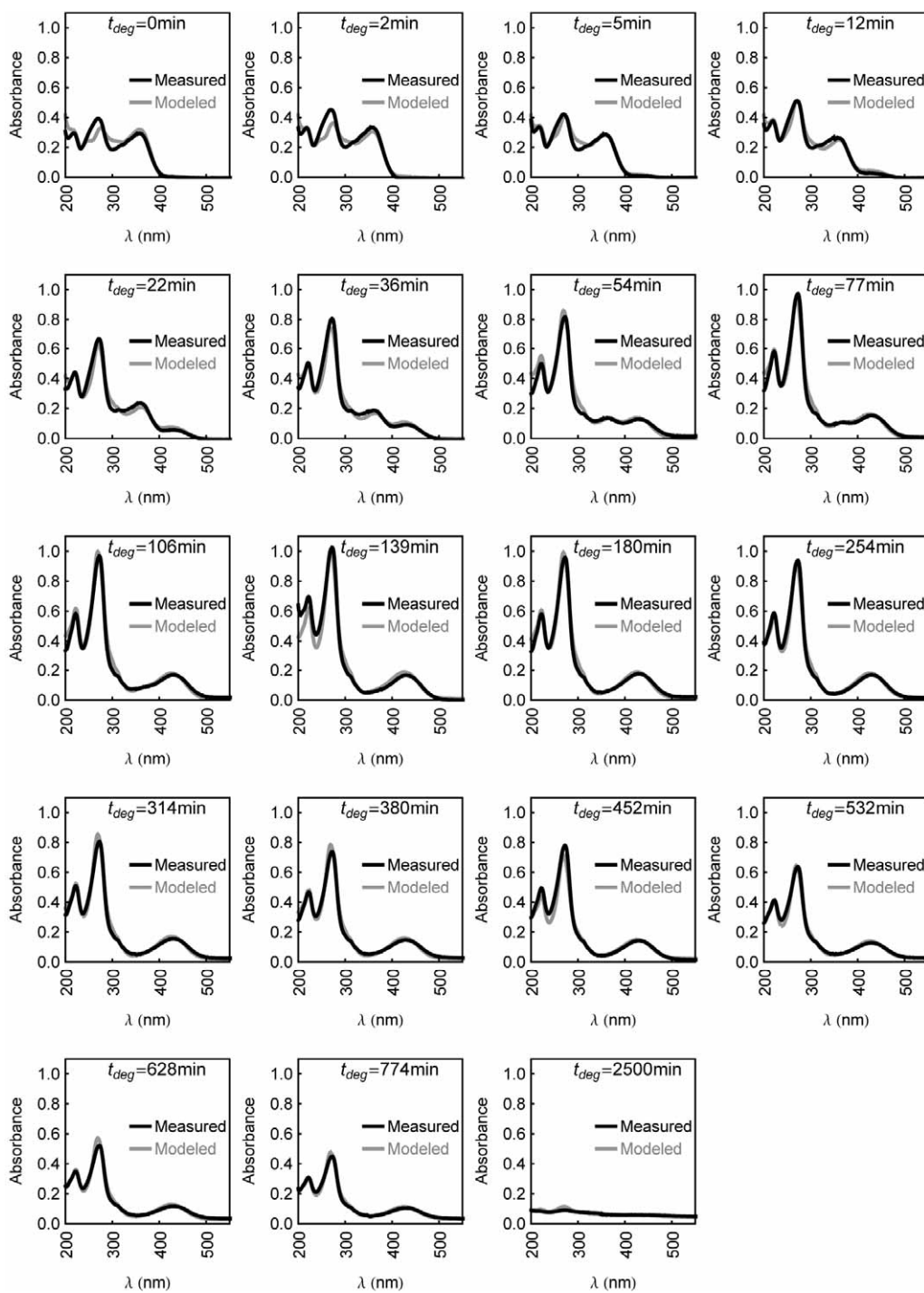
Supplementary Figure 1.2. Measured and modeled spectra of degraded tetracycline solutions. (Continued)

$$\text{TET} \xrightarrow{k_3} \text{ATC} \xrightarrow{k_{\text{loss}}} \emptyset$$

$$k_{-1} \Big\Uparrow\!\!\Downarrow k_1 \qquad k_{-2} \Big\Uparrow\!\!\Downarrow k_2$$

$$\text{ETC} \xrightarrow[k_4]{} \text{EATC} \xrightarrow[k_{\text{loss}}]{} \emptyset$$

$$\frac{\text{d[Tet]}}{\text{dt}} = k_{-1}\times[\text{ETC}] - (k_1 + k_3)\times[\text{Tet}]$$

$$\frac{\text{d[ETC]}}{\text{dt}} = k_1\times[\text{Tet}] - (k_{-1} + k_4)\times[\text{ETC}]$$

$$\frac{\text{d[ATC]}}{\text{dt}} = k_3\times[\text{Tet}] + k_{-2}\times[\text{EATC}] - (k_2 + k_{loss})\times[\text{ATC}]$$

$$\frac{\text{d[EATC]}}{\text{dt}} = k_4\times[\text{ETC}] + k_2\times[\text{ATC}] - (k_{-2} + k_{loss})\times[\text{EATC}]$$

$$\frac{\text{d}[\emptyset]}{\text{dt}} = k_{loss}\times([\text{ATC}] + [\text{EATC}])$$

Supplementary Figure 1.3. Kinetic model of tetracycline decay. Reaction scheme for the kinetic model of tetracycline decay constructed by (Yuen and Sokoloski, 1977), extended to account for the slow loss of degradation products at very long timescales (k_{loss}). The shaded areas in Figure 1.1c are constructed from this model, utilizing values of k_1, k_{-1}, k_2, k_{-2}, k_3 and k_4 which were experimentally determined by (Yuen and Sokoloski, 1977), and a fitted value of k_{loss} (Supplementary Table 1.1).

Supplementary Figure 1.4. Parameter sensitivity of the kinetic model of tetracycline decay. Plotting the error between measured and modeled spectra of degraded tetracycline solutions (Supplementary Figure 1.2) demonstrates the consistency of the rate constants measured by (Yuen and Sokoloski, 1977) with this study. Note that only the characteristic wavelength ranges 250-290nm and 325-400nm were utilized. The parameter values used in the kinetic model (Supplementary Table 1.1) are marked in red. k_{loss} was absent from the kinetic model of (Yuen and Sokoloski, 1977), and so was fitted to minimize the sum of square errors.
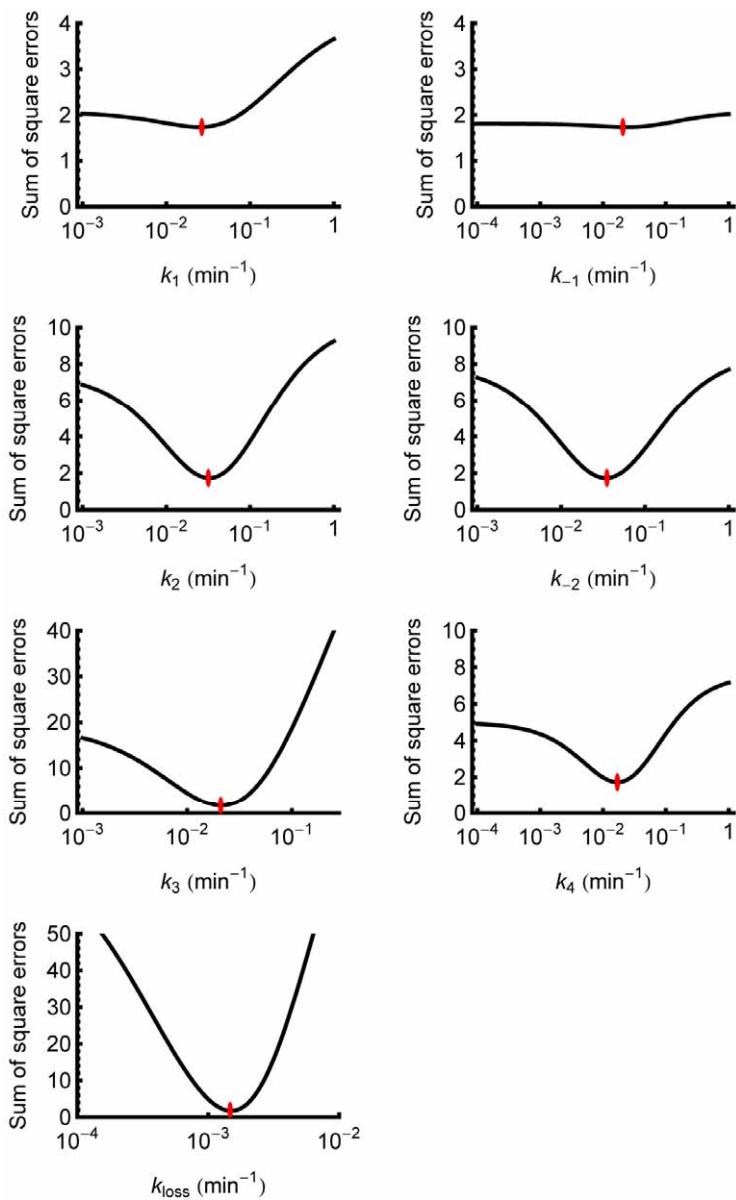
**Supplementary Figure 1.4. Parameter sensitivity of the kinetic model of tetracycline decay. (Continued)**
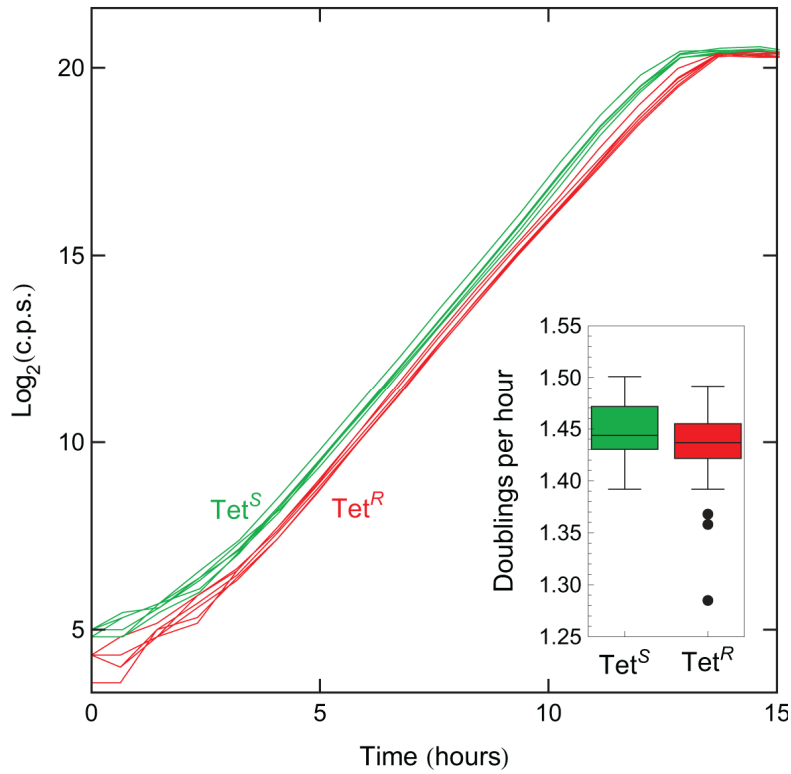
Supplementary Figure 1.5. Tet^S and Tet^R strains have equal growth rates in the absence of tetracycline. Growth rates were measured with high resolution over the course of 15 doublings using bioluminescence based measurements of cell density (Kishony and Leibler, 2003; Yeh et al., 2006) (Methods). Six representative growth curves each are presented for the Tet^S (green) and Tet^R (red) strains. Inset: Boxplot of growth rate measurements of the Tet^S and Tet^R strains (n=36 each).
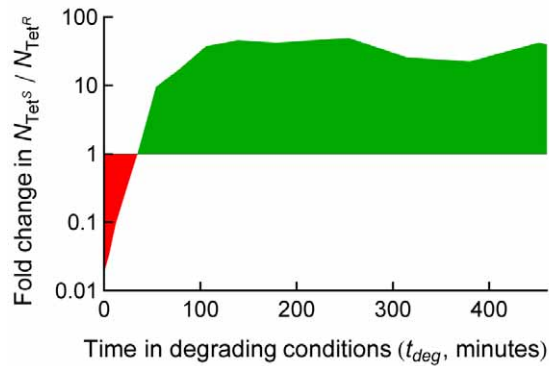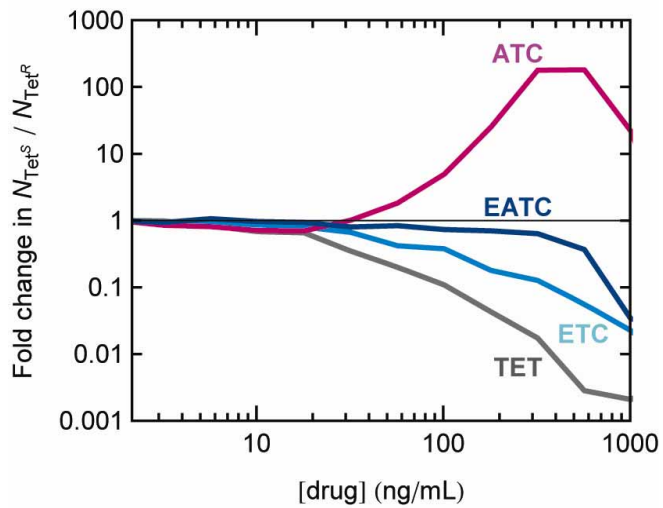
Supplementary Figure 1.6. Tetracycline degradation products and fusaric acid select against chromosomally-integrated tetracycline resistance. The cost of expression of tetracycline resistance is dependent upon the dosage of resistance genes(Lenski et al., 1994; Moyed et al., 1983). We have observed that Tet degradation products select against resistance (Fig 2c,d) when resistance is provided from a plasmid whose level of expression of the *tetA* efflux pump maximizes fitness in 10μg/mL Tet (Daniels and Bertrand, 1985; Lenski et al., 1994); Methods). When tetracycline resistance is supplied by a lower dosage of resistance genes, the extent of selection against resistance will presumably be weaker, as the phenotype approaches that of a fully sensitive strain. We therefore measured the effect Tet degradation products on competition between sensitive and resistant strains, when the Tn10 tetracycline resistance determinant was integrated in single-copy in the chromosome. In this scenario we can reproduce the net selection against resistance seen in Figure 1.2c,d (trajectory 1) when Tet degradation products (initial Tet concentration 2000 ng/mL) are supplied together with 40 μg/mL fusaric acid, a naturally-occurring compound which sensitizes bacteria to the expression of the *tetA* efflux pump(Bochner et al., 1980). Fold change in N_{tet}^S / N_{tet}^R is determined relative to wells lacking Tet or its degradation products, but containing fusaric

117

acid (Methods), and so excludes the selection imposed by fusaric acid alone, but reflects its combined effect with Tet and Tet degradation products. Fusaric acid is produced by many species of the *Fusarium* fungi (Bacon et al., 1996) and thus may be an ecologically relevant factor contributing to selection against low-copy or high-copy tetracycline resistance. In poor nutritional conditions and specific salt concentrations, fusaric acid can be made to select against tetracycline resistance in *Salmonella typhimurium* and *Escherichia coli* (Bochner et al., 1980; Maloy and Nunn, 1981). In these rich nutritional conditions, fusaric acid combined with undegraded tetracycline continues to select for resistance, but as tetracycline degrades, the combination of fusaric acid and decay products selects against resistance. This demonstrates that degradation influences the interaction between an antibiotic and its decay products (collectively) with other compounds which may conditionally select against resistance.
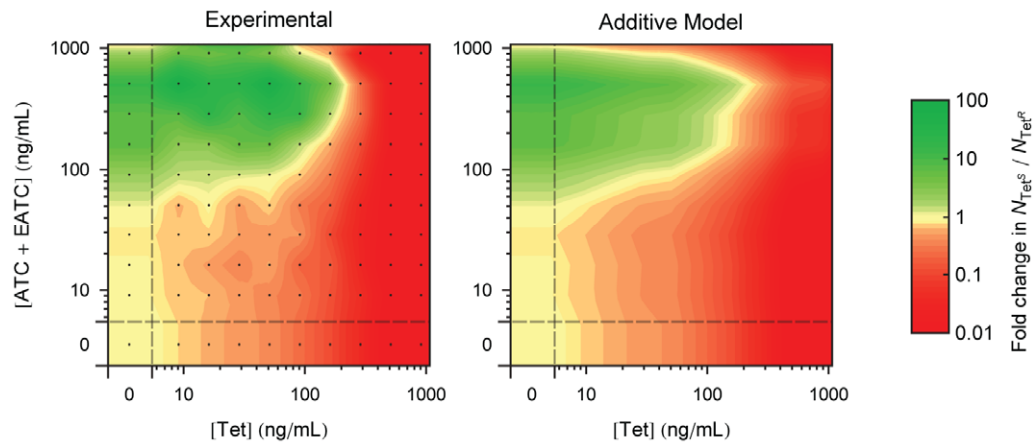
Supplementary Figure 1.7. Net selection for/against tetracycline resistance depends upon both the means of drug loss and the initial drug concentration. For any given initial drug concentration and rates of dilution and degradation (λ_{dil} and λ_{deg}, respectively), a linear trajectory is defined across the surface of Figure 1.2c, describing how selective pressure changes over time as the drug and its degradation products are lost from the environment: examples are trajectories 1, 2, and 3 from Figures 1.2c and 1.2d. Integrating $\log(N_{Tet}^S / N_{Tet}^R)$ along a trajectory provides the net selective pressure resulting from a given initial drug concentration and ratio of dilution and degradation rates, $\lambda_{dil} / \lambda_{deg}$. On the left edge of the plot drug loss is by degradation only, with the dilution rate increasing in relative magnitude towards the right; on the right edge drug loss is by dilution only. Trajectory 1 illustrates a timecourse of selection resulting in net selection against resistance. Trajectory 2 illustrates neutral net selection, where periods of selection for and against resistance cancel out over time. Trajectory 3 illustrates net selection for resistance.
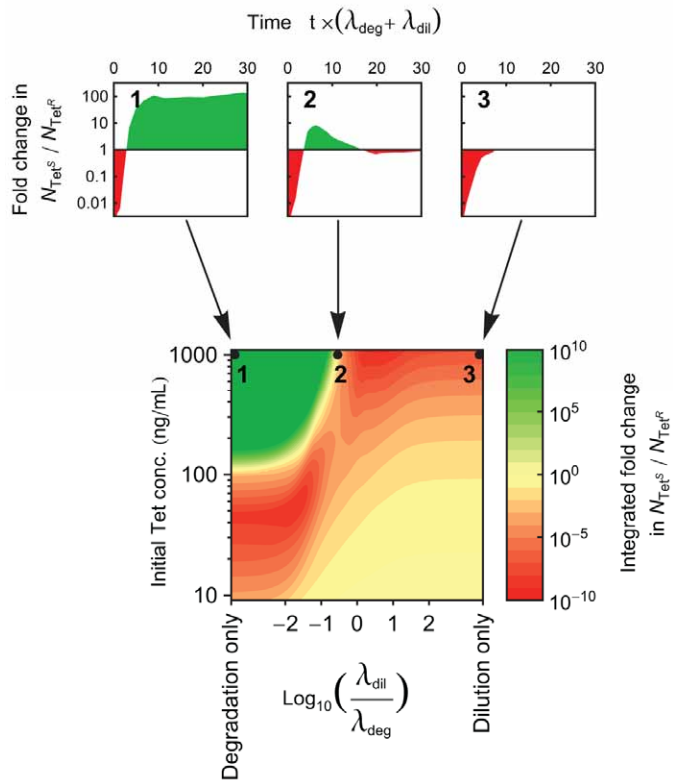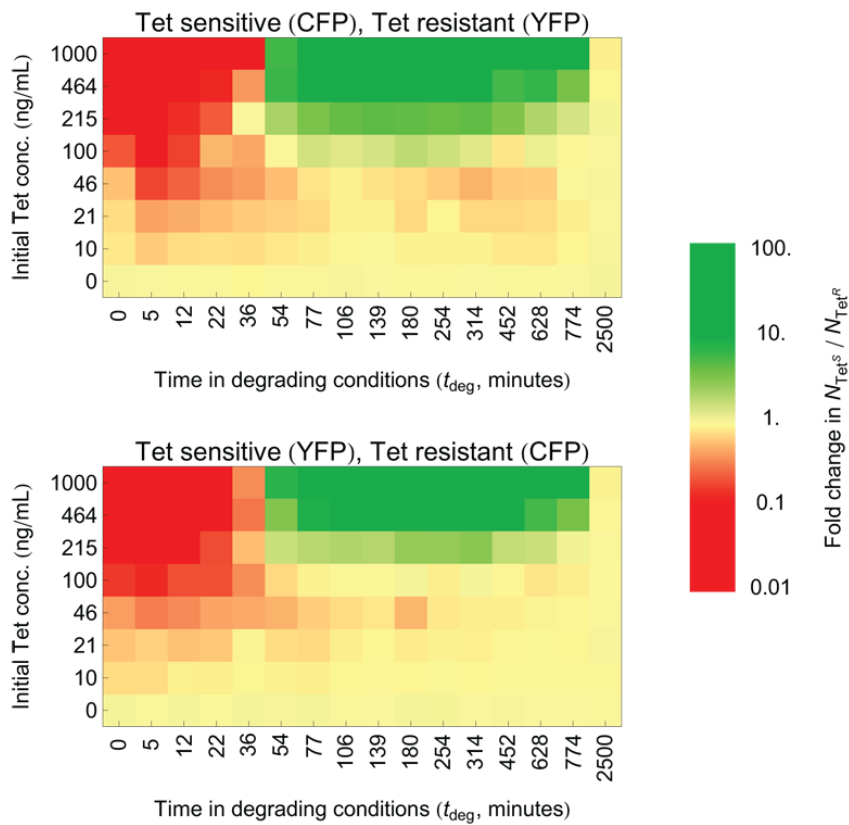
Supplementary Figure 1.7. Net selection for/against tetracycline resistance depends upon both the means of drug loss and the initial drug concentration. (Continued)

Supplementary Figure 1.8. Tetracycline and its degradation products each have a different impact on selection for resistance. Selective pressures of Tet and individual degradation products ETC, ATC, and EATC, measured by competition between Tet^S and Tet^R strains (see Figure 1.2a).
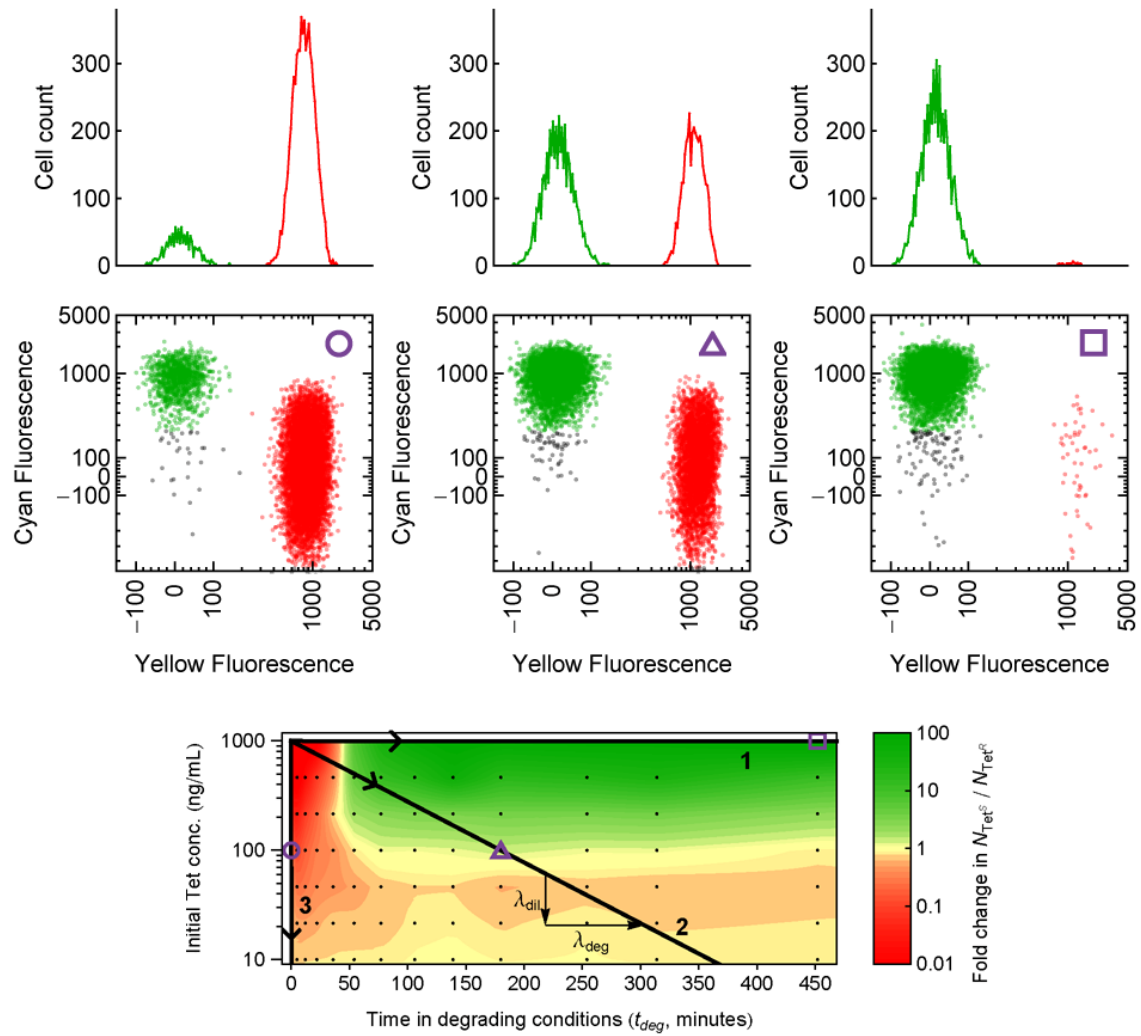
Supplementary Figure 1.9. Combinations of tetracycline and its degradation products produce selective pressures which are well predicted by Bliss additivity. Selective pressure for (red) or against (green) resistance across a drug gradient of Tet and a 1:1 mixture of ATC and EATC; on the left experimentally measured (as per Figure 1.2a) and on the right ('Additive Model') calculated from the effects along the axes of the 'Experimental' panel, assuming additive drug interactions, i.e. by summing the changes in $\log(N_{\text{Tet}}^{S} / N_{\text{Tet}}^{R})$.

Supplementary Figure 1.10. Different permutations of fluorescent labels do not influence selection for/against resistance by tetracycline degradation products. Selective pressure for (red) or against resistance (green) by Tet and its degradation products (Figure 1.2c) was measured by averaging the results of two competition experiments: between Tet^S-CFP and Tet^R-YFP; and between Tet^S-YFP and Tet^R-CFP. Here these measurements are presented separately, where it can be seen that competition between Tet^S and Tet^R strains is not influenced by the permutation of fluorescent labels.

Supplementary Figure 1.11. Measurement of selection for/against resistance by flow cytometry. Flow cytometry measurements of $N_{\text{Tet}}^{\text{S}}$ and $N_{\text{Tet}}^{\text{R}}$, for representative data points in Figure 1.2c (reproduced here with selected data points marked in purple). These scatter plots of raw measurements of cyan and yellow fluorescence are presented in 'logicle' scale to prevent distortion of low signals by logarithmic scaling(Parks et al., 2006). These points demonstrate selection for resistance (circle), no selection (triangle), and selection against resistance (square). Above the cyan-yellow scatter plots are histograms summing the number of resistant cells (red; $N_{\text{Tet}}^{\text{R}}$) and sensitive cells (green; $N_{\text{Tet}}^{\text{S}}$).

Supplementary Figure 1.11. Measurement of selection for/against resistance by flow cytometry. (Continued)

Supplementary Table 1.1. Parameter values of the kinetic model of tetracycline decay

Parameter	Value (min⁻¹)	Source	ΔE (%)
k_1	0.0265	(Yuen and Sokoloski, 1977)	0.04
k_{-1}	0.0207	(Yuen and Sokoloski, 1977)	0.04
k_2	0.0317	(Yuen and Sokoloski, 1977)	0.06
k_{-2}	0.0352	(Yuen and Sokoloski, 1977)	0.08
k_3	0.0209	(Yuen and Sokoloski, 1977)	0.09
k_4	0.0169	(Yuen and Sokoloski, 1977)	0.001
k_{loss}	0.00147	fitted*	N/A*

The consistency of parameters measured in (Yuen and Sokoloski, 1977) with this study's spectra of degraded tetracycline solutions (Supplementary Figure 1.2) can be quantitated by the error in the alignment between measured and modeled spectra. Specifically, we define the error E as

$$E = \sum_{t_{deg}} \int (A_\lambda^{\text{measured}} - A_\lambda^{\text{modelled}})^2 d\lambda$$,

where λ is integrated over the ranges 250-290nm and 325-400nm. E can be evaluated with modeled spectra produced either by the parameters in (Yuen and Sokoloski, 1977), or by parameters which are fitted to minimize E. For each single parameter then, we determine $\Delta E = E$ ((Yuen and Sokoloski, 1977) parameter) / E(best fit parameter) -1, which describes how close the parameters in (Yuen and Sokoloski, 1977) are to minimizing E. We see that they are indeed extremely close to minimizing the alignment error (see also Supplementary Figure 1.4). When all parameters are simultaneously fitted, $\Delta E = 2\%$. Values taken from (Yuen and Sokoloski, 1977) are averages of duplicate measurements at 75°C. Note that

although Tet and ATC exert the strongest selective effects (Supplementary Figure 1.8), the kinetic model cannot be accurately simplified to these two compounds alone. The equilibrium constant for epimerization between Tet and ETC (k_1/k_{-1} = 1.3) is different from the equilibrium constant between ATC and EATC (k_2/k_{-2} = 0.90). Consequently, even after epimerization reactions have reached equilibrium, the dehydration reaction does not bring about a net 1:1 conversion between Tet and ATC.

Supplementary Material for Chapter 2.

A multi-peaked adaptive landscape arising from high-order genetic interactions

Supplementary Figure 2.1. Growth rates of *E.coli* strains with mutant *DHFR* genes as a function of trimethoprim concentration. The growth rates of strains carrying all possible combinations of seven trimethoprim resistance-conferring mutuations were measured across a range of trimethoprim concentrations. Each column is one strain, whose mutations are indicated in the color coded grid atop the plot. Mutant strains are sorted by the overall number of mutations. A black to yellow heatmap indicates growth rate. Six columns that are entirely black are genotypes that could not be successfully integrated into the chromosome of *E.coli* despite repeated attempts.
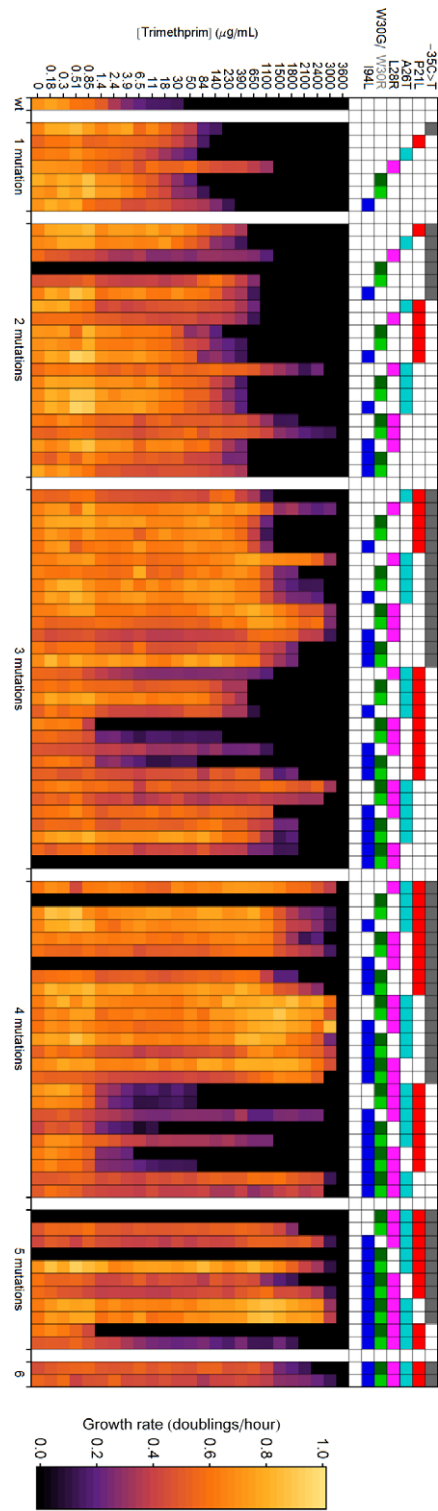
Supplementary Figure 2.1. Growth rates of *E.coli* strains with mutant *DHFR* genes as a function of trimethoprim concentration. (Continued)

Supplementary Material for Chapter 3.

Diverse pathways to drug resistance by changes in gene expression

**Supplementary Figure 3.1. Pooled diffusion-based selection for changes in gene expression that confer antibiotic resistance.** 10^7 colony forming units of a clonal wildtype strain or a pooled library of gene deletion or gene over-expression mutants were plated on M63 glucose minimal media agar. An aliquot of antibiotic was added to the center and plates were incubated for 48 hours at 37°C before imaging. Images here show the presence of gene expression mutants with resistance to antibiotics that act upon: **a**, cell wall synthesis; **b**, the cell membrane; **c**, transcription; **d, e**, translation; **f**, DNA synthesis; **g**, free radical production. Plates treated with sulfacetamide and sulfamethoxazole were incubated for 1 week before imaging due to the slow growth of sulfonamide resistant colonies.
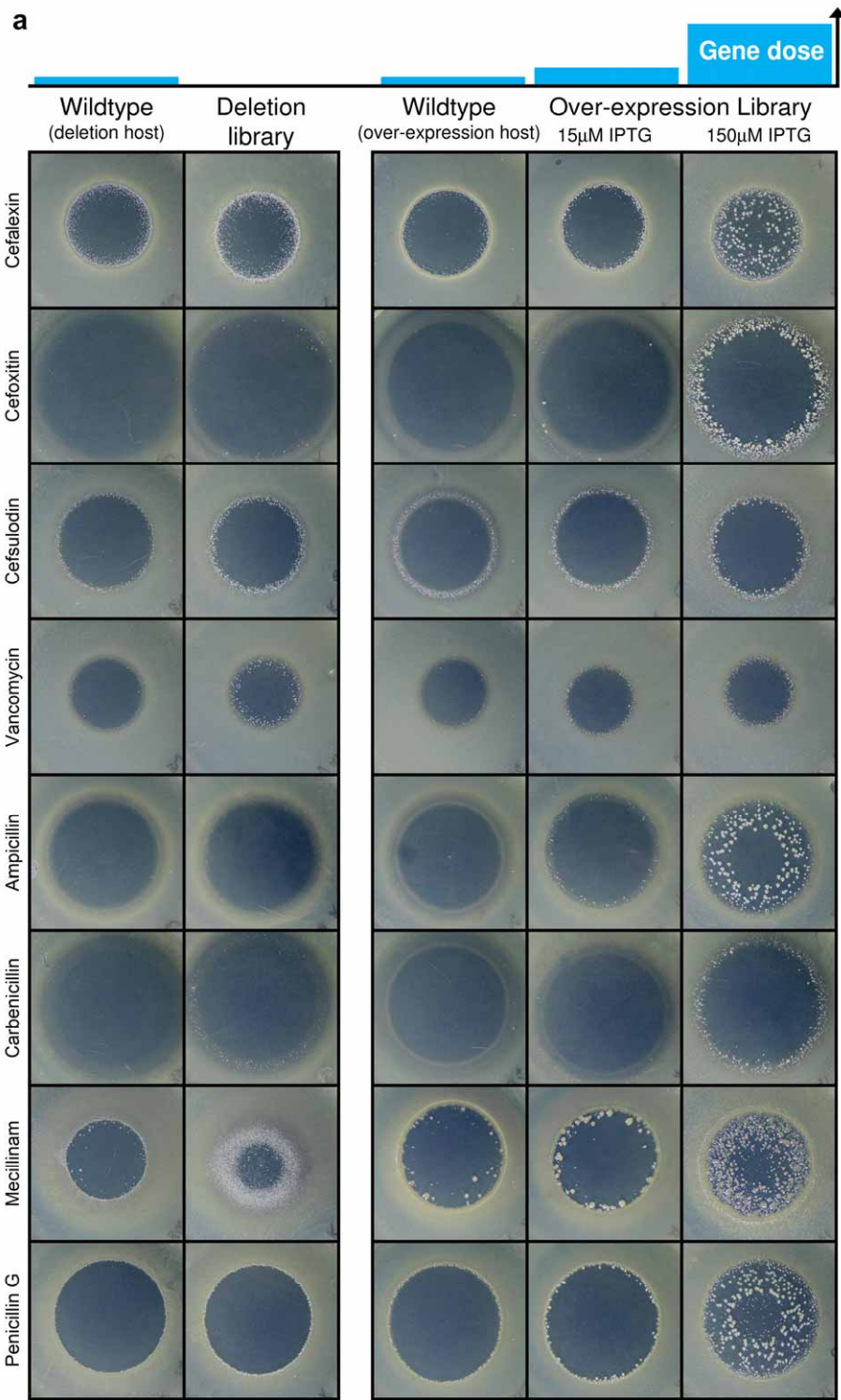
Supplementary Figure 3.1 (continued).
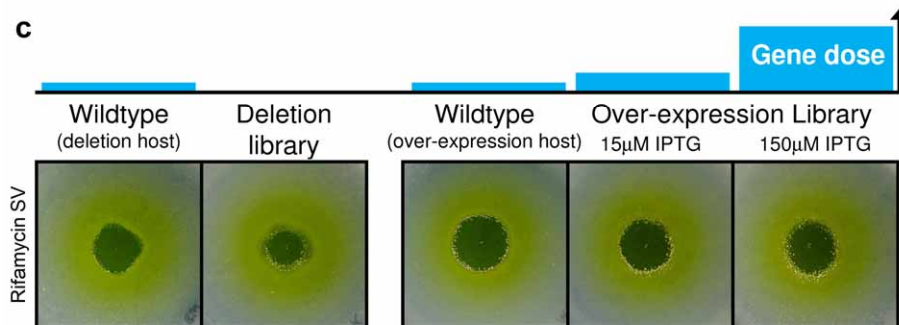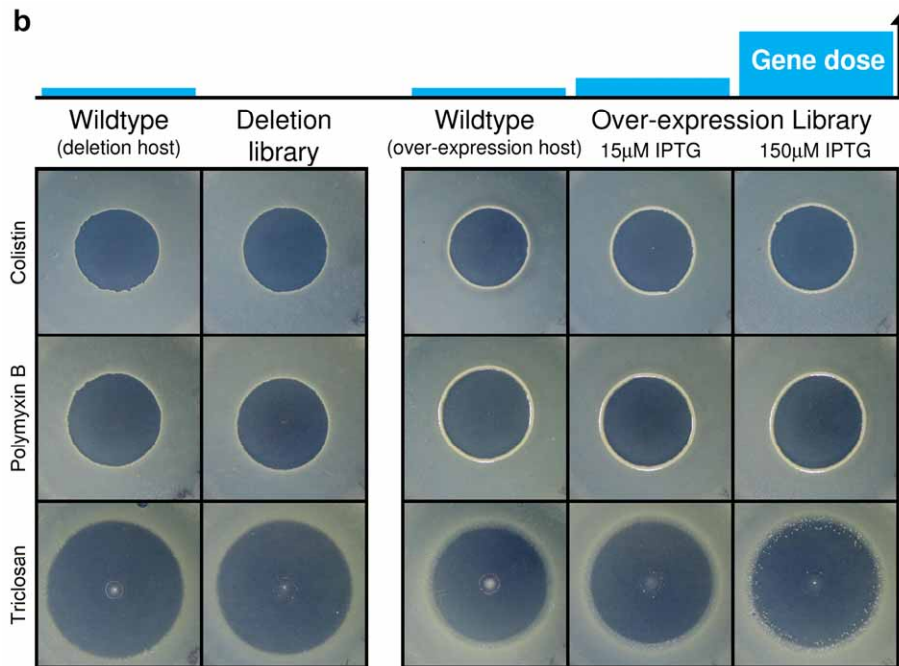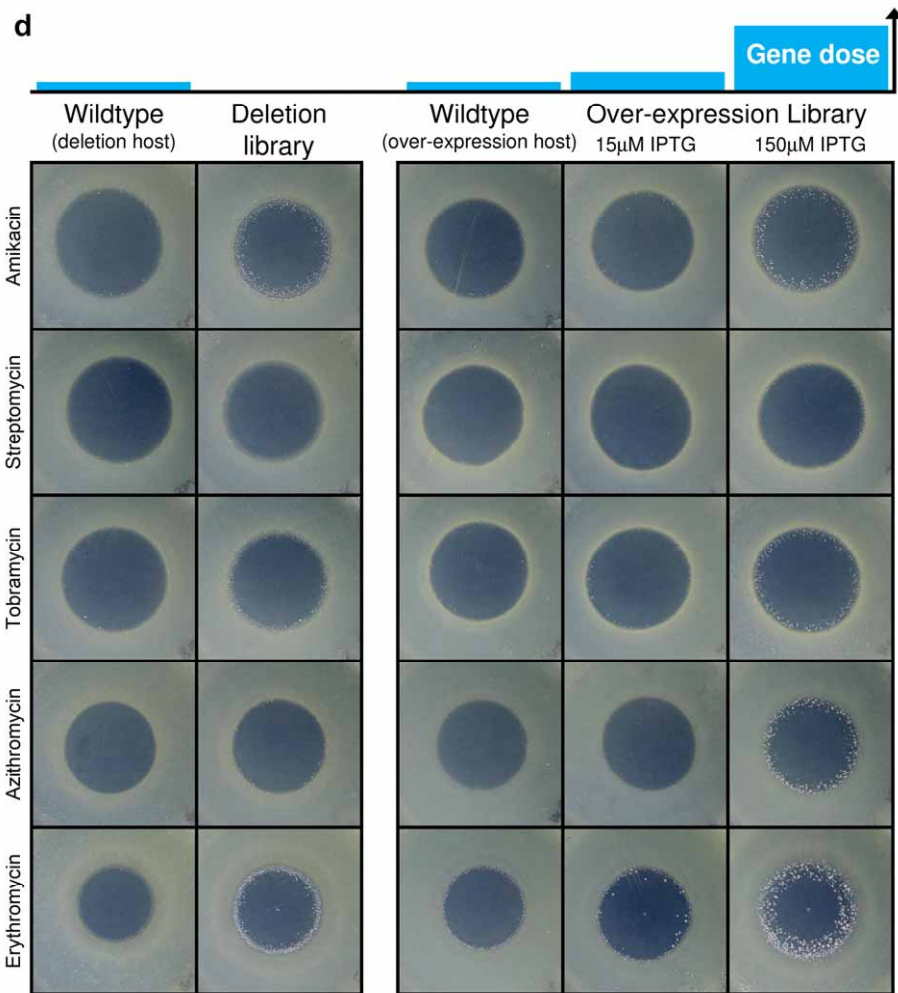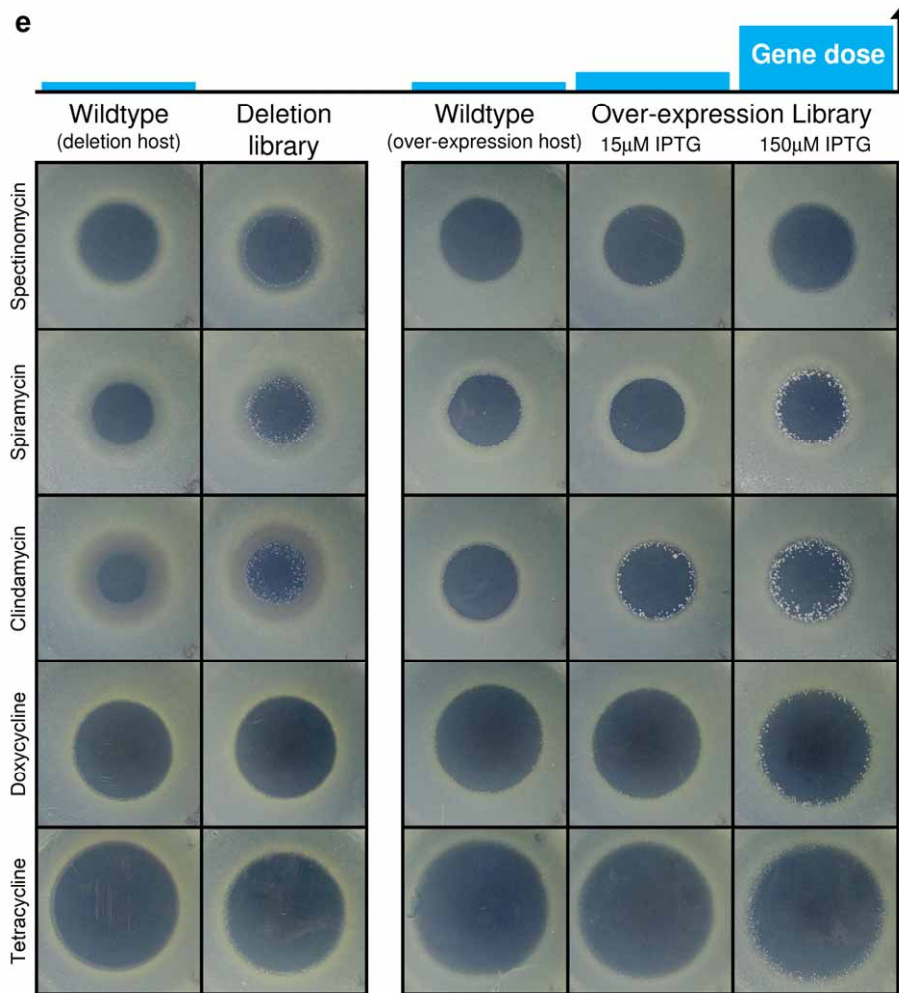
b

c

Supplementary Figure 3.1 (continued).
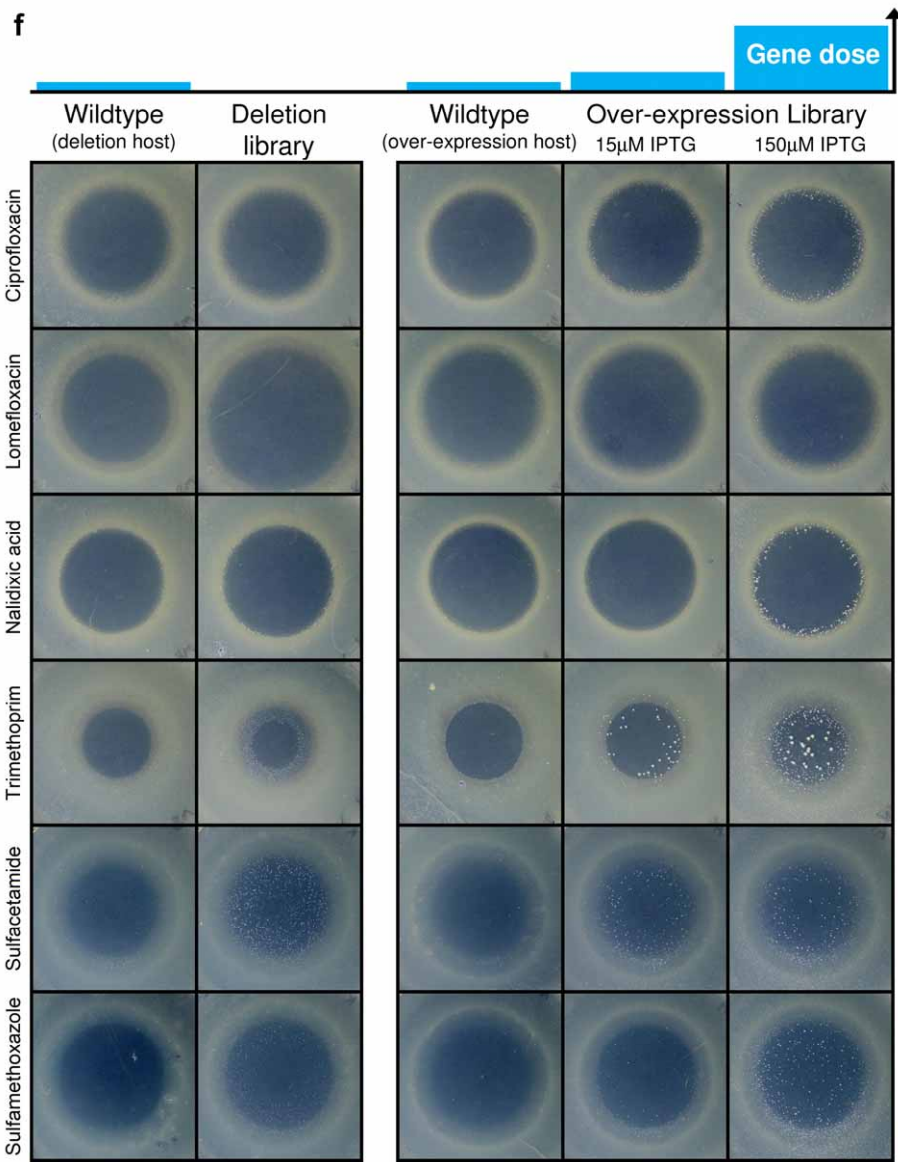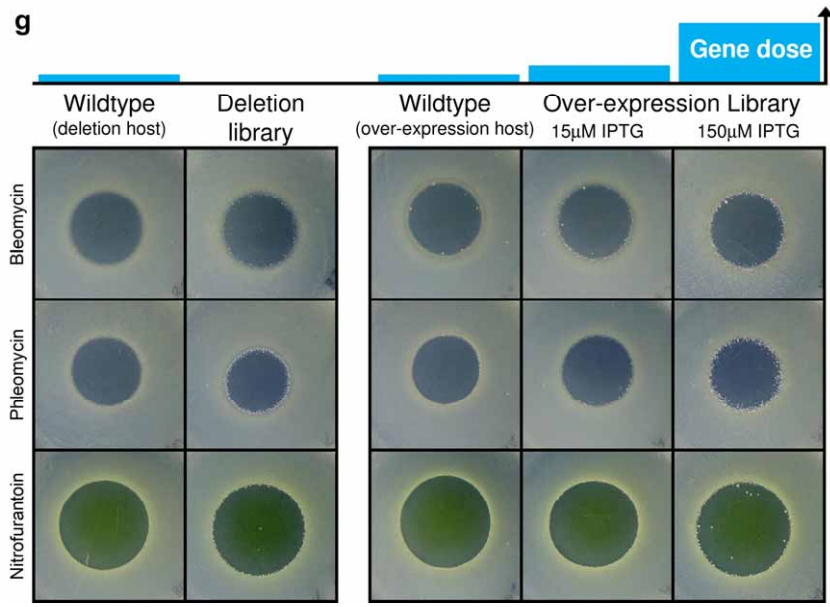
Supplementary Figure 3.1 (continued).

Supplementary Figure 3.1 (continued).

Supplementary Figure 3.1 (continued).

Supplementary Figure 3.1 (continued).

Supplementary Table 3.1. Changes in gene expression that increase antibiotic resistance.

Gene-drug interactions from Figure 3.2 are tabulated with gene functions curated from the

Ecocyc database (Keseler et al., 2011)

Change in gene expression	Gene name	Drugs resisted	Gene function	Previously associated with drug resistance?	Notes
Overexpression	hemD	AMK, MEC, PHM, TOB	uroporphyrinogen III synthase	N	
Overexpression	yhbT	AMK, PHM, TOB	predicted lipid carrier protein	N	
Overexpression	ampC	AMP, CLX, CRB, FOX, PEN	β-lactamase	Y	(Linstrom et al., 1970)
Overexpression	marA	AMP, BLM, CLI, CLX, CPR, DOX, ERY, NAL, PEN, TET	MarA DNA-binding transcriptional dual regulator	Y	(Cohen et al., 1993)
Overexpression	nanA	AMP	N-acetylneuraminate lyase	N	nanA is the first enzyme in pathway for degradation of sialic acid (Vimr and Troy, 1985).
Overexpression	soxS	AMP, AZI, BLM, CLI, CPR, DOX, ERY, FOX, NAL, PEN, SPR, TET, TMP	SoxS DNA-binding transcriptional dual regulator	Y	(Amabile-Cuevas and Demple, 1991)
Overexpression	yidF	AMP, CLX, PEN	predicted DNA-binding transcriptional regulator	N	
Overexpression	gadW	AZI, BLM	GadW DNA-binding transcriptional dual regulator	N	gadW is a regulator of Glutamic acid decarboxylase (GAD) acid resistance system (Tucker et al., 2003).
Overexpression	rpmH	AZI, ERY, SPR	50S ribosomal subunit protein L34	N	Overexpression of rpmH decreases the production of polyamine (Panagiotidis et al., 1995).
Overexpression	ydeO	AZI	YdeO DNA-binding transcriptional dual regulator	N	ydeO activates transcription of acid resistance genes (Masuda and Church, 2003).

Supplementary Table 3.1. Changes in gene expression that increase antibiotic resistance. (continued)

Change in gene expression	Gene name	Drugs resisted	Gene function	Previously associated with drug resistance?	Notes
Overexpression	yeaH	AZI, ERY, SPR	conserved protein	N	
Overexpression	sbmC	BLM, PHM	DNA gyrase inhibitor	Y	Overexpression of sbmC confers resistance to mitomycin C (Wei et al., 2001) and microcin B17 (Baquero et al., 1995).
Overexpression	yjcH	BLM	conserved inner membrane protein	N	
Overexpression	ddpF	CFS, CLX, MEC, PHM	putative ATP-binding component of an ABC transporter	N	While ddpF overexpression resists CFS, CLX, MEC, PHD, ddpF deletion resists AMK
Overexpression	degQ	CFS	serine endoprotease	N	
Overexpression	mrcB	CFS	Murein polymerase (PBP1b)	Y	mrcB and mrcA are the primary targets of Cefsulodin (Kong et al., 2010).
Overexpression	nlpE	CFS, CRB, PEN	outer membrane lipoprotein	N	
Overexpression	adk	CLI	adenylate kinase	N	
Overexpression	cadA	CLI	lysine decarboxylase 1	N	cadA is part of the lysine-dependent acid resistance system 4 (Takayama et al., 1994).
Overexpression	hflX	CLI, ERY	GTPase associated with the 50S subunit of the ribosome	N	
Overexpression	lepA	CLI	elongation factor 4	N	
Overexpression	proQ	CLI	RNA chaperone	N	
Overexpression	ybiT	CLI	putative ATP-binding component of an ABC transporter	N	

Supplementary Table 3.1. Changes in gene expression that increase antibiotic resistance. (continued)

Change in gene expression	Gene name	Drugs resisted	Gene function	Previously associated with drug resistance?	Notes
Overexpression	yheS	CLI	putative ATP-binding component of an ABC transporter	N	
Overexpression	aroB	CLX	3-dehydroquinate synthase	N	
Overexpression	bssR	CLX, CPR, FOX, NIT	regulator of biofilm formation	N	
Overexpression	gmr	CLX, FOX, NIT, PEN	modulator of RNase II stability	N	
Overexpression	gntT	CLX	gluconate transporter	N	
Overexpression	nanK	CLX, FOX	*N*-acetylmannosamine kinase	N	
Overexpression	rcsD	CLX	Regulator of capsular polysaccharide synthesis	N	
Overexpression	rluA	CLX	23S rRNA and tRNA pseudouridine synthase	N	
Overexpression	yccT	CLX, PEN, VAN	conserved protein	N	
Overexpression	yjjQ	CLX, PEN	predicted DNA-binding transcriptional regulator	N	yjjQ is associated with methylglyoxal sensitivity (Kim et al., 2007).
Overexpression	rbsR	CPR, FOX, PEN	'Ribose Repressor' DNA-binding transcriptional repressor	N	
Overexpression	baeR	CRB	BaeR transcriptional regulator	Y	baeR activates the MdtABC drug efflux system (Nagakubo et al., 2002).
Overexpression	iap	CRB, PEN	alkaline phosphatase isozyme conversion protein	N	

Supplementary Table 3.1. Changes in gene expression that increase antibiotic resistance. (continued)

Change in gene expression	Gene name	Drugs resisted	Gene function	Previously associated with drug resistance?	Notes
Overexpression	amiA	ERY, SPR	N-acetylmuramoyl-L-alanine amidase 1	N	
Overexpression	appY	ERY	'acid phosphatase' DNA-binding transcriptional activator	N	
Overexpression	rluE	ERY, SPR	23S rRNA pseudouridine synthase	N	
Overexpression	rng	ERY	ribonuclease G	N	
Overexpression	btuE	FOX	thioredoxin/glutathione peroxidase	N	
Overexpression	ycgZ	FOX, PEN	predicted protein	N	ycgZ is a member of the cold shock stimulon (Polissi et al., 2003).
Overexpression	dxs	MEC	1-deoxyxylulose-5-phosphate synthase	N	Dxs is the first enzyme in the methylerythritol phosphate pathway of isoprenoid biosynthesis (Sprenger et al., 1997).
Overexpression	gcvA	MEC	'Glycine cleavage A' DNA-binding transcriptional dual regulator	N	
Overexpression	glnB	MEC	nitrogen regulatory protein P-II 1	N	
Overexpression	glyQ	MEC	glycyl-tRNA synthetase, α subunit	N	
Overexpression	mrdA	MEC	peptidoglycan synthetase (PBP2)	Y	mrdA is the primary target of Mecillinam (Kong et al., 2010).
Overexpression	rplJ	MEC	50S ribosomal subunit protein L10	N	
Overexpression	rutR	MEC, PEN	'pyrimidine utilization, rut repressor' DNA-binding transcriptional dual regulator	N	

Supplementary Table 3.1. Changes in gene expression that increase antibiotic resistance. (continued)

Change in gene expression	Gene name	Drugs resisted	Gene function	Previously associated with drug resistance?	Notes
Overexpression	trpR	MEC	tryptophan transcriptional repressor	N	
Overexpression	yehK	MEC	predicted protein	N	
Overexpression	ygbE	MEC	conserved inner membrane protein	N	
Overexpression	ycjR	NIT	predicted component of the SdsRQP multidrug efflux pump	Y	(Dinh et al., 1994)
Overexpression	yibF	NIT	glutathione transferase-like protein	N	
Overexpression	eptB	PEN, VAN	phosphoethanolamine transferase	N	eptB modifies lipopolysaccharide (Reynolds et al., 2005).
Overexpression	nadK	PEN	NAD kinase	N	
Overexpression	cpdA	PHM	cAMP phosphodiesterase	N	Overproduction of cpdA confers acid resistance (Barth et al., 2009).
Overexpression	frsA	PHM	fermentation/respiration switch protein	N	
Overexpression	metB	PHM	O-succinylhomoserine lyase / O-succinylhomoserine(thiol)-lyase	N	
Overexpression	pdhR	PHM	pyruvate dehydrogenase complex DNA-binding transcriptional dual regulator	N	
Overexpression	slyA	PHM	SlyA DNA-binding transcriptional activator	N	
Overexpression	yejG	PHM	predicted protein	N	

Supplementary Table 3.1. Changes in gene expression that increase antibiotic resistance. (continued)

Change in gene expression	Gene name	Drugs resisted	Gene function	Previously associated with drug resistance?	Notes
Overexpression	ylcG	PHM	DLP12 prophage; small membrane protein	N	
Overexpression	yrbL	PHM	predicted protein	N	
Overexpression	entS	RIF	enterobactin efflux transporter	Y	An entS insertion mutant has increased susceptibility to mitomycin C (Han et al., 2010).
Overexpression	gadE	RIF	'Glutamic acid decarboxylase' DNA-binding transcriptional activator	Y	gadE activates the glutamic acid decarboxylase (GAD) acid resistance system, and multi-drug efflux genes (Tucker et al., 2003).
Overexpression	gfcC	RIF	conserved protein	N	
Overexpression	nuoI	RIF	NADH:ubiquinone oxidoreductase, chain I	N	
Overexpression	cynS	SCM	cyanase	N	cynS may function in detoxification of cyanate (Anderson et al., 1990).
Overexpression	nudB	SCM, SMX	dihydroneopterin triphosphate pyrophosphohydrolase	N	nudB catalyzes the first committed step in the synthesis of folate (Suzuki and Brown, 1974).
Overexpression	pyrG	SCM, SMX	CTP synthetase	N	
Overexpression	ydiZ	SCM	predicted protein	N	
Overexpression	ykfF	SCM	predicted protein	N	
Overexpression	ymgG	SCM	predicted protein	N	
Overexpression	dksA	SMX	RNA polymerase-binding transcription factor	N	While dksA overexpression resists SMX, dksA deletion resists RIF

Supplementary Table 3.1. Changes in gene expression that increase antibiotic resistance. (continued)

Change in gene expression	Gene name	Drugs resisted	Gene function	Previously associated with drug resistance?	Notes
Overexpression	puuP	SPX	proton dependent putrescine transporter	N	
Overexpression	fabI	TCL	enoyl acyl carrier protein reductase	Y	fabI is the target of Triclosan (Heath et al., 1998).
Overexpression	folA	TMP	dihydrofolate reductase	Y	folA is the target of Trimethoprim (Miovic and Pizer, 1971).
Overexpression	folM	TMP	dihydromonapterin reductase / dihydrofolate reductase	Y	folM is a dihydromonapterin reductase with weak activity as a dihydrofolate reductase (Giladi et al., 2003). While folM over-expression confers trimethoprim resistance, folM deletion confers sulfonamide resistance.
Overexpression	creA	VAN	conserved protein	N	
Deletion	ddpF	AMK	putative ATP-binding component of an ABC transporter	N	While ddpF overexpression resists CFS, CLX, MEC, PHD, ddpF deletion resists AMK
Deletion	gnsA	AMK	predicted regulator of phosphatidylethanolamine synthesis	N	
Deletion	pheM	AMK	phenylalanyl-tRNA synthetase operon leader peptide	N	
Deletion	ydjI	AMK	predicted aldolase	N	
Deletion	sbmA	BLM	peptide antibiotic transporter	Y	Loss of sbmA function confers resistance to proline-rich antimicrobial peptides (Mattiuzzo et al., 2007).
Deletion	asmA	CFS	predicted outer membrane protein assembly protein	N	asmA is required for assembly of the porins through which cephalosporins enter the cell (Misra and Miao, 1995).

Supplementary Table 3.1. Changes in gene expression that increase antibiotic resistance. (continued)

Change in gene expression	Gene name	Drugs resisted	Gene function	Previously associated with drug resistance?	Notes
Deletion	hrpB	CFS	predicted ATP-dependent helicase	N	
Deletion	yceG	CFS, VAN	predicted aminodeoxychorismate lyase	N	
Deletion	cadB	CLI	lysine:cadaverine antiporter	N	cadB is part of the lysine-dependent acid resistance system 4 (Meng and Bennett, 1992).
Deletion	rpmG	CLI	50S ribosomal subunit protein L33	N	
Deletion	speA	CLI	biosynthetic arginine decarboxylase	N	speA catalyzes the first step in putrescine biosynthesis (Wu and Morris, 1973).
Deletion	speB	CLI	agmatinase	N	speB catalyzes the second step in putrescine biosynthesis (Satishchandran and Boyle, 1986).
Deletion	lon	CLX	DNA-binding, ATP-dependent protease	Y	Loss of lon function stabilizes marA to confer antibiotic resistance (Nicoloff et al., 2006).
Deletion	ompF	CLX, FOX	outer membrane porin F	Y	ompF is the primary route of cell entry for many beta-lactams, particularly cephalosporins (Nikaido, 1989).
Deletion	ompR	CLX, FOX	OmpR response regulator	Y	ompR is the transcriptional activator of ompF; loss of ompR prevents synthesis of ompF (Tsui et al., 1988).
Deletion	atpB	CRB	ATP synthase F0 complex - a subunit	N	
Deletion	atpE	CRB	ATP synthase F0 complex - c subunit	N	
Deletion	cpxA	CRB	CpxA sensory histidine kinase	N	cpxA is part of the stress response pathway to cell envelope damage (Pogliano et al., 1997).
Deletion	rnhA	ERY	RNase HI	N	

Supplementary Table 3.1. Changes in gene expression that increase antibiotic resistance. (continued)

Change in gene expression	Gene name	Drugs resisted	Gene function	Previously associated with drug resistance?	Notes
Deletion	sulA	ERY	SOS cell division inhibitor	N	
Deletion	ycbZ	ERY, SPR	putative ATP-dependent protease	N	
Deletion	fepB	MEC	ferric enterobactin ABC transporter	N	
Deletion	fepC	MEC	ferric enterobactin ABC transporter	N	
Deletion	fepG	MEC	ferric enterobactin ABC transporter	N	
Deletion	fes	MEC	enterochelin esterase	N	fes hydrolyzes ferric enterobactin (Langman et al., 1972).
Deletion	glnD	MEC	uridylyltransferase	N	
Deletion	pdxA	MEC	4-hydroxy-L-threonine phosphate dehydrogenase, NAD-dependent	N	pdxA is required for pyridoxal phosphate synthesis (Lam et al., 1992).
Deletion	rodZ	MEC	transmembrane component of cytoskeleton	N	rodZ interacts with the target of mecillinam (mrdA) through the MreB cytoskeleton (Bendezu et al., 2009).
Deletion	ybjI	MEC	FMN phosphatase	N	ybjI possesses phosphatase activity against pyridoxal phosphate (Kuznetsova et al., 2006).
Deletion	dbpA	NIT	ATP-dependent RNA helicase, specific for 23S rRNA	N	
Deletion	lpcA	NIT	D-sedoheptulose 7-phosphate isomerase	N	lpcA catalyzes the first step in the synthesis of a core component of lipopolysaccharide; lpcA deletion confers sensitivity to some antibiotics by increasing cell permeability (Tamaki et al., 1971).

Supplementary Table 3.1. Changes in gene expression that increase antibiotic resistance. (continued)

| Change in gene expression	Gene name	Drugs resisted	Gene function	Previously associated with drug resistance?	Notes
Deletion	nfsA	NIT	NADPH nitroreductase	Y	nfsA is required to activate nitrofurantoin to toxic reactive species, and so nfsA deletion confers nitrofurantoin resistance (McCalla et al., 1978).
Deletion	pstC	NIT	phosphate ABC transporter - membrane subunit	N	
Deletion	rfaC	NIT	ADP-heptose:LPS heptosyltransferase I	N	rfaC transfers heptose onto lipopolysaccharide (Kadrmas and Raetz, 1998)
Deletion	rfaD	NIT	ADP-L-glycero-D-mannoheptose-6-epimerase	N	rfaD catalyzes a step in the synthesis of lipopolysaccharide (Kneidinger et al., 2002).
Deletion	sspA	NIT	stringent starvation protein A	N	
Deletion	ybjC	NIT	predicted inner membrane protein	N	ybjC is co-transcribed with nfsA (Paterson et al., 2002). Polar effects on nfsA are a likely mechanism of resistance to nitrofurantoin.
Deletion	ratA	PHM	toxin of a predicted toxin-antitoxin pair	N	
Deletion	ubiF	PHM	2-octaprenyl-3-methyl-6-methoxy-1,4-benzoquinone hydroxylase	Y	uniF catalyzes a step in the ubiquinone biosynthesis pathway. Previously identified as a phleomycin resistant mutant (Collis and Grigg, 1989).
Deletion	ubiG	PHM	bifunctional 3-demethylubiquinone-8 3-O-methyltransferase and 2-octaprenyl-6-hydroxyphenol methylase	Y	ubiG catalyzes a step in the ubiquinone biosynthesis pathway. ubiG deletion produces a similar defect to a Phleomycin-resistant mutation in ubiF
Deletion	ubiH	PHM	2-octaprenyl-6-methoxyphenol hydroxylase	Y	ubiH catalyzes a step in the ubiquinone biosynthesis pathway. ubiH deletion produces a similar defect to a Phleomycin-resistant mutation in ubiF

Supplementary Table 3.1. Changes in gene expression that increase antibiotic resistance. (continued)

Change in gene expression	Gene name	Drugs resisted	Gene function	Previously associated with drug resistance?	Notes
Deletion	ycgB	PHM	conserved protein	N	
Deletion	ymgG	PHM	predicted protein	N	
Deletion	dksA	RIF	RNA polymerase-binding transcription factor DksA	N	While dksA overexpression resists SMX, dksA deletion resists RIF
Deletion	marC	RIF	predicted transporter	N	
Deletion	ptsN	RIF	phosphotransferase system enzyme IIA, regulation of potassium transport	N	
Deletion	rlmL	RIF	fused dual 23S rRNA methyltransferase	N	
Deletion	yfgH	RIF	predicted outer membrane lipoprotein	N	
Deletion	ccmH	SCM, SMX	cytochrome c biogenesis protein	N	
Deletion	folM	SCM, SMX	dihydromonapterin reductase / dihydrofolate reductase	Y	While folM over-expression confers trimethoprim resistance, folM deletion confers sulfonamide resistance. A folM deletion has been previously observed to confer sulfonamide resistance (Girgis et al., 2009).
Deletion	folX	SCM, SMX	dihydroneopterin triphosphate 2'-epimerase	Y	A folX deletion has been previously observed to confer sulfonamide resistance (Girgis et al., 2009).
Deletion	ybiP	SPR	predicted hydrolase, inner membrane	N	

Supplementary Table 3.1. Changes in gene expression that increase antibiotic resistance. (continued)

Change in gene expression	Gene name	Drugs resisted	Gene function	Previously associated with drug resistance?	Notes
Deletion	ygeO	SPR	predicted protein	N	ygeO is involved in the production of Extracellular Death Factor (Kolodkin-Gal et al., 2007).
Deletion	ymfJ	SPR	predicted protein	N	
Deletion	rsxC	TMP	member of SoxR-reducing complex	Y	rsxC deletion produces constitutive transcription of sox operon (Koo et al., 2003).
Deletion	dacA	VAN	D-alanyl-D-alanine carboxypeptidase IA (PBP5)	N	dacA is involved in production of the cellular target of vancomycin binding (D-alanyl-D-alanine). dacA deletion confers increased beta-lactam susceptibility (Sarkar et al., 2010).
Deletion	ycgB	PHM	conserved protein	N	

Supplementary Table 3.1. Changes in gene expression that increase antibiotic resistance. (continued)
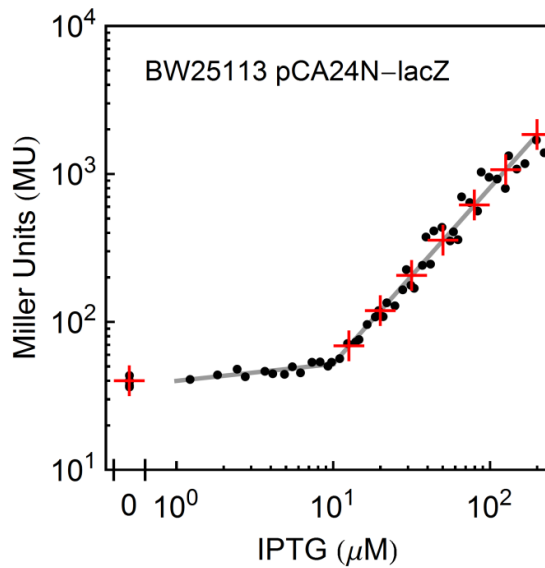
Supplementary Figure 3.2. Measurement of IPTG-induced transcription of antibiotic resistance genes by beta-galactosidase assays. The pCA24N plasmid used to express Open Reading Frames in the ASKA library was engineered to express *lacZ*, and transformed into BW25113. Liquid cultures of this strain were prepared as for growth rate assays, across a gradient of IPTG concentrations. In early log phase, promoter activity was measured in Miller Units by a kinetic beta-galactosidase assay (black points). The resulting data is well described by two straight lines on a double-log plot (gray lines). From this data, eight IPTG concentrations were chosen for the growth rate assays in Figures 3 and 4, that produced evenly log-distributed amounts of promoter activity (in Miller Units) over a 50-fold dynamic range (red crosses).

Supplementary Figure 3.3. Non-optimal use of antibiotic resistance genes under antibiotic stress. Microtiter plates containing 2-dimensional gradients of IPTG and antibiotic were inoculated with either a wildtype strain (WT = BW25113 pCA24N-ΔpT5lac-*yfp* pCSλ), a strain lacking a gene of interest (Δ*gene* = BW25113 *gene*::FRT pCA24N-ΔpT5lac-*yfp* pCSλ), or a strain with experimentally controlled expression of the gene of interest (BW25113 *gene*::FRT pCA24N-*gene* pCSλ). Plates were incubated at 30°C in a scintillation counter and growth rates were measured based on bioluminescence, generated by the pCSλ plasmid (Methods). **a**, The use of marA and soxS was measured in a panel of 9 antibiotics. **b**, The use of ampC was measured in ampicillin and cephalexin, and the use of sbmC was measured in phleomycin.
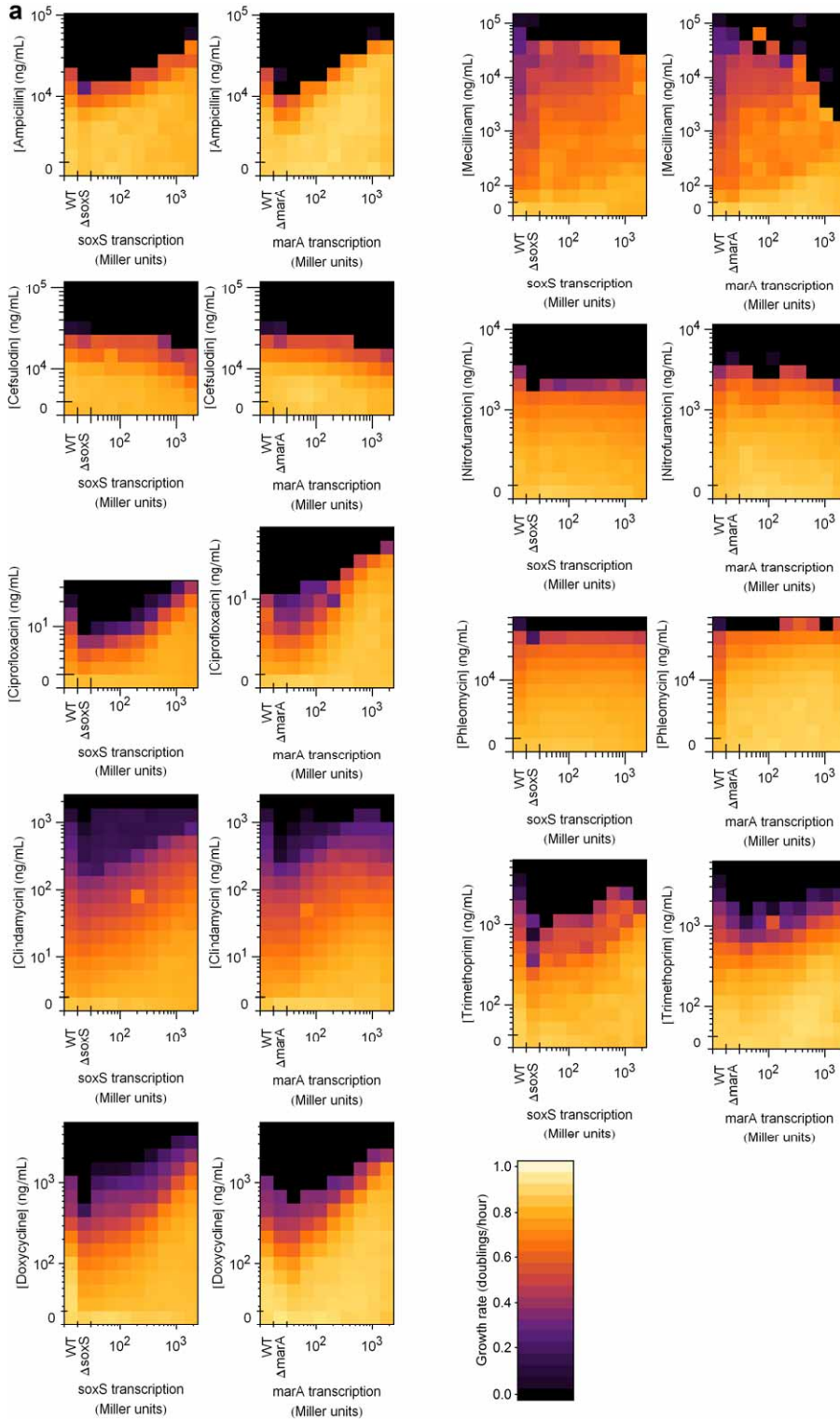
Supplementary Figure 3.3 (continued).
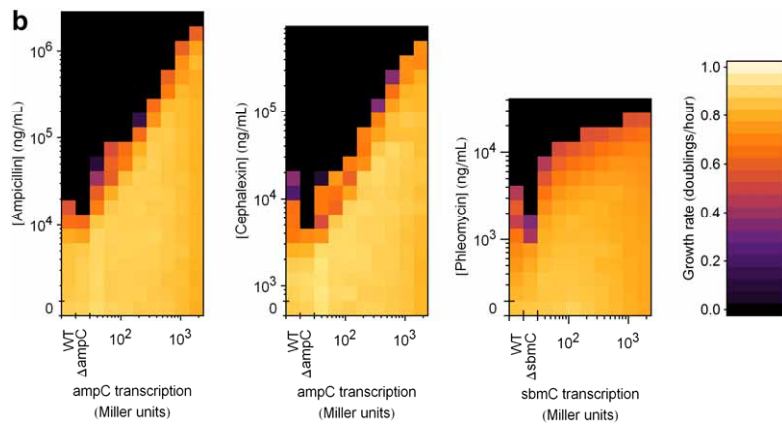
Supplementary Figure 3.3 (continued).

Supplementary Material for Chapter 4.

The dependence of antibiotic resistance on target expression
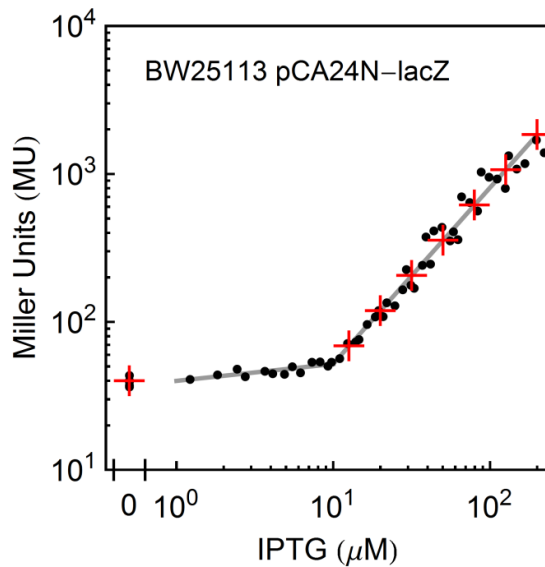
Supplementary Figure 4.1. Measurement of IPTG-induced transcription of drug target genes by beta-galactosidase assays. A strain was constructed where lacZ was encoded in place of a drug target gene (BW25113 pCA24N-*lacZ*). Liquid cultures of this strain were prepared as for growth rate assays, across a gradient of IPTG concentrations. In early log phase, promoter activity was measured in Miller Units by a kinetic beta-galactosidase assay (black points). The resulting data is well described by two straight lines on a double-log plot (gray lines). From this data, eight IPTG concentrations were chosen for the growth rate assays in Figure 1b, that produced evenly log-distributed amounts of promoter activity (in Miller Units) over a 50-fold dynamic range (red crosses).

Supplementary Figure 4.2. Mass-action kinetic models reveal the relations between enzyme concentration and drug resistance.

In sections **a** and **b** we first derive the relation between drug target over-expression and drug resistance for the simple model shown in Figure 4.2a. In sections **c**, **d**, **e** and **f** we show that mass-action kinetic models of competitive and non-competitive inhibition produce identical results to the initial simple models.

(**a**) Simple model of a drug that solely inhibits an enzyme

$$k_{Ion}[E][I] = k_{Ioff}[EI]$$

$$K_i = \frac{k_{Ioff}}{k_{Ion}} = \frac{[E][I]}{[EI]}$$
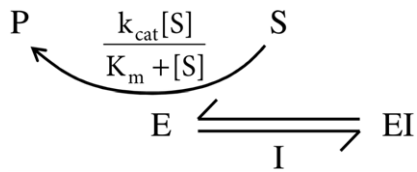
$$[E]_{total} = [E] + [EI] = [E] + \frac{[E][I]}{K_i} = [E]\left(1 + [I]/K_i\right)$$

$$[E] = \frac{[E]_{total}}{1 + [I]/K_i}$$

$$\frac{d[P]}{dt} = [E]\frac{k_{cat}[S]}{K_m + [S]} = \frac{[E]_{total}}{1 + [I]/K_i}\frac{k_{cat}[S]}{K_m + [S]}$$

Supplementary Figure 4.2. (continued)

Let $[E]_{total} = (E_{wt} + E_{additional})$.

Solve for IC50, first without considering fitness costs of additional enzyme production:

$$\left(\begin{array}{c} \text{drug - inhibited flux with} \\ \text{additional enzyme} \end{array}\right) = 50\% \times \left(\begin{array}{c} \text{uninhibited flux with} \\ \text{wildtype enzyme abundance} \end{array}\right)$$

$$\left(E_{wt} + E_{additional}\right) \times \left(\frac{1}{1 + [I]/K_i} \times \frac{k_{cat}\,[S]}{K_m + [S]}\right) = \frac{1}{2} \times E_{wt} \times \left(\frac{k_{cat}\,[S]}{K_m + [S]}\right)$$

$$2 \times \left(\frac{E_{wt} + E_{additional}}{E_{wt}}\right) = 1 + [I]/K_i$$

$$[I] = K_i \times \left(2 \times \left(\frac{E_{wt} + E_{additional}}{E_{wt}}\right) - 1\right)$$

$$IC50_{wt} = [I]\big|_{E_{additional} = 0} = K_i$$

$$\frac{IC50}{IC50_{wt}} = \frac{K_i \times \left(2 \times \left(\frac{E_{wt} + E_{additional}}{E_{wt}}\right) - 1\right)}{K_i}$$

$$\frac{IC50}{IC50_{wt}} = 2 \times \left(\frac{E_{wt} + E_{additional}}{E_{wt}}\right) - 1$$

Supplementary Figure 4.2. (continued)

Solve for IC50, considering fitness costs of additional enzyme production, cost($E_{additional}$):

$$\begin{pmatrix} \text{drug - inhibited flux with} \\ \text{additional enzyme} \end{pmatrix} \times \begin{pmatrix} 1 - \dfrac{\text{fitness cost of}}{\text{additional enzyme}} \end{pmatrix} = 50\% \times \begin{pmatrix} \text{uninhibited flux with} \\ \text{wildtype enzyme abundance} \end{pmatrix}$$

$$\left(E_{wt} + E_{additional} \right) \times \left(\frac{1}{1 + [I]/K_i} \times \frac{k_{cat}\,[S]}{K_m + [S]} \right) \times \left(1 - cost(E_{additional}) \right) = \frac{1}{2} \times E_{wt} \times \left(\frac{k_{cat}\,[S]}{K_m + [S]} \right)$$

$$2 \times \left(\frac{E_{wt} + E_{additional}}{E_{wt}} \right) \times \left(1 - cost(E_{additional}) \right) = 1 + [I]/K_i$$

$$[I] = K_i \times \left(2 \times \left(\frac{E_{wt} + E_{additional}}{E_{wt}} \right) \times \left(1 - cost(E_{additional}) \right) - 1 \right)$$

$$IC50_{wt} = [I]\big|_{E_{additional}=0} = K_i \text{ , given that } cost(0) = 0$$

$$\frac{IC50}{IC50_{wt}} = \frac{K_i \times \left(2 \times \left(\dfrac{E_{wt} + E_{additional}}{E_{wt}} \right) \times \left(1 - cost(E_{additional}) \right) - 1 \right)}{K_i}$$

$$\frac{IC50}{IC50_{wt}} = 2 \times \left(\frac{E_{wt} + E_{additional}}{E_{wt}} \right) \times \left(1 - cost(E_{additional}) \right) - 1$$

Supplementary Figure 4.2. (continued)

(**b**) Simple model of a drug that induces a harmful enzyme-catalyzed reaction.

The mechanism of inhibition modeled here can result in a depletion of substrate S, and so to

model this effect S is treated as a dynamical variable, synthesized at rate α.

$$\downarrow \alpha$$

$$P \quad \frac{k_{cat}[S]}{K_m+[S]} \quad S \quad \frac{k_{cat}[S]}{K_m+[S]} \quad X$$

$$E \rightleftharpoons EI$$
$$I$$
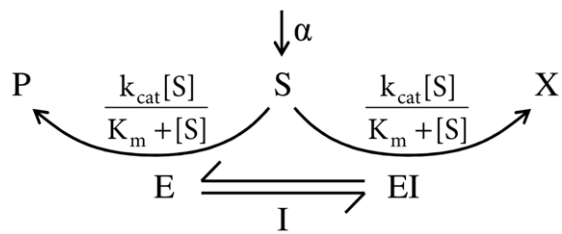
Supplementary Figure 4.2. (continued)

$$k_{Ion}[E][I] = k_{Ioff}[EI]$$

$$K_i = \frac{k_{Ioff}}{k_{Ion}} = \frac{[E][I]}{[EI]}$$

$$[E]_{total} = [E] + [EI] = [E] + \frac{[E][I]}{K_i} = [E]\left(1 + [I]/K_i\right)$$

$$\frac{d[S]}{dt} = \alpha - [E]\frac{k_{cat}[S]}{K_m + [S]} - [EI]\frac{k_{cat}[S]}{K_m + [S]} = \alpha - [E]_{total}\frac{k_{cat}[S]}{K_m + [S]}$$

Solve for $\dfrac{d[S]}{dt} = 0$:

$$[S] = \frac{K_m\,\alpha}{[E]_{total}\,k_{cat} - \alpha}$$

Note that a steady - state solution for [S] is only possible when $[E]_{total} > \dfrac{\alpha}{k_{cat}}$,

i.e. Enzyme is sufficiently abundant for substrate consumption to keep pace with substrate production.

$$\frac{d[P]}{dt} = [E]\frac{k_{cat}[S]}{K_m + [S]}$$

Substitute steady state solutions for [S] and [E] :

$$\frac{d[P]}{dt} = \frac{[E]_{total}}{1 + [I]/K_i}\frac{k_{cat}\left(\frac{K_m\,\alpha}{[E]_{total}\,k_{cat} - \alpha}\right)}{K_m + \left(\frac{K_m\,\alpha}{[E]_{total}\,k_{cat} - \alpha}\right)}$$

$$\frac{d[P]}{dt} = \frac{[E]_{total}}{1 + [I]/K_i}\frac{k_{cat}\,K_m\,\alpha}{K_m\,[E]_{total}\,k_{cat} - K_m\,\alpha + K_m\,\alpha}$$

$$\frac{d[P]}{dt} = \frac{[E]_{total}}{1 + [I]/K_i}\frac{\alpha}{[E]_{total}}$$

$$\Rightarrow \frac{d[P]}{dt} = \frac{\alpha}{1 + [I]/K_i}$$

Supplementary Figure 4.2. (continued)

Let $[E]_{total} = (E_{wt} + E_{additional})$. Note that in contrast to the model of enzyme inhibition in Supplementary Figure 4.2a, this substitution now has no effect on reaction rate.

Solve for IC50, first without considering fitness costs of additional enzyme production:

$$\left(\begin{array}{c} \text{drug - inhibited flux with} \\ \text{additional enzyme} \end{array}\right) = 50\% \times \left(\begin{array}{c} \text{uninhibited flux with} \\ \text{wildtype enzyme abundance} \end{array}\right)$$

$$\left(\frac{\alpha}{1 + [I]/K_i}\right) = \frac{1}{2} \times \alpha$$

$$2 = 1 + [I]/K_i$$

$$\text{IC50}_{wt} = [I]\big|_{E_{additional} = 0} = K_i$$

$$\frac{\text{IC50}}{\text{IC50}_{wt}} = \frac{K_i}{K_i} = 1$$

Solve for IC50, considering fitness costs of additional enzyme production, cost($E_{additional}$):

Supplementary Figure 4.2. (continued)

$$\left(\begin{array}{c} \text{drug - inhibited flux with} \\ \text{additional enzyme} \end{array}\right) \times \left(1 - \begin{array}{c} \text{fitness cost of} \\ \text{additional enzyme} \end{array}\right) = 50\% \times \left(\begin{array}{c} \text{uninhibited flux with} \\ \text{wildtype enzyme abundance} \end{array}\right)$$

$$\left(\frac{\alpha}{1 + [I]/K_i}\right) \times \left(1 - \text{cost}(E_{\text{additional}})\right) = \frac{1}{2} \times \alpha$$

$$2 \times \left(1 - \text{cost}(E_{\text{additional}})\right) = 1 + [I]/K_i$$

$$[I] = K_i \times \left(2 \times \left(1 - \text{cost}(E_{\text{additional}})\right) - 1\right)$$

$$\text{IC50}_{\text{wt}} = [I]\big|_{E_{\text{additional}} = 0} = K_i \text{ , given that } \text{cost}(0) = 0$$

$$\frac{\text{IC50}}{\text{IC50}_{\text{wt}}} = \frac{K_i \times \left(2 \times \left(1 - \text{cost}(E_{\text{additional}})\right) - 1\right)}{K_i}$$

$$\frac{\text{IC50}}{\text{IC50}_{\text{wt}}} = 2 \times \left(1 - \text{cost}(E_{\text{additional}})\right) - 1$$

Supplementary Figure 4.2. (continued)

(**c**). Competitive enzyme inhibition

Example: E = Dihydrofolate reductase (DHFR), S = dihydrofolic acid, P = tetrahydrofolic acid, I = trimethoprim (Supplementary Figure 4.4b).

$$EI \xrightleftharpoons[]{I} E \xrightleftharpoons[]{S} ES$$
$$\downarrow$$
$$P$$
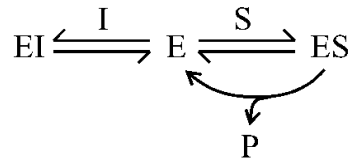
$$\frac{d[E]}{dt} = k_{Ioff}[EI] + (k_{Soff} + k_{cat})[ES] - (k_{Son}[S] + k_{Ion}[I])[E]$$

$$\frac{d[EI]}{dt} = k_{Ion}[E][I] - k_{Ioff}[EI]$$

$$\frac{d[ES]}{dt} = k_{Son}[E][S] - (k_{Soff} + k_{cat})[ES]$$

$$\frac{d[P]}{dt} = k_{cat}[ES]$$

$$K_m = \frac{k_{cat} + k_{Soff}}{k_{Son}}, \quad K_i = \frac{k_{Ioff}}{k_{Ion}}$$

Assume separation of timescales $(k_{cat} \ll k_{Soff})$

$$\Rightarrow \frac{d[P]}{dt} = [E]_{total} . k_{cat} \frac{[S]}{K_m(1 + [I]/K_i) + [S]}$$

Supplementary Figure 4.2. (continued)

Let $[E]_{total} = (E_{wt} + E_{additional})$.

Solve for IC50, first without considering fitness costs of additional enzyme production:

$$\begin{pmatrix} \text{drug - inhibited flux with} \\ \text{additional enzyme} \end{pmatrix} = 50\% \times \begin{pmatrix} \text{uninhibited flux with} \\ \text{wildtype enzyme abundance} \end{pmatrix}$$

$$\left(E_{wt} + E_{additional}\right) \times \left(\frac{k_{cat}\,[S]}{K_m\left(1 + [I]/K_i\right) + [S]}\right) = \frac{1}{2} \times E_{wt} \times \left(\frac{k_{cat}\,[S]}{K_m + [S]}\right)$$

$$2 \times \left(\frac{E_{wt} + E_{additional}}{E_{wt}}\right) \times \left(K_m + [S]\right) = K_m\left(1 + [I]/K_i\right) + [S]$$

$$2 \times \left(\frac{E_{wt} + E_{additional}}{E_{wt}}\right) \times \left(1 + [S]/K_m\right) = \left(1 + [S]/K_m\right) + [I]/K_i$$

$$[I] = K_i \times \left(1 + [S]/K_m\right) \times \left(2 \times \left(\frac{E_{wt} + E_{additional}}{E_{wt}}\right) - 1\right)$$

$$IC50_{wt} = [I]\big|_{E_{additional}=0} = K_i \times \left(1 + [S]/K_m\right)$$

$$\frac{IC50}{IC50_{wt}} = \frac{K_i \times \left(1 + [S]/K_m\right) \times \left(2 \times \left(\frac{E_{wt} + E_{additional}}{E_{wt}}\right) - 1\right)}{K_i \times \left(1 + [S]/K_m\right)}$$

$$\frac{IC50}{IC50_{wt}} = 2 \times \left(\frac{E_{wt} + E_{additional}}{E_{wt}}\right) - 1$$

Supplementary Figure 4.2. (continued)

Let $[E]_{total} = (\,E_{wt} + E_{additional}\,)$.

Solve for IC50, considering fitness costs of additional enzyme production, cost($E_{additional}$):

$$\begin{pmatrix} \text{drug - inhibited flux with} \\ \text{additional enzyme} \end{pmatrix} \times \begin{pmatrix} 1 - \dfrac{\text{fitness cost of}}{\text{additional enzyme}} \end{pmatrix} = 50\% \times \begin{pmatrix} \text{uninhibited flux with} \\ \text{wildtype enzyme abundance} \end{pmatrix}$$

$$\left(E_{wt} + E_{additional}\right) \times \left(\frac{k_{cat}\,[S]}{K_m\left(1+[I]/K_i\right)+[S]}\right) \times \left(1-\text{cost}\left(E_{additional}\right)\right) = \frac{1}{2} \times E_{wt} \times \left(\frac{k_{cat}\,[S]}{K_m+[S]}\right)$$

$$2 \times \left(\frac{E_{wt}+E_{additional}}{E_{wt}}\right) \times \left(1-\text{cost}\left(E_{additional}\right)\right) \times \left(K_m+[S]\right) = K_m\left(1+[I]/K_i\right)+[S]$$

$$2 \times \left(\frac{E_{wt}+E_{additional}}{E_{wt}}\right) \times \left(1-\text{cost}\left(E_{additional}\right)\right) \times \left(1+[S]/K_m\right) = \left(1+[S]/K_m\right)+[I]/K_i$$

$$[I] = K_i \times \left(1+[S]/K_m\right) \times \left(2 \times \left(\frac{E_{wt}+E_{additional}}{E_{wt}}\right) \times \left(1-\text{cost}\left(E_{additional}\right)\right) - 1\right)$$

$$\text{IC50}_{wt} = [I]\big|_{E_{additional}=0} = K_i \times \left(1+[S]/K_m\right) \text{, given that cost}(0)=0$$

$$\frac{\text{IC50}}{\text{IC50}_{wt}} = \frac{K_i \times \left(1+[S]/K_m\right) \times \left(2 \times \left(\dfrac{E_{wt}+E_{additional}}{E_{wt}}\right) \times \left(1-\text{cost}\left(E_{additional}\right)\right) - 1\right)}{K_i \times \left(1+[S]/K_m\right)}$$

$$\frac{\text{IC50}}{\text{IC50}_{wt}} = 2 \times \left(\frac{E_{wt}+E_{additional}}{E_{wt}}\right) \times \left(1-\text{cost}\left(E_{additional}\right)\right) - 1$$

Supplementary Figure 4.2. (continued)

(**d**). Non-competitive enzyme inhibition

$$\begin{array}{ccc}
EI & \xrightleftharpoons{S} & EIS \\
\big\updownarrow I & & \big\updownarrow I \\
E & \xrightleftharpoons{S} & ES \\
& \searrow & \downarrow \\
& P &
\end{array}$$
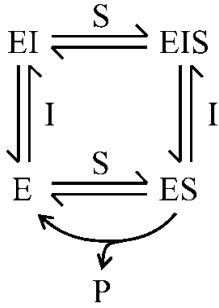
$$\frac{d[E]}{dt} = k_{Ioff}[EI] + \left(k_{Soff} + k_{cat}\right)[ES] - k_{Son}[E][S] - k_{Ion}[E][I]$$

$$\frac{d[EI]}{dt} = k_{Ion}[E][I] + k_{Soff}[EIS] - k_{Ioff}[EI] - k_{Son}[EI][S]$$

$$\frac{d[ES]}{dt} = k_{Son}[E][S] + k_{Ioff}[EIS] - \left(k_{Soff} + k_{cat} + k_{Ion}[I]\right)[ES]$$

$$\frac{d[EIS]}{dt} = k_{Ion}[ES][I] + k_{Son}[EI][S] - \left(k_{Ioff} + k_{Soff}\right)[EIS]$$

$$\frac{d[P]}{dt} = k_{cat}[ES]$$

$$K_m = \frac{k_{cat} + k_{Soff}}{k_{Son}}, \quad K_i = \frac{k_{Ioff}}{k_{Ion}}$$

Assume separation of timescales $(k_{cat} \ll k_{Soff})$

$$\Rightarrow \frac{d[P]}{dt} = \frac{[E]_{total} \cdot k_{cat}}{1 + [I]/K_i} \frac{[S]}{K_m + [S]}$$

The remainder of the derivation is identical to that in Supplementary Figure 4.2a, yielding

$$\frac{IC50}{IC50_{wt}} = 2 \times \left(\frac{E_{wt} + E_{additional}}{E_{wt}}\right) - 1 \quad \text{or} \quad \frac{IC50}{IC50_{wt}} = 2 \times \left(\frac{E_{wt} + E_{additional}}{E_{wt}}\right) \times \left(1 - cost\left(E_{additional}\right)\right) - 1$$

depending on the absence or presence of fitness costs for drug target over-expression.

Supplementary Figure 4.2. (continued)

(**e**). Competitive substrate damage

The mechanism of inhibition modeled here can result in a depletion of substrate S_2, and so to model this effect S_2 is treated as a dynamical variable, synthesized at rate α; while S_1 is treated as a constant.

Example: E = Dihydropteroate synthase (DHPS), S_1 = para-aminobenzoic acid (PABA), S_2 = pteridine diphosphate, P = dihydropteroate, I = sulfamethoxazole, I-S_2 = dihydropterin-sulfamethoxazole (Supplementary Figure 4.4a).
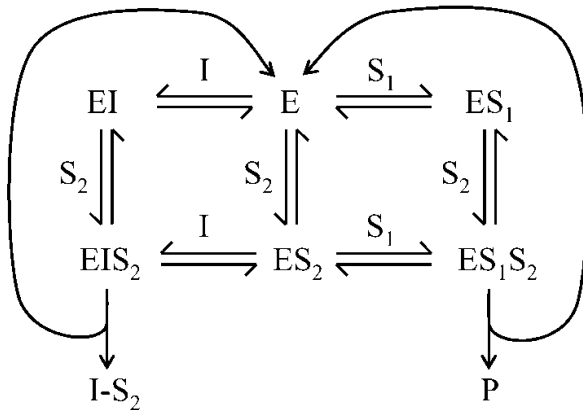
Supplementary Figure 4.2. (continued)

$$\frac{d[E]}{dt} = k_{Ioff}[EI] + k_{S1off}[ES_1] + k_{S2off}[ES_2] + k_{cat}([ES_1S_2] + [EIS_2]) - (k_{S1on}[S_1] + k_{S2on}[S_2] + k_{Ion}[I])[E]$$

$$\frac{d[EI]}{dt} = k_{Ion}[E][I] + k_{S2off}[EIS_2] - (k_{Ioff} + k_{S2on}[S_2])[EI]$$

$$\frac{d[ES_1]}{dt} = k_{S1on}[E][S_1] + k_{S2off}[ES_1S_2] - (k_{S1off} + k_{S2on}[S_2])[ES_1]$$

$$\frac{d[ES_2]}{dt} = k_{S2on}[E][S_2] + k_{S1off}[ES_1S_2] + k_{Ioff}[EIS_2] - (k_{S2off} + k_{S1on}[S_1] + k_{Ion}[I])[ES_2]$$

$$\frac{d[ES_1S_2]}{dt} = k_{S1on}[ES_2][S_1] + k_{S2on}[ES_1][S_2] - (k_{S1off} + k_{S2off} + k_{cat})[ES_1S_2]$$

$$\frac{d[EIS_2]}{dt} = k_{Ion}[ES_2][I] + k_{S2on}[EI][S_2] - (k_{Ioff} + k_{S2off} + k_{cat})[EIS_2]$$

$$\frac{d[S_2]}{dt} = \alpha + k_{S2off}([ES_2] + [ES_1S_2] + [EIS_2]) - k_{S2on}([E] + [ES_1] + [EI])[S]$$

$$\frac{d[P]}{dt} = k_{cat}[ES_1S_2]$$

$$K_i = \frac{k_{Ioff}}{k_{Ion}}, \ K_{S1} = \frac{k_{S1off}}{k_{S1on}}$$

$$\Rightarrow \frac{d[P]}{dt} = \frac{\alpha}{1 + \dfrac{[I]/K_i}{[S_1]/K_{S1}}}$$

Supplementary Figure 4.2. (continued)

Let $[E]_{total} = (E_{wt} + E_{additional})$.

Solve for IC50, considering fitness costs of additional enzyme production, cost($E_{additional}$):

$$\begin{pmatrix} \text{drug - inhibited flux with} \\ \text{additional enzyme} \end{pmatrix} \times \begin{pmatrix} 1 - \begin{matrix} \text{fitness cost of} \\ \text{additional enzyme} \end{matrix} \end{pmatrix} = 50\% \times \begin{pmatrix} \text{uninhibited flux with} \\ \text{wildtype enzyme abundance} \end{pmatrix}$$

$$\left(\frac{\alpha}{1 + \dfrac{[I]/K_i}{[S_1]/K_{S1}}} \right) \times \left(1 - \text{cost}(E_{additional})\right) = \frac{1}{2} \times \alpha$$

$$2 \times \left(1 - \text{cost}(E_{additional})\right) = 1 + \frac{[I]/K_i}{[S_1]/K_{S1}}$$

$$[I] = \frac{[S_1].K_i}{K_{S1}} \times \left(2 \times \left(1 - \text{cost}(E_{additional})\right) - 1\right)$$

$$IC50_{wt} = [I]\big|_{E_{additional}=0} = \frac{[S_1].K_i}{K_{S1}}, \text{given that } \text{cost}(0) = 0$$

$$\frac{IC50}{IC50_{wt}} = \frac{\dfrac{[S_1].K_i}{K_{S1}} \times \left(2 \times \left(1 - \text{cost}(E_{additional})\right) - 1\right)}{\dfrac{[S_1].K_i}{K_{S1}}}$$

$$\frac{IC50}{IC50_{wt}} = 2 \times \left(1 - \text{cost}(E_{additional})\right) - 1$$

Supplementary Figure 4.2. (continued)

(f). Non-competitive substrate damage

The mechanism of inhibition modeled here can result in a depletion of substrate S, and so to

model this effect S is treated as a dynamical variable, synthesized at rate α.
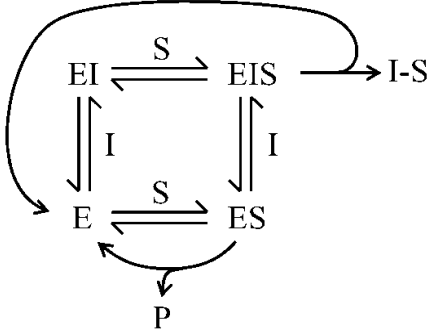
$$\frac{d[E]}{dt} = k_{Ioff}[EI] + (k_{Soff} + k_{cat})[ES] + k_{cat}[EIS] - (k_{Son}[S] + k_{Ion}[I])[E]$$

$$\frac{d[EI]}{dt} = k_{Ion}[E][I] + k_{Soff}[EIS] - k_{Ioff}[EI] - k_{Son}[EI][S]$$

$$\frac{d[ES]}{dt} = k_{Son}[E][S] + k_{Ioff}[EIS] - (k_{Soff} + k_{cat} + k_{Ion}[I])[ES]$$

$$\frac{d[EIS]}{dt} = k_{Ion}[ES][I] + k_{Son}[EI][S] - (k_{Ioff} + k_{Soff} + k_{cat})[EIS]$$

$$\frac{d[S]}{dt} = \alpha - k_{Son}([E] + [EI])[S] + k_{Soff}([ES] + [EIS])$$

$$\frac{d[P]}{dt} = k_{cat}[ES]$$

$$K_i = \frac{k_{Ioff}}{k_{Ion}}$$

$$\Rightarrow \frac{d[P]}{dt} = \frac{\alpha}{1 + [I]/K_i}$$

169

Supplementary Figure 4.2. (continued)

The remainder of the derivation is identical to that in Supplementary Figure 4.2b, yielding

$$\frac{IC50}{IC50_{wt}} = 1 \quad \text{or} \quad \frac{IC50}{IC50_{wt}} = 2 \times \left(1 - \text{cost}\left(E_{additional}\right)\right) - 1$$

depending on the absence or presence of fitness costs for drug target over-expression.

Supplementary Figure 4.3. Wildtype enzyme abundance quantitatively affects the resistance obtained upon drug target over-expression. Over-expression of a non-costly target gene of an enzyme inhibitor confers increased drug resistance according to the equation $IC50/IC50_{wt} = 2 \times (E_{wt} + E_{additional}) / E_{wt} - 1$ (Supplementary Figure 4.3a, b). Consequently, variation in E_{wt} affects the change in resistance for a given value of $E_{additional}$: when plotted against $\log(E_{additional})$ the response curve retains its shape but is translated along the $\log(E_{additional})$ axis by the log of the ratio of E_{wt} values. This phenomenon explains the quantitative difference in resistance between trimethoprim and triclosan on the over-expression of each drug's target (DHFR and ENR, respectively). Known differences in E_{wt} explain most of the observed variation: Taniguchi *et al* measured wildtype protein abundances in *E. coli* with single-molecule sensitivity using fluorescent protein fusions(Taniguchi et al., 2010), and measured the mean single-cell abundance of DHFR (*folA*) as 38 proteins / cell, while ENR (*fabI*) was more highly expressed at 342 proteins / cell (Supplementary Table 6 of (Taniguchi et al., 2010). While $\log10(E_{wt\ ENR} / E_{wt\ DHFR}) \approx 1$, the measured curves $(IC50/IC50_{wt})_{DHFR}$ and $(IC50/IC50_{wt})_{ENR}$ differ by 1.5 units on the $\log10(E_{additional})$ axis (Figure 4.2b). The additional difference of 0.5 may be explained by differences in transcript stability or translation efficiency between the exogenous (plasmid-expressed) transcript and the endogenous (chromosomal) transcript. An altered number of proteins produced per exogenous transcript can be characterized by a coefficient in front of $E_{additional}$, which is mathematically equivalent to variation in E_{wt} and thus results in a shift along the $\log(E_{additional})$ axis. One feature of the response to ENR over-expression is still not

explained by this theory: an elevated baseline level of resistance, conferred by carriage of the ENR-expressing plasmid even without IPTG (Figure 4.1b). This effect, and a similar effect for DNA Gyrase and Topo IV (reduced baseline resistance), can be explained by an elevated baseline transcription of these genes from weak internal promoters (Supplementary Figure 4.5).
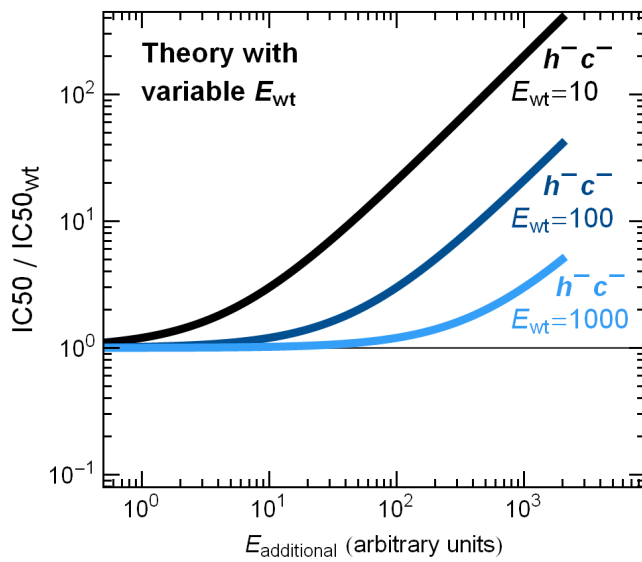

Supplementary Figure 4.3. Wildtype enzyme abundance quantitatively affects the resistance obtained upon drug target over-expression. (Continued)

Supplementary Figure 4.4. Sulfonamides and trimethoprim inhibit their targets by different molecular mechanisms. (**a**) Sulfonamide class antibiotics, such as sulfamethoxazole, compete with para-aminobenzoic acid for binding to Dihydropteroate synthase (DHPS). When sulfonamides bind to DHPS they do not inhibit catalysis, but are covalently linked by DHPS to the substrate pteridine diphosphate. This substrate-diverting reaction constitutes a distinction from competitive inhibition that profoundly changes the relation between enzyme concentration and drug resistance (Supplementary Figure 4.2) (**b**) Trimethoprim competes with dihydrofolic acid for binding to Dihydrofolate reductase (DHFR), and exemplifies the traditional concept of a competitive enzyme inhibitor: DHFR has no catalytic activity when bound by trimethoprim.
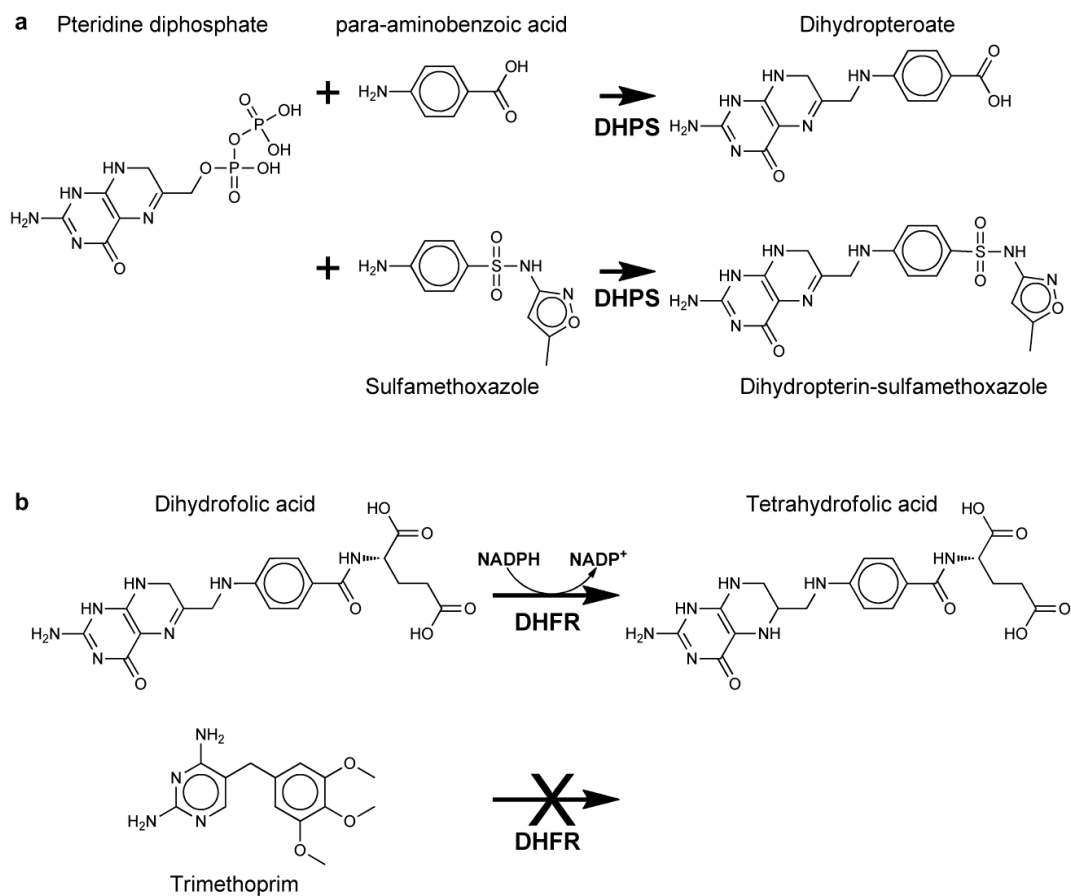
Supplementary Figure 4.4. Sulfonamides and trimethoprim inhibit their targets by different molecular mechanisms. (Continued)

Supplementary Figure 4.5. Small differences in baseline drug resistance can be explained by weak internal promoters in drug target genes. Plasmids encoding the drug target genes ENR, Gyrase, and Topo IV induce small changes in resistance that do do not appear to be caused by basal IPTG-regulated transcription (Supplementary Figure 4.1), since this baseline change in resistance does not change further until a greater than 5-fold increase in IPTG-induced transcription (Figure 4.1b). These effects may be explained by weak internal promoters in these drug target genes, that will induce a baseline level of additional transcription that is not IPTG-responsive. This figure demonstrates the theoretical responses to ENR (h^-c^-), Gyrase (h^+c^+ *lethal*) and Topo IV (h^+c^+ *partial*) in the presence of a weak internal promoter. Small amounts of additional drug target production have the effect of inducing small changes in drug resistance; positive for h^-c^- and negative for h^+c^+; that persist even as IPTG-regulated $E_{additional}$ approaches zero. In the examples shown here, the h^-c^- gene (compare to ENR, Figure 4.1b) contains an internal promoter of 0.5% of the wildtype promoter strength. As this gene is encoded on a plasmid with, conservatively, 50 copies per cell(Kitagawa et al., 2005; Lutz and Bujard, 1997), this 0.5% activity per gene copy leads to a baseline synthesis of 25% of E_{wt}, and consequently a measurable increase in baseline IC50. This quantitative calibration (internal promoter = 0.5% of E_{wt}) is made possible by the relative increase in drug resistance; such an estimation is not possible for genes that only incur costs, not protection (e.g. Gyrase and Topo IV).
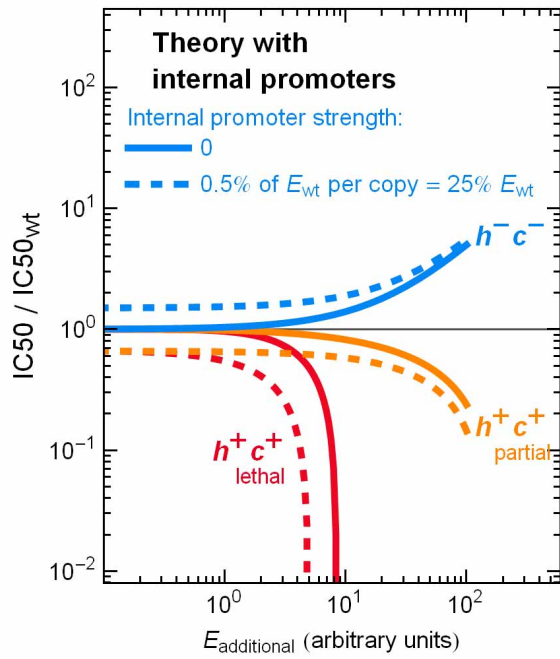
Supplementary Figure 4.5. Small differences in baseline drug resistance can be explained by weak internal promoters in drug target genes. (Continued)

References

Amabile-Cuevas, C.F., and Demple, B. (1991). Molecular characterization of the soxRS genes of Escherichia coli: two genes control a superoxide stress regulon. Nucleic acids research *19*, 4479-4484.

Anderson, P.M., Sung, Y.C., and Fuchs, J.A. (1990). The cyanase operon and cyanate metabolism. FEMS microbiology reviews *7*, 247-252.

Bacon, C.W., Porter, J.K., Norred, W.P., and Leslie, J.F. (1996). Production of fusaric acid by Fusarium species. Appl Environ Microbiol *62*, 4039-4043.

Baquero, M.R., Bouzon, M., Varea, J., and Moreno, F. (1995). sbmC, a stationary-phase induced SOS Escherichia coli gene, whose product protects cells from the DNA replication inhibitor microcin B17. Mol Microbiol *18*, 301-311.

Barth, E., Gora, K.V., Gebendorfer, K.M., Settele, F., Jakob, U., and Winter, J. (2009). Interplay of cellular cAMP levels, {sigma}S activity and oxidative stress resistance in Escherichia coli. Microbiology *155*, 1680-1689.

Bendezu, F.O., Hale, C.A., Bernhardt, T.G., and de Boer, P.A. (2009). RodZ (YfgA) is required for proper assembly of the MreB actin cytoskeleton and cell shape in E. coli. The EMBO journal *28*, 193-204.

Bochner, B.R., Huang, H.C., Schieven, G.L., and Ames, B.N. (1980). Positive selection for loss of tetracycline resistance. J Bacteriol *143*, 926-933.

Cohen, S.P., Hachler, H., and Levy, S.B. (1993). Genetic and functional analysis of the multiple antibiotic resistance (mar) locus in Escherichia coli. J Bacteriol *175*, 1484-1492.

Collis, C.M., and Grigg, G.W. (1989). An Escherichia coli mutant resistant to phleomycin, bleomycin, and heat inactivation is defective in ubiquinone synthesis. J Bacteriol *171*, 4792-4798.

Daniels, D.W., and Bertrand, K.P. (1985). Promoter mutations affecting divergent transcription in the Tn10 tetracycline resistance determinant. J Mol Biol *184*, 599--610.

Dinh, T., Paulsen, I.T., and Saier, M.H., Jr. (1994). A family of extracytoplasmic proteins that allow transport of large molecules across the outer membranes of gram-negative bacteria. J Bacteriol *176*, 3825-3831.

Giladi, M., Altman-Price, N., Levin, I., Levy, L., and Mevarech, M. (2003). FolM, a new chromosomally encoded dihydrofolate reductase in Escherichia coli. J Bacteriol *185*, 7015-7018.

Girgis, H.S., Hottes, A.K., and Tavazoie, S. (2009). Genetic architecture of intrinsic antibiotic susceptibility. PLoS One *4*, e5629.

Han, X., Dorsey-Oresto, A., Malik, M., Wang, J.Y., Drlica, K., Zhao, X., and Lu, T. (2010). Escherichia coli genes that reduce the lethal effects of stress. BMC microbiology *10*, 35.

Heath, R.J., Yu, Y.T., Shapiro, M.A., Olson, E., and Rock, C.O. (1998). Broad spectrum antimicrobial biocides target the FabI component of fatty acid synthesis. The Journal of biological chemistry *273*, 30316-30320.

Kadrmas, J.L., and Raetz, C.R. (1998). Enzymatic synthesis of lipopolysaccharide in Escherichia coli. Purification and properties of heptosyltransferase i. The Journal of biological chemistry *273*, 2799-2807.

Keseler, I.M., Collado-Vides, J., Santos-Zavaleta, A., Peralta-Gil, M., Gama-Castro, S., Muniz-Rascado, L., Bonavides-Martinez, C., Paley, S., Krummenacker, M., Altman, T.*, et al.* (2011). EcoCyc: a comprehensive database of Escherichia coli biology. Nucleic acids research *39*, D583-590.

Kim, I., Kim, J., Min, B., Lee, C., and Park, C. (2007). Screening of genes related to methylglyoxal susceptibility. J Microbiol *45*, 339-343.

Kishony, R., and Leibler, S. (2003). Environmental stresses can alleviate the average deleterious effect of mutations. J Biol *2*, 14.

Kitagawa, M., Ara, T., Arifuzzaman, M., Ioka-Nakamichi, T., Inamoto, E., Toyonaga, H., and Mori, H. (2005). Complete set of ORF clones of Escherichia coli ASKA library (a complete set of E. coli K-12 ORF archive): unique resources for biological research. DNA research : an international journal for rapid publication of reports on genes and genomes *12*, 291-299.

Kneidinger, B., Marolda, C., Graninger, M., Zamyatina, A., McArthur, F., Kosma, P., Valvano, M.A., and Messner, P. (2002). Biosynthesis pathway of ADP-L-glycero-beta-D-manno-heptose in Escherichia coli. J Bacteriol *184*, 363-369.

Kolodkin-Gal, I., Hazan, R., Gaathon, A., Carmeli, S., and Engelberg-Kulka, H. (2007). A linear pentapeptide is a quorum-sensing factor required for mazEF-mediated cell death in Escherichia coli. Science *318*, 652-655.

Kong, K.F., Schneper, L., and Mathee, K. (2010). Beta-lactam antibiotics: from antibiosis to resistance and bacteriology. APMIS : acta pathologica, microbiologica, et immunologica Scandinavica *118*, 1-36.

Koo, M.S., Lee, J.H., Rah, S.Y., Yeo, W.S., Lee, J.W., Lee, K.L., Koh, Y.S., Kang, S.O., and Roe, J.H. (2003). A reducing system of the superoxide sensor SoxR in Escherichia coli. The EMBO journal *22*, 2614-2622.

Kuznetsova, E., Proudfoot, M., Gonzalez, C.F., Brown, G., Omelchenko, M.V., Borozan, I., Carmel, L., Wolf, Y.I., Mori, H., Savchenko, A.V.*, et al.* (2006). Genome-wide analysis of substrate specificities of the Escherichia coli haloacid dehalogenase-like phosphatase family. The Journal of biological chemistry *281*, 36149-36161.

Lam, H.M., Tancula, E., Dempsey, W.B., and Winkler, M.E. (1992). Suppression of insertions in the complex pdxJ operon of Escherichia coli K-12 by lon and other mutations. J Bacteriol *174*, 1554-1567.

Langman, L., Young, I.G., Frost, G.E., Rosenberg, H., and Gibson, F. (1972). Enterochelin system of iron transport in Escherichia coli: mutations affecting ferric-enterochelin esterase. J Bacteriol *112*, 1142-1149.

Lenski, R.E., Souza, V., Duong, L.P., Phan, Q.G., Nguyen, T.N., and Bertrand, K.P. (1994). Epistatic effects of promoter and repressor functions of the Tn10 tetracycline-resistance operon of the fitness of Escherichia coli. Mol Ecol *3*, 127--135.

Linstrom, E.B., Boman, H.G., and Steele, B.B. (1970). Resistance of Escherichia coli to penicillins. VI. Purification and characterization of the chromosomally mediated penicillinase present in ampA-containing strains. J Bacteriol *101*, 218-231.

Lutz, R., and Bujard, H. (1997). Independent and tight regulation of transcriptional units in Escherichia coli via the LacR/O, the TetR/O and AraC/I1-I2 regulatory elements. Nucleic Acids Res *25*, 1203-1210.

Maloy, S.R., and Nunn, W.D. (1981). Selection for loss of tetracycline resistance by Escherichia coli. J Bacteriol *145*, 1110-1111.

Masuda, N., and Church, G.M. (2003). Regulatory network of acid resistance genes in Escherichia coli. Mol Microbiol *48*, 699-712.

Mattiuzzo, M., Bandiera, A., Gennaro, R., Benincasa, M., Pacor, S., Antcheva, N., and Scocchi, M. (2007). Role of the Escherichia coli SbmA in the antimicrobial activity of proline-rich peptides. Mol Microbiol *66*, 151-163.

McCalla, D.R., Kaiser, C., and Green, M.H. (1978). Genetics of nitrofurazone resistance in Escherichia coli. J Bacteriol *133*, 10-16.

Meng, S.Y., and Bennett, G.N. (1992). Nucleotide sequence of the Escherichia coli cad operon: a system for neutralization of low extracellular pH. J Bacteriol *174*, 2659-2669.

Miovic, M., and Pizer, L.I. (1971). Effect of trimethoprim on macromolecular synthesis in Escherichia coli. J Bacteriol *106*, 856-862.

Misra, R., and Miao, Y. (1995). Molecular analysis of asmA, a locus identified as the suppressor of OmpF assembly mutants of Escherichia coli K-12. Mol Microbiol *16*, 779-788.

Moyed, H.S., Nguyen, T.T., and Bertrand, K.P. (1983). Multicopy Tn10 tet plasmids confer sensitivity to induction of tet gene expression. J Bacteriol *155*, 549--556.

Nagakubo, S., Nishino, K., Hirata, T., and Yamaguchi, A. (2002). The putative response regulator BaeR stimulates multidrug resistance of Escherichia coli via a novel multidrug exporter system, MdtABC. J Bacteriol *184*, 4161-4167.

Nicoloff, H., Perreten, V., McMurry, L.M., and Levy, S.B. (2006). Role for tandem duplication and lon protease in AcrAB-TolC- dependent multiple antibiotic resistance (Mar) in an Escherichia coli mutant without mutations in marRAB or acrRAB. J Bacteriol *188*, 4413-4423.

Nikaido, H. (1989). Outer membrane barrier as a mechanism of antimicrobial resistance. Antimicrob Agents Chemother *33*, 1831-1836.

Panagiotidis, C.A., Huang, S.C., and Canellakis, E.S. (1995). Relationship of the expression of the S20 and L34 ribosomal proteins to polyamine biosynthesis in Escherichia coli. The international journal of biochemistry & cell biology *27*, 157-168.

Parks, D.R., Roederer, M., and Moore, W.A. (2006). A new "Logicle" display method avoids deceptive effects of logarithmic scaling for low signals and compensated data. Cytometry A *69*, 541-551.

Paterson, E.S., Boucher, S.E., and Lambert, I.B. (2002). Regulation of the nfsA Gene in Escherichia coli by SoxS. J Bacteriol *184*, 51-58.

Pogliano, J., Lynch, A.S., Belin, D., Lin, E.C., and Beckwith, J. (1997). Regulation of Escherichia coli cell envelope proteins involved in protein folding and degradation by the Cpx two-component system. Genes & development *11*, 1169-1182.

Polissi, A., De Laurentis, W., Zangrossi, S., Briani, F., Longhi, V., Pesole, G., and Deho, G. (2003). Changes in Escherichia coli transcriptome during acclimatization at low temperature. Research in microbiology *154*, 573-580.

Reynolds, C.M., Kalb, S.R., Cotter, R.J., and Raetz, C.R. (2005). A phosphoethanolamine transferase specific for the outer 3-deoxy-D-manno-octulosonic acid residue of Escherichia coli lipopolysaccharide. Identification of the eptB gene and Ca2+ hypersensitivity of an eptB deletion mutant. The Journal of biological chemistry *280*, 21202-21211.

Sarkar, S.K., Chowdhury, C., and Ghosh, A.S. (2010). Deletion of penicillin-binding protein 5 (PBP5) sensitises Escherichia coli cells to beta-lactam agents. International journal of antimicrobial agents *35*, 244-249.

Satishchandran, C., and Boyle, S.M. (1986). Purification and properties of agmatine ureohydrolyase, a putrescine biosynthetic enzyme in Escherichia coli. J Bacteriol *165*, 843-848.

Sprenger, G.A., Schorken, U., Wiegert, T., Grolle, S., de Graaf, A.A., Taylor, S.V., Begley, T.P., Bringer-Meyer, S., and Sahm, H. (1997). Identification of a thiamin-dependent synthase in Escherichia coli required for the formation of the 1-deoxy-D-xylulose 5-phosphate precursor to isoprenoids, thiamin, and pyridoxol. Proc Natl Acad Sci U S A *94*, 12857-12862.

Suzuki, Y., and Brown, G.M. (1974). The biosynthesis of folic acid. XII. Purification and properties of dihydroneopterin triphosphate pyrophosphohydrolase. The Journal of biological chemistry *249*, 2405-2410.

Takayama, M., Ohyama, T., Igarashi, K., and Kobayashi, H. (1994). Escherichia coli cad operon functions as a supplier of carbon dioxide. Mol Microbiol *11*, 913-918.

Tamaki, S., Sato, T., and Matsuhashi, M. (1971). Role of lipopolysaccharides in antibiotic resistance and bacteriophage adsorption of Escherichia coli K-12. J Bacteriol *105*, 968-975.

Taniguchi, Y., Choi, P.J., Li, G.W., Chen, H., Babu, M., Hearn, J., Emili, A., and Xie, X.S. (2010). Quantifying E. coli proteome and transcriptome with single-molecule sensitivity in single cells. Science *329*, 533-538.

Tsui, P., Helu, V., and Freundlich, M. (1988). Altered osmoregulation of ompF in integration host factor mutants of Escherichia coli. J Bacteriol *170*, 4950-4953.

Tucker, D.L., Tucker, N., Ma, Z., Foster, J.W., Miranda, R.L., Cohen, P.S., and Conway, T. (2003). Genes of the GadX-GadW regulon in Escherichia coli. J Bacteriol *185*, 3190-3201.

Vimr, E.R., and Troy, F.A. (1985). Identification of an inducible catabolic system for sialic acids (nan) in Escherichia coli. J Bacteriol *164*, 845-853.

Wei, Y., Vollmer, A.C., and LaRossa, R.A. (2001). In vivo titration of mitomycin C action by four Escherichia coli genomic regions on multicopy plasmids. J Bacteriol *183*, 2259-2264.

Wu, W.H., and Morris, D.R. (1973). Biosynthetic arginine decarboxylase from Escherichia coli. Purification and properties. The Journal of biological chemistry *248*, 1687-1695.

Yeh, P., Tschumi, A.I., and Kishony, R. (2006). Functional classification of drugs by properties of their pairwise interactions. Nat Genet *38*, 489--494.

Yuen, P.H., and Sokoloski, T.D. (1977). Kinetics of concomitant degradation of tetracycline to epitetracycline, anhydrotetracycline, and epianhydrotetracycline in acid phosphate solution. J Pharm Sci *66*, 1648--1650.